INCLUSION OF A GLYCOGEN REGULATION MATHEMATICAL MODEL INTO A CONTEXTUAL METABOLIC FRAMEWORK

Abby Jo Todd

A dissertation submitted to the faculty of the University of North Carolina at Chapel Hill in partial fulfillment of the requirements for the degree of Doctor of Philosophy in the Department of Mathematics.

Chapel Hill

2008

Approved by:

Timothy C. Elston

Kevin T. Morgan

David Adalsteinsson

M. Gregory Forest

Richard McLaughlin

ABSTRACT

Abby Jo Todd: Inclusion of a Glycogen Regulation Mathematical Model into a Contextual Metabolic Framework
(Under the direction of Timothy C. Elston)

While we generally eat infrequently, metabolic processes within our body tightly regulate blood glucose levels. The metabolic system is comprised of various tissues, each of which contains specific regulatory pathways that determine the function of the tissue within the system. These tissues and their localized metabolic functions, complement one another through inter-tissue metabolic highways to form the entire metabolic system. The liver is a key control center of metabolism and thus, the mathematical model described in this thesis is heavily 'liver-centric.' Though all hepatocytes, or liver cells, are capable of similar metabolic functions, the rate at which these functions are carried out depends on the location of the hepatocytes within the liver. At the intracellular level, the various metabolic pathways contain many intersections. Though the intracellular components of the metabolic system are spatially localized, I assume a well-mixed cell and ignore spatial heterogeneity

While physiological layering is important to accurately model metabolism, the layering of regulation within the system is also of interest for our model. The biochemical processes that make up metabolic pathways are regulated on many levels, such as by metabolites, hormones and enzymes, and also at a pre-protein level through transcription. While the model developed here does not include all levels of metabolic

control it does address the need for understanding of metabolism from a multi-level perspective. The main conclusions from this study are that while fats are utilized to help produce glucose during periods of low blood glucose levels, resulting ketone bodies are kept at a minimal level and that heatmaps are an effective visual tool in evaluating model simulations. The enzyme circuit of the glycogen regulatory system allows for efficient modification of activity of enzymes to quickly increase the rate at which excess glucose is stored as glycogen. Also, as blood glucose levels drop, this enzyme circuitry is modified so that glycogen, amino acids and fats are broken down to produce glucose so that blood glucose levels are stabilized. The proposed model suggests that while fats are utilized in this process, ketone bodies resulting from lipolysis are kept at low levels, which is essential to protect the system from ketoacidosis. A mathematical model of a reduced glycogen regulatory circuit was developed and compared to a model of the full glycogen regulatory circuit. Though simulations of these models were similar in isolation, they produced different results when immersed in a contextual model which captured the multiple tissue environment of the metabolic system. This method allowed investigation into the effects of the enzyme cascade in the glycogen regulatory system. Heatmaps enabled quick assessment of model simulations and were vital for obtaining an overall 'fluxomic' picture of the state of the system.

To my family.

ACKNOWLEDGEMENTS

I extend many thanks to Dr. Tim Elston for his unending patience and his confidence in and support for me. I can not thank him enough for his invaluable help and dedication over the recent years. I would certainly have missed out on some wonderful conversations and learning experiences had I not had the opportunity to work with Dr. Kevin Morgan. His constant zest for life and learning is something we should all hope to experience, even if but for a moment.

Thank you to my other committee members, Dr. M. Gregory Forest, Dr. David Adalsteinsson and Dr. Richard McLaughlin, for helping me through my journey at Carolina. Your dedication to the UNC Mathematics Department and its students is commendable.

Not only am I thankful for the financial support I received as a research assistant from Sanofi-aventis Pharmaceuticals but I also appreciate the opportunity to have gained some insight into the workings behind drug development and experimentation.

I have been extremely blessed with my family whose love and encouragement over the years allowed me to reach this level of achievement. Thank you also to the many faithful friends who have cheered me in uncountable ways.

I am grateful to my Lord and Savior Who has blessed me along the way with wonderful people to work with and with the opportunity to use mathematics to explore His amazing world.

PREFACE

My initial interest in the application of mathematics to biological systems was inspired by an example given in one of my classes for a mathematical application to cancer detection. The thought of using mathematics to further medical knowledge and thus help people encouraged me to work in the field of mathematical biology. From an educational perspective, this is a very exciting time to work in this field of research as we are currently in the beginning of a great revolution of bringing together disciplines that have traditionally been separated. Life does not separate itself into history, English, biology, mathematics, etcetera but is a continuous blend of cross-disciplinary concepts. I believe that as we continue in this movement to modify education to learn using this connected viewpoint, we will be more successful in learning about ourselves and the world around us. The challenge of investigating the metabolic system from a systems biology point of view through mathematical modeling is daunting but very important as there has been a drastic increase in the prevalence of obesity, diabetes and other concerns relating to metabolism. By obtaining a better understanding of metabolic processes, especially during transitional feeding periods, we will have a broader knowledge base from which to determine effective methods for controlling diabetes and obesity as well as other undesirable metabolic conditions.

TABLE OF CONTENTS

LIST OF TABLES

Table

LIST OF FIGURES

Figure

LIST OF ABBREVIATIONS

ATP	Adenosine triphosphate
ADP	Adenosine diphosphate
CoA	Coenzyme A
CO2	Carbon dioxide molecule (1 atom of carbon + 2 atoms of oxygen)
FAD	Flavin adenine dinucleotide
FADH2	Energy carrying flavin adenine dinucleotide (FAD + 2 hydrogen molecules)
H+	Hydrogen atom with a positive charge, proton
H2O	Water molecule (2 atoms of hydrogen + 1 atom of oxygen)
NAD+	Oxidized form of nicotinamide adenine dinucleotide
NADH	Reduced form of nicotinamide adenine dinucleotide (NAD + 1 hydrogen molecule)

CHAPTER 1

Introduction

A vast amount of biological data has been obtained through technological advances over the past decade. Advances in scientific computing have allowed mathematical modeling to become a very useful tool in understanding this data and thus increasing out knowledge of particular systems. The metabolic system is quite complex and though many of its components have been explored through modeling, these models have been investigated in isolation. The level of glucose, the main fuel for most cells, is tightly regulated by the metabolic system. Glycogen is a stored form of glucose and is made when there is excess glucose and degraded to make glucose during times of a glucose shortage. This thesis aims to explore the mechanisms behind this synthesis and utilization of glycogen by connecting an isolated mathematical model of the glycogen regulation system to a larger model of the metabolic system.

1.1 Overview of Metabolism

The human body is a complex system that has a constant demand for energetic resources. These energetic resources are made available to the body through the diet, and as people typically experience separate times of eating and fasting, the body must establish a method of using energy derived from the digestion of meals in such a way as

to provide a constant source of fuel to meet its energetic demands. To maintain continuous provision of energetic substrates, the human body has a sophisticated method of storing these products. Liver glycogen, a form of transient storage for energetic resources, was discovered by Claude Bernard in 1857 [1] and though much is now known about the role of glycogen in metabolism, there is still much to be explored. This thesis develops and analyzes a mathematical model of the control mechanisms that regulate the storage and utilization of liver glycogen.

Food is introduced to the body mainly as a mixture of carbohydrates, proteins and fats which are digested in the gut to form glucose, amino acids and free fatty acids, respectively. Glucose enters the liver from the gut via the hepatic portal vein and is the main metabolic fuel of most cells and the sole metabolic fuel for certain cells such as erythrocytes [2]. Blood glucose levels must be tightly regulated to ensure a constant provision of glucose to these cells. Amino acids, which also enter the liver through the hepatic portal vein, can be used to build tissue protein or be converted to metabolites through transamination or the switching of amino groups from one molecule to another. Free fatty acids, either obtained from the diet or from biochemical conversion of excess dietary carbohydrates, are then stored in adipose, or fat, tissue.

During feeding, glucose is plentiful and there is a net conversion of glucose into glycogen for short term storage and fats for long term storage. (Figure 1.1.) As the system transitions from a feeding state into a post-absorptive state, blood glucose levels decrease and the body switches from storing glucose to utilizing glycogen and fat to make glucose. (Figure 1.2.) Specific mechanisms which facilitate this directional change of net flux are discussed later. These changes within the system in response to a loss of

glucose input create interesting dynamics due to the nonlinear feedback mechanisms used to maintain homeostasis. Thus, investigations of this thesis focus on regulatory mechanisms during the post-absorptive, or fasted, state.

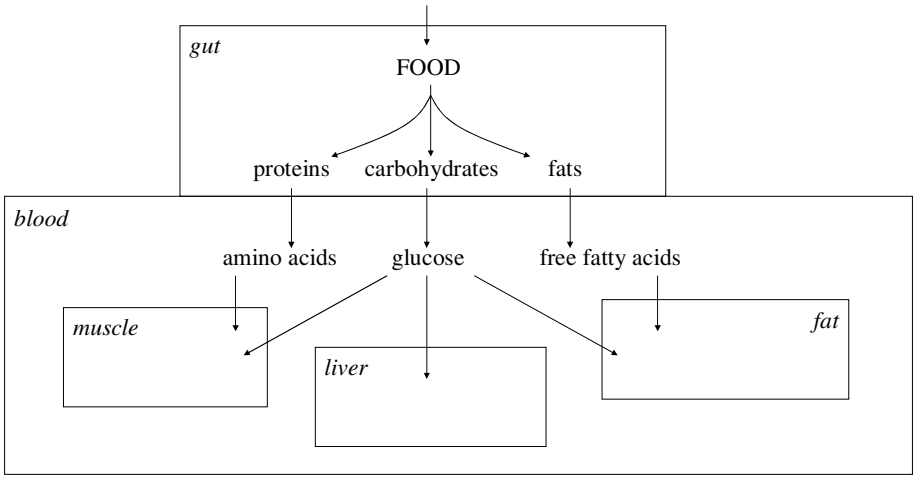

Figure 1.1 Sources of Blood Glucose During a Meal. Food is digested in the gut to form proteins, carbohydrates and fats. These products are converted to amino acids, glucose and free fatty acids, respectively. Glucose is taken up by all tissues while amino acids are mainly taken up by the muscle and free fatty acids are mainly taken up by fat tissue.

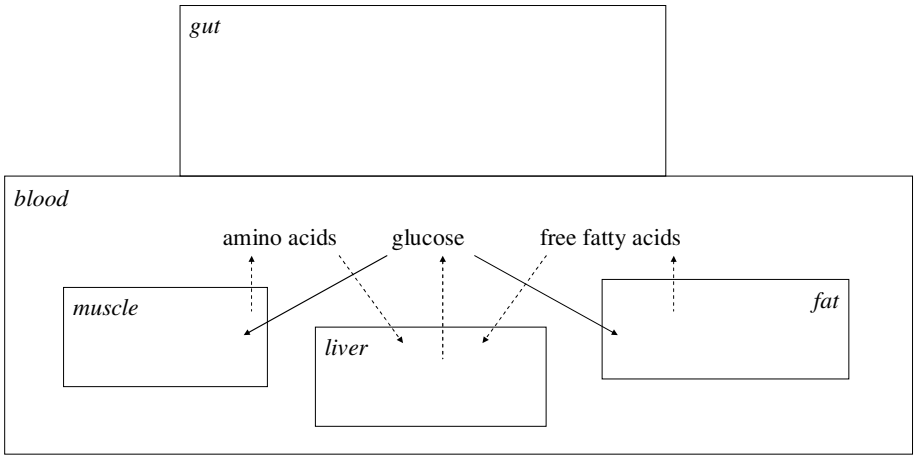

Figure 1.2 Sources of Blood Glucose During Fasting. Fluxes denoted by solid lines are shared by the fed state. Fluxes denoted by dashed lines differ from the fed state.

1.2 The Problem

Two of the main regulators of metabolic pathways are the hormones insulin and glucagon, secreted from the beta cells and alpha cells of the pancreas, respectively. It has been well documented that calcium oscillations lead to oscillations in the secretion of insulin [3, 4] and these oscillations, in turn, create oscillatory dynamics in blood glucose concentrations. Though a number of mathematical models have been developed to capture the oscillatory features of glucose, insulin and glucagon [5-8], none of these include a detailed description of the feedback regulation of insulin and glucagon on blood glucose levels. Through intermediary signals, these two hormones regulate multiple metabolic pathways [9, 10]. Insulin and glucagon also regulate levels of the second messenger cyclic adenosine monophosphate (cAMP) which in turn regulates multiple metabolic processes. The mechanism by which oscillations in blood glucose levels occur

as a result of oscillations in insulin secretion have not been determined. The model introduced in this thesis aims to explain a possible cause for the resulting behavior of blood glucose levels in response to dynamical changes in the regulatory components during the transition from a fed to a fasted state.

Some metabolic pathways, such as glycogen synthesis and degradation, are irreversible due to processes that are highly favored to be unidirectional but function in an opposite manner. Glycogen synthesis will convert a molecule of glucose 6-phosphate into glycogen while glycogen degradation takes glycogen and converts it into glucose 6-phosphate [10]. When both pathways are active at the same time, a phenomenon known as futile cycling occurs [11, 12]. While the exact effects of futile cycling on the metabolic system are unknown, it has been observed with glycogen synthesis and degradation during a fasted state. It is hypothesized that the amount of futile cycling present during the fasting period determines the response time, the time in which the system returns to a fed homeostatic state, once food is reintroduced to the system.

1.3 The Purpose

It is estimated that around 4% of the American population had diabetes in 2000 and that this will increase to around 7% by 2050 [13]. Diabetes has long been around and continues to be an expensive health issue. Symptoms of this disease include an excess of sugar in the urine due to the high levels of glucose in the blood and the inability of the metabolic system to regulate these glucose levels. Type I diabetes occurs when the beta cells of the pancreas are unable to produce insulin resulting in compromised secretion of this key regulatory hormone. Type II diabetes occurs when insulin secretion is normal

but the signaling of this hormone is dysfunctional leading to compromised regulation by this hormone. A better understanding of the regulatory mechanisms of insulin on the enzyme cascade for storage and utilization of glycogen can help build a better understanding of diabetes and possible treatments.

CHAPTER 2

Framework of Metabolism

Metabolism can be defined as the collection of biochemical processes by which digested food is converted into energy through pathways that contain both anabolic and catabolic processes [10]. The metabolic system is very complex and so to become familiar with this system, I first look at an overview of main metabolic pathways. After looking at different tissues which make up this framework, I discuss the main metabolic pathways in more detail to better understand the functions of the various tissues and how they work together to form the metabolic system.

2.1 Overview of Metabolic Pathways

It is important to understand the functionality of metabolic pathways before discussing the main tissues involved with metabolism. For modeling purposes, I only focus on select pathways but in this section I take a brief glance at pathways not included in our model as well as those I chose as key metabolic pathways. Table 2.1 provides a list of the various metabolic pathways and their main functions. It is important to note that while we speak of separate pathways, the metabolic system is in fact not so neatly separated in reality but is a collection of numerous messy reactions constricted within a small area of a cell. For simplicity, I assume that once a molecule has entered a reaction

that the molecule is committed to completing this reaction. We also assume no metabolite concentration is in an intermediate state of these biochemical processes.

Pathway	Function
Glycolysis	breakdown of glucose to pyruvate which then can release ATP by being converted to lactate (anaerobic glycolysis) or being converted to acetyl-CoA and entering the TCA cycle (aerobic glycolysis)
Gluconeogenesis	Conversion of amino acids to glucose
TCA cycle	Set of biochemical reactions common to glucose, amino acid and fat metabolism, an intersection for these pathways. Under aerobic conditions, factors released during reactions of the TCA cycle enter oxidative phosphorylation resulting in ATP synthesis
Glycogenesis	Glucose is converted to glycogen, a transient storage form of glucose
Glycogenolysis	Glycogen is converted to glucose
Lipogenesis	Biosynthesis of fats from excess glucose
Lipolysis	Breakdown of fats, most products from this pathway are unable to enter gluconeogenesis but are beneficial in producing ATP via oxidative phosphorylation
Ketogenesis	Synthesis of ketone bodies, a byproduct of lipolysis and alternate metabolic fuel for some tissues such as muscle and brain

Table 2.1. Overview of Metabolic Pathways. These are the metabolic pathways considered for the model proposed in this thesis.

With the exception of two pathways listed in the table, the model is concerned with paired pathways which results in the production and degradation of certain metabolites. Glycolysis and gluconeogenesis describes the formation and conversion of glucose; glycogenesis and glycogenolysis are the pathways by which glycogen is produced and degraded; lipogenesis and lipolysis are the pathways by which fats are built up and broken down. Though many of the biochemical reactions of each pathway are

reversible, some of them are not requiring different enzymes for the synthesis and degradation of these metabolites. The differences within these pathways will be discussed in Section 2.3. The two pathways which do not have opposite functions are the TCA cycle and ketogenesis.

2.2 Physiology of the Metabolic System

Now that we are somewhat familiar with the functions of metabolic pathways, we will look at the various tissues involved in the metabolic system. The model contains four of the main metabolic tissues: liver, blood, muscle and fat. Table 2.2 lists these tissues along with other tissues and the metabolic pathways found within each tissue.

Tissue	Pathways Present
Liver	Glycolysis, gluconeogenesis, glycogenesis, glycogenolysis, TCA cycle, lipogenesis, lipolysis, ketogenesis
Blood	None
Muscle	Glycolysis, glycogenesis, glycogenolysis, TCA cycle, lipolysis, ketone body utilization
Fat	Glycolysis, TCA cycle, lipogenesis, lipolysis
*Kidney	Glycolysis, gluconeogenesis, TCA cycle
*Brain	Glycolysis, TCA cycle, lipolysis, ketone body utilization
*Heart	Glycolysis, TCA cycle, lipolysis, ketone body utilization
*Erythrocytes	Glycolysis (anaerobic)

Table 2.2. Tissue-Specific Metabolic Pathways. Tissues denoted by * are not represented in the model proposed in this thesis.

2.2.1 Liver

As Table 2.2 shows, hepatic cells are capable of most metabolic pathways. Liver and muscle tissues are also the site of major stores of glycogen. The regulation of glycogenesis and glycogenolysis in the liver is such that hepatic glycogen is a main source of glucose during times of fasting, allowing hepatic glycogen to eventually be converted to metabolic fuel for other tissues. Erythrocytes, among other cells, are solely reliant on glucose as they lack the presence of the TCA cycle needed to use fats or ketone bodies as alternative fuels. Muscle glycogen is primarily used to provide energy for the cell in which the glycogen is stored. The role of hepatic glycogen, to be used for glucose production for the liver and other tissues, and the ability of liver to process amino acid and fat metabolism help make the liver the control center of the metabolic system.

2.2.2 Blood

Though biochemical processes occur in the blood we assume that the blood is simply a transport vehicle for metabolites.

2.2.3 Fat

Fat is useful to the body in many ways, including regulating body temperature, insulating body organs and storage of important excess metabolic fuels. A certain amount of fat is necessary for optimal functioning of the body but can start to have negative effects when there is too much of it. Excess dietary glucose is transported directly to fat tissue and is also converted into free fatty acids within the liver and then transferred to fat tissue for storage. When glucose levels drop, these stored fats are then

transported back to the liver and enter lipolysis providing substrate for the TCA cycle within the liver as well as increasing the rate at which gluconeogenesis occurs resulting in glucose being released from the liver to the blood. Fats can also be transported to other tissues with mitochondria capable of lipolysis and directly provide energy.

2.2.4 Muscle

Though muscle has its own store of glycogen, this store is conserved for when a sudden demand for energy occurs. Muscle utilizes glucose as substrate of glycogen storage and also for immediate metabolic fuel. Muscle tissue is capable of lipolysis and contains the TCA cycle so is able to process alternate metabolic fuels during a fasted state. This preserves blood glucose levels for tissues that are incapable of switching to alternate fuels. Muscle cells lack an enzyme required for making glucose from both gluconeogenesis and glycogenolysis. Assistance from muscle tissue in regulating blood glucose comes from using less blood glucose during fasting and also from providing substrate for gluconeogenesis to the liver through the Cori cycle [9, 10].

2.2.5 Others

All tissues affect and are affected by the regulation of metabolism in some way. Other tissues that contribute a significant amount of interaction with the metabolic system are heart, brain, kidney and pancreatic tissues. For simplification purposes, these do not explicitly appear in the mathematical model in this paper.

2.3 Select Metabolic Pathways

Though this thesis focuses on the fate of glucose as an energy source, the proposed mathematical model is capable of investigating other forms of fuel and this concept is included in the chapter addressing future work. The main result of a functional metabolic system is providing the correct supply of energy to the system at each moment in time. As discussed earlier, in order for this to occur, blood glucose levels must be tightly regulated within a set concentration threshold. This section describes the main metabolic pathways that help regulate these blood glucose levels.

2.3.1 Glycolysis

Glycolysis is the pathway by which glucose is converted into pyruvate which then can enter exergonic processes, releasing energy through either aerobic or anaerobic means [9, 10]. Glycolysis and the anaerobic (oxygen independent) pathway of producing energy are found in the cytosol of all cells whereas the machinery required to aerobically produce energy requires the presence of mitochondria. Figure 2.1 shows the complete pathway from glucose to pyruvate and also includes the anaerobic step from pyruvate to lactate.

Though including each reaction of the metabolic system in a mathematical model would result in a comprehensive model, the analysis of such an extensive system would be very challenging. To simplify the analysis of the contextual or whole-physiological model, only those reactions which limit the flux through the pathways of interest are included in the model. This introduction to these pathways will include a figure and table

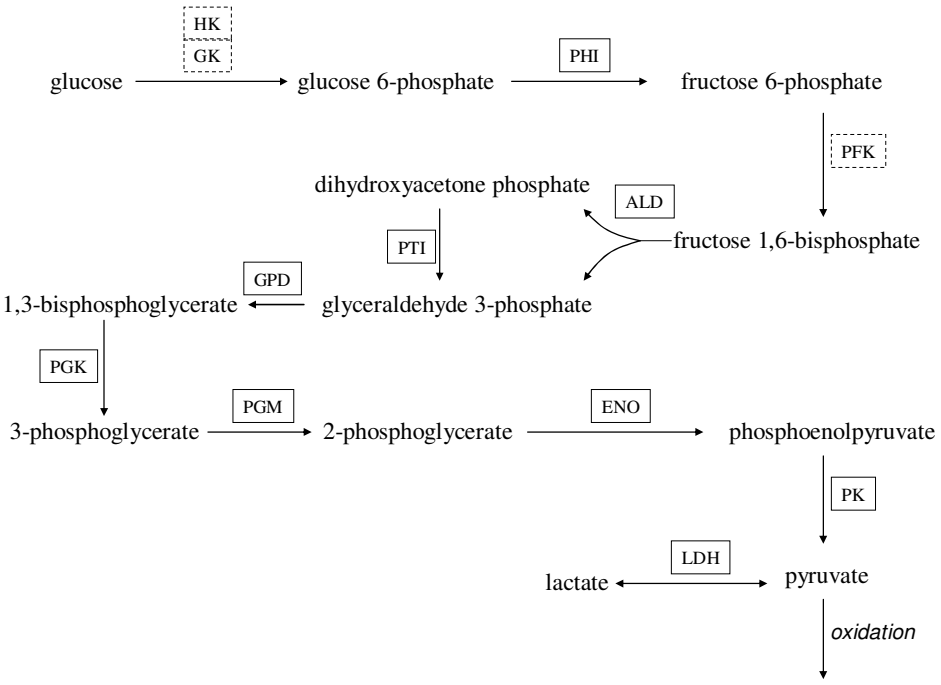

Figure 2.1. The Complete Pathway of Glycolysis. Enzymes catalyzing specific reactions are denoted in boxes next to the arrow of each corresponding reaction. Enzymes with dashed outlines are specific to glycolysis while those with outlined in solid are also found in gluconeogenesis. Abbreviations are as follows: HK, hexokinase; GK, glucokinase; PHI, phosphokexose isomerase; PFK, phosphofructokinase; ALD, aldolase; PTI, phosphotriose isomerase; GPD, glyceraldehyde-3-phosphate dehydrogenase; PGK, phosphoglycerate kinase; PGM, phosphoglycerate mutase; ENO, enolase; PK, pyruvate kinase; LDH, lactate dehydrogenase.

that detail the specific steps of the pathway. A reduction of these pathways in Chapter 4 is given in context of the mathematical model developed to describe their behavior. Table 2.3, which corresponds with Figure 2.1, lists the detailed reactions of glycolysis.

In many of the reactions listed in this thesis and other metabolic and non-metabolic reactions not listed, ATP exists as a cofactor. ATP, the main energy carrying compound for the body, is the result of glucose metabolism. In Figure 2.1, anaerobic

ENZYME (Enzyme Commission number and name) REACTION
HK, GK (EC 2.7.1.1 hexokinase, EC 2.7.1.2 glucokinase) ATP + glucose = ADP + glucose 6-phosphate
PHI (EC 5.3.1.9 phosphohexose isomerase) glucose 6-phosphate = fructose 6-phosphate
PFK (EC 2.7.1.11 phosphofructose kinase) ATP + fructose 6-phosphate = ADP + fructose 1,6-bisphosphate
ALD (EC 4.1.2.13 aldolase) fructose 1,6-bisphosphate = glycerone phosphate + glyceraldehyde 3-phosphate
PTI (EC 5.3.1.1 phosphotriose isomerase) glycerone phosphate = glyceraldehyde 3-phosphate
GPD (EC 1.2.1.12 glyceraldehyde 3-phosphate dehydrogenase) glyceraldehyde 3-phosphate + phosphate + NAD+ = 1,3-bisphosphoglycerate + NADH + H+
PGK (EC 2.7.2.3 phosphoglycerate kinase) ADP + 1,3-bisphosphoglycerate = ATP + 3-phospho-glycerate
PGM (EC 5.4.2.1 phosphoglycerate mutase) 3-phospho-glycerate = 2-phospho-glycerate
ENO (EC 4.2.1.11 enolase) 2-phospho-glycerate = phosphoenolpyruvate + H2O
PK (EC 2.7.1.40 pyruvate kinase) ADP + phosphoenolpyruvate = ATP + pyruvate
LDH (EC 1.1.1.27 lactate dehydrogenase) pyruvate + NADH + H+ = lactate + NAD+

Table 2.3. Reactions of the Pathway of Glycolysis. Enzyme abbreviations correspond with those in Figure 2.1. For each reaction, the full enzyme name and Enzyme Commission number is listed as well as the full reaction with all substrates, products and cofactors.

glycolysis was included, that being from pyruvate to lactate. In Table 2.3, we see that the reaction catalyzed by lactate dehydrogenase, LDH, results in a molecule of NAD+. This NAD+ can act as substrate for the reaction catalyzed by glyceraldehyde 3-phosphate dehydrogenase, GPD, thus encouraging glycolysis to continue. Anaerobic glycolysis provides a net gain of two ATP molecules. Due to aldolase splitting fructose 1,6-bisphosphate into two separate compounds and phosphotriose isomerase converting one

of these compounds into the other, we see the stoichiometry of 2:1 for glucose: glyceraldehyde 3-phosphate. So though the glucokinase and phosphofructose kinase reactions use up one molecule each of ATP, PGK and PK both release one ATP resulting in 2 ATP molecules used to 4 ATP molecules released, or a net gain of 2 ATP molecules [10].

Anaerobic glycolysis is unable to keep up with the normal energetic demands of the body for long periods and we will see it is much more efficient to release energy through aerobic glycolysis. As this method requires oxygen, aerobic glycolysis is the preferred method of ATP

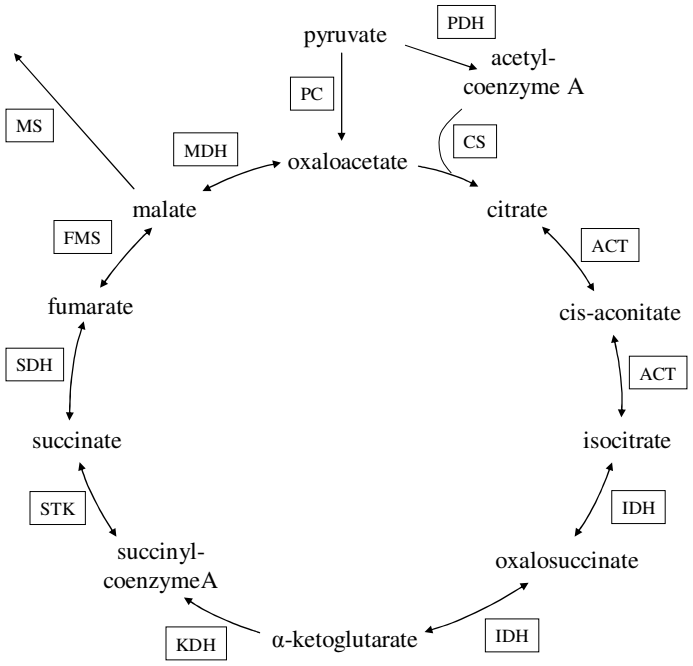

Figure 2.2. The Tricarboxylic Acid (TCA) Cycle. Enzymes catalyzing specific reactions are denoted in boxes next to the arrow of each corresponding reaction. Abbreviations are as follows: PC, pyruvate carboxylase; PDH, pyruvate dehydrogenase; CS, citrate synthase; ACT, aconitase; IDH, isocitrate dehydrogenase; KDH, α-ketoglutarate dehydrogenase; STK, succinate thiokinase; SDK, succinate dehydrogenase; FMS, fumarase; MDH, malate dehydrogenase; MS, malate shuttle.

production and is usually the most prominent method unless there is a sudden drop of oxygen concentration, such as during extreme exercise. Aerobic glycolysis occurs in the mitochondria and requires the presence of the tricarboxylic acid (TCA) cycle machinery. In Figure 2.1, an arrow shows continued metabolism of pyruvate through oxidation. This oxidative pathway is the entrance into the TCA cycle; its components are shown in Figure 2.2.

ENZYME (Enzyme Commission number and name) REACTION
PDH (EC 1.2.1.51 pyruvate dehydrogenase) pyruvate + CoA + NAD+ = acetyl-CoA + CO2 + NADH
PC (EC 6.4.1.1 pyruvate carboxylase) ATP + oxaloacetate = ADP + phosphoenolpyruvate + CO2
CS (EC 2.3.3.8 citrate synthase) ADP + phosphate + acetyl-CoA + oxaloacetate = ATP + citrate + CoA
ACT (EC 4.2.1.3 aconitase) (1) citrate = cis-aconitate + H2O; (2) cis-aconitate + H2O = isocitrate
IDH (EC 1.1.1.42 isocitrate dehydrogenase) (1) isocitrate + NAD+ = 2-oxoglutarate + CO2 + NADH + H+; (2) oxalosuccinate + NAD+ = 2-oxoglutarate + CO2 + NADH + H+
KDH (EC 1.2.7.3 α-ketoglutarate dehydrogenase complex) 2-oxoglutarate + CoA + NAD = succinyl-CoA + CO2 + NADH
STK (EC 6.2.1.5 succinate thiokinase) ADP + phosphate + succinyl-CoA = ATP + succinate + CoA
SDH (EC 1.3.5.1 succinate dehydrogenase) succinate + FAD = fumarate + FADH2
FMS (EC 4.2.1.2 fumarase) fumarate + H2O = malate
MDH (EC 1.1.1.37 malate dehydrogenase) malate + NAD+ = oxaloacetate + NADH + H+
MS (malate shuttle) transports malate across mitochondrial membrane

Table 2.4. Reactions of the Tricarboxylic Acid (TCA) Cycle. Enzyme abbreviations correspond with those in Figure 2.2. For each reaction, the full enzyme name and Enzyme Commission number is listed as well as the full reaction with all substrates, products and cofactors.

Though many of these reactions are reversible, the favored direction of this cycle is typically clockwise. In this direction, we can see in Table 2.4 that the reactions corresponding to IDH, KDH and MDH each release one molecule of NADH while the SDH reaction releases an FADH2. These molecules enter phosphorylative oxidation to form 3 ATP for each molecule of NADH and 2 ATP for one molecule of FADH2. Pyruvate kinase activity is reduced when the glycolytic pathway is up-regulated. Assuming that pyruvate resulting from glycolytic activity enters the TCA cycle as acetyl-CoA, then one glucose molecule entering glycolysis will result in two molecules of acetyl-CoA which allows for two turns of the TCA cycle. We saw previously that there is a net gain of 2 ATP molecules during glycolysis from glucose to pyruvate. Along with the 6 NADH and 2 FADH2 released during 2 turns of the TCA cycle and 2 NADH released during conversion of 2 molecules of pyruvate to 2 of acetyl-CoA by PDH, we now have: 2 ATP + 8 NADH + 2 FADH2 = 2 ATP + 24 ATP + 4 ATP = 30 ATP. In the glycolytic pathway from glucose to pyruvate, the 2 molecules of NADH released during the GPD reaction yield 2 ATP molecules each through oxidative phosphorylation resulting in a total of 4 ATP molecules. So in total, one glucose molecule completing the aerobic glycolysis pathway will release 34 ATP molecules, 32 more ATP molecules than through anaerobic glycolysis [10]. This magnifies the importance of maintaining blood glucose levels for those cells which lack mitochondria and thus lack the ability to produce ATP through oxidative phosphorylation. The TCA cycle is a common ‘intersection’ of glucose, amino acid and fat metabolism.

2.3.2 Gluconeogenesis

When blood glucose levels drop below a certain threshold, the metabolic pathways in certain tissues are regulated so that alternate metabolic fuels such as amino acids, fats and ketone bodies are used to complement glycolysis in order to preserve

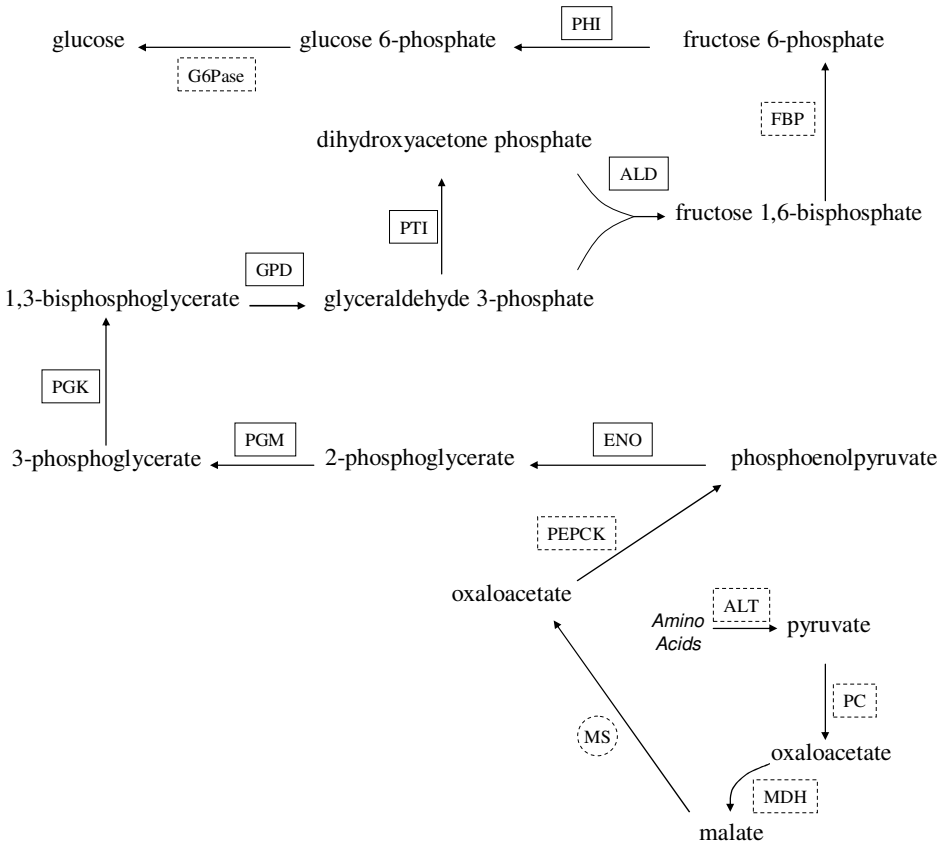

Figure 2.3. The Complete Pathway of Gluconeogenesis. Enzymes catalyzing specific reactions are denoted in boxes next to the arrow of each corresponding reaction. Enzymes with dashed outlines are specific to glycolysis while those with outlined in solid are also found in gluconeogenesis. Abbreviations are as follows: G6Pase, glucose 6-phosphatase; PEPCK, phosphoenolpyruvate carboxykinase; MDH, malate dehydrogenase; MS, malate shuttle; TCA, tricarboxylic acid; ALT, alanine transaminase; PC, pyruvate carboxylase.

ENZYME (Enzyme Commission number and name) REACTION
ALT (EC 2.6.1.2 alanine transaminase) alanine + α-ketoglutarate = pyruvate + glutamate
PC (EC 6.4.1.1 pyruvate carboxylase) ATP + oxaloacetate = ADP + phosphoenolpyruvate + CO2
MS (malate shuttle) transports malate across mitochondrial membrane
MDH (EC 1.1.1.37 malate dehydrogenase) malate + NAD+ = oxaloacetate + NADH + H+
PEPCK (EC 4.1.1.49 PEP carboxykinase) ATP + oxaloacetate = ADP + phosphoenolpyruvate + CO2
ENO (EC 4.2.1.11 enolase) phosphoenolpyruvate + H2O = 2-phospho-glycerate
PGM (EC 5.4.2.1 phosphoglycerate mutase) 2-phospho-glycerate = 3-phospho-glycerate
PGK (EC 2.7.2.3 phosphoglycerate kinase) ATP + 3-phospho-glycerate = ADP + 1,3-bisphosphoglycerate
GPD (EC 1.2.1.12 glyceraldehyde 3-phosphate dehydrogenase) 1,3-bisphosphoglycerate + NADH + H+ = glyceraldehyde 3-phosphate + phosphate + NAD+
PTI (EC 5.3.1.1 phosphotriose isomerase) glyceraldehyde 3-phosphate = glycerone phosphate
ALD (EC 4.1.2.13 aldolase) glycerone phosphate + glyceraldehyde 3-phosphate = fructose 1,6-bisphosphate
FBP (EC 3.1.3.11 fructose-1,6-bisphosphatase) fructose 1,6-bisphosphate + H2O = fructose 6-phosphate + phosphate
PHI (EC 5.3.1.9 phosphohexose isomerase) fructose 6-phosphate = glucose 6-phosphate
G6Pase (EC 3.1.3.9 glucose-6-phosphatase) glucose 6-phosphate + H2O = glucose + phosphate

Table 2.5. Reactions of the Pathway of Gluconeogenesis. Enzyme abbreviations correspond with those in Figure 2.3. For each reaction, the full enzyme name and Enzyme Commission number is listed as well as the full reaction with all substrates, products and cofactors.

glucose for those tissues that rely solely on glucose for energy production. Along with switching over to using alternate fuels, some tissues also increase the rate at which gluconeogenesis occurs. Gluconeogenesis is the metabolic pathway by which amino

acids are used to form glucose and occurs in select tissues, mainly liver and kidney. The complete pathway of gluconeogenesis can be seen in Figure 2.3.

Regulation of the reactions in these pathways causes a switching to occur so that one is emphasized more than the other depending on the state of glucose intake of the system, futile cycling occurs since each pathway still has some amount of flux no matter the state of glucose intake. Some futile cycling occurs but it has been observed that the net flux of these pathways is what switches in response to an increase or decrease of blood glucose levels. Though observation of futile cycling of these two pathways has been documented, there is still much unknown about costs and benefits to the system as a result of this phenomenon.

2.3.3 Glycogenesis

As glycogen is the stored form of glucose, we will consider glucose the starting substrate when considering the pathway of glycogenesis, leading to the formation of glycogen. The first step in this pathway is the same as that of glycolysis, hexokinase or glucokinase converting glucose to glucose 6-phosphate. Glucose 6-phosphate is an interesting metabolite to study as multiple pathways connect through this compound. For simplification purposes Only four of these pathways are considered: glycolysis, gluconeogenesis, glycogenesis, and glycogenolysis. One neglected pathway worth mentioning is the pentose phosphate pathway which is an alternate pathway for the conversion of glucose 6-phosphate to phosphoenolpyruvate, a participant in glycolysis and gluconeogenesis. Another noteworthy pathway to mention is that from glucose 6-

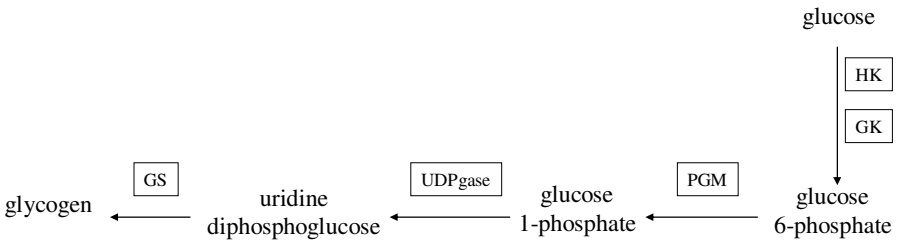

Figure 2.4. The Complete Pathway of Glycogenesis. Enzymes catalyzing specific reactions are denoted in boxes next to the arrow of each corresponding reaction. Abbreviations are as follows: HK, hexokinase; GK, glucokinase; PGM, phosphoglucomutase; UDPgase, uridine diphosphoglucose pyrophosphorylase; GS, glycogen synthase.

ENZYME (Enzyme Commission number and name) REACTION
HK, GK (EC 2.7.1.1 hexokinase, EC 2.7.1.2 glucokinase) ATP + glucose = ADP + glucose 6-phosphate
PGM (EC 5.4.2.2 phosphoglucomutase) glucose 6-phosphate = glucose 1-phosphate
UDPgase (EC 2.7.7.9 UDP glucose pyrophosphorylase) UTP + glucose 1-phosphate = diphosphate + UDP-glucose
GS (EC 2.4.1.11 glycogen synthase) UDP-glucose + (1,4-glucosyl)n = UDP + (1,4-glucosyl)(n+1)

Table 2.6. Reactions of the Complete Pathway of Glycogenesis. Enzyme abbreviations correspond with those in Figure 2.4. For each reaction, the full enzyme name and Enzyme Commission number is listed as well as the full reaction with all substrates, products and cofactors.

phosphate to glycerol. Although these pathways are not considered here it is important to keep in mind the complexity of this system in its true environment. The rate at which glycogenesis occurs increases when glucose levels are high. In order for glycogen to

form, an initial or starter compound called glycogenin is needed. The glucose partitions of intermediary compounds in this pathway bind to glycogenin and then to each other resulting in a branched chain-like structure of glucose molecules. A diagram of glycogenolysis is shown in Figure 2.3.

2.3.4 Glycogenolysis

Using glycogen as a source of glucose is the fastest pathway to regulate when blood glucose levels drop and a supply of glucose is needed immediately. Just as gluconeogenesis did not use the same pathway as glycolysis in reverse, glycogenolysis does not simply reverse the reactions in glycogenesis. One less step is needed for glycogenolysis as uridine diphosphoglucose is not a component of this pathway. Figure 2.4 shows details the glycogenolytic pathway.

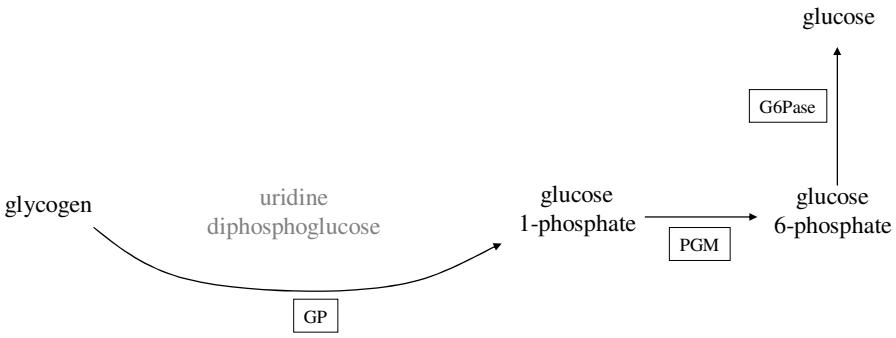

Figure 2.5. The Complete Pathway of Glycogenolysis. Enzymes catalyzing specific reactions are denoted in boxes next to the arrow of each corresponding reaction. Abbreviations are as follows: G6Pase, glucose 6-phosphatase; PGM, phosphoglucomutase; GP, glycogen phosphorylase.

In this pathway, not only are different enzymes required but glycogen is directly converted to glucose-1-phosphate and the step involving uridine diphosphoglucose is not needed. The only enzyme that this pathway has in common with glycogenesis is phosphoglucomutase. The activation of glycogen synthase and glycogen phosphorylase is tightly regulated by complex circuit of enzymes. This regulatory circuit will be described in more detail in Chapter 3.

ENZYME (Enzyme Commission number and name) REACTION
GP (EC 2.4.1.1 glycogen phosphorylase) ATP + glucose = ADP + glucose 6-phosphate
PGM (EC 5.4.2.2 phosphoglucomutase) glucose 1-phosphate = glucose 6-phosphate
G6Pase (EC 3.1.3.9 glucose-6-phosphatase) glucose 6-phosphate + H2O = glucose + phosphate

Table 2.7. Reactions of the Pathway of Glycogenolysis. Enzyme abbreviations correspond with those in Figure 2.5. For each reaction, the full enzyme name and Enzyme Commission number is listed as well as the full reaction with all substrates, products and cofactors.

2.3.5 Lipogenesis

Lipogenesis is a very complex process involving numerous conversion steps. The enzymes involved in this process are listed in Table 2.8.

ENZYME (Enzyme Commission number and name) REACTION
CL (EC 2.3.3.8 ATP citrate lyase) ATP + citrate + CoA = ADP + phosphate + acetyl-CoA + oxaloacetate
AC (EC 6.4.1.2 acetyl-CoA carboxylase) ATP + acetyl-CoA + HCO3- = ADP + phosphate + malonyl-CoA
ACT (EC 2.3.1.38 acetyl transacylase) acetyl-CoA + [acyl-carrier protein] = CoA + acetyl-[acyl-carrier protein]
MT (EC 2.3.1.39 malonyl transacylase) malonyl-CoA + [acyl-carrier protein] = CoA + malonyl-[acyl-carrier protein]
KAS (EC 2.3.1.41 3-ketoacyl synthase) acyl-[acyl-carrier protein] + malonyl-[acyl-carrier protein] = 3-oxoacyl-[acyl-carrier protein] + CO2 + [acyl-carrier protein]
KAR (EC 1.1.1.100 3-ketoacyl reductase) 3-oxoacyl-[acyl-carrier protein] + NADPH + H+ = 3-hydroxyacyl-[acyl-carrier protein] + NADP+
HT (EC 4.2.1.58 hydratase) 3-hydroxybutanoyl-[acyl-carrier protein] = but-2-enoyl-[acyl-carrier protein] + H2O
ER (EC 1.3.1.10 enoyl reductase) CoA + 3-oxoacyl-CoA = acyl-CoA + acetyl-CoA
after cycling through last 4 reactions: **TE** (EC 3.1.2.14 thioesterase) oleoyl-[acyl-carrier protein] + H2O = [acyl-carrier protein] + oleate

Table 2.8. Reactions of the Pathway of Lipogenesis. For each reaction, the full enzyme name and Enzyme Commission number is listed as well as the full reaction with all substrates, products and cofactors.

2.3.6 Lipolysis

It is common knowledge that exercise is effective in reducing the amount of fat in the body. The properties of one's diet also assists in reducing fat. Fat from the diet directly is stored as fat in the body. Excess glucose is also converted to and stored as fat.

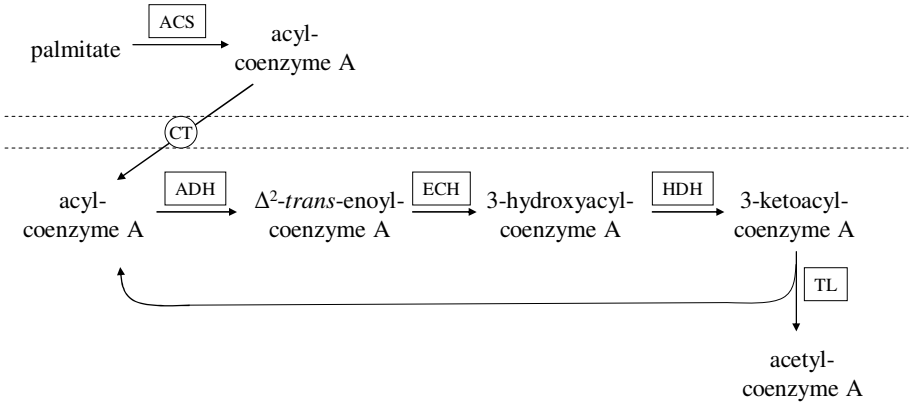

Figure 2.6. The Complete Pathway of Lipolysis. Enzymes catalyzing specific reactions are denoted in boxes next to the arrow of each corresponding reaction. Abbreviations are as follows: ACS, acyl-coenzyme A synthetase; CT, carnitine transporter; ADH, acyl- coenzyme A dehydrogenase; ECH, Δ^2-trans-enoyl-coenzyme A hydratase; HDH, 3-hydraoxyacyl-coenzyme A dehydrogenase; TL, thiolase.

When glucose levels drop, the rate at which fat stores break down is increased as they will serve to pick up some of the slack for energy production due to a lack of glucose. Fats are unable to enter the gluconeogenic pathway to form glucose. This is discussed later with the roles of various tissues within metabolism. Fats cannot be made into glucose. However, fats are able to, through lipolysis, be metabolized to acetyl-CoA which is oxidized through the TCA cycle, providing necessary substrate for the respiratory chain, producing energy. So fats do provide energy for the tissue in which they reside but are unable to provide energy to other tissues. Fats are transported to other tissues and provide energy to use amino acids as a source of glucose in those tissues. As glucose is plentiful during feeding, lipolysis occurs as a slow rate as fats are not needed. As glucose levels drop, we see a rise in the rate of lipolytic reactions. Figure 2.7 and table 2.9 detail the steps of lipolysis.

ENZYME (Enzyme Commission number and name) REACTION
ACS (EC 6.2.1.3 acyl-CoA synthetase) ATP + a long-chain carboxylic acid + CoA = AMP + diphosphate + an acyl-CoA
CT (Carnitine Transporter) transports acyl-CoA across the mitochondrial membrane
ADH (EC 1.3.99.3 acyl-CoA dehydrogenase) acyl-CoA + acceptor = 2,3-dehydroacyl-CoA + reduced acceptor
ECH (EC 4.2.1.17 Δ^2-enoyl-CoA hydratase) trans-2(or 3)-enoyl-CoA + H2O = 3-hydroxyacyl-CoA
HDH (EC 1.1.1.35 3-hydroxyacyl-CoA dehydrogenase) 3-hydroxyacyl-CoA + NAD+ = 3-oxoacyl-CoA + NADH + H+
TL (EC 2.3.1.16 3-ketoacyl-CoA thiolase) CoA + 3-oxoacyl-CoA = acyl-CoA + acetyl-CoA

Table 2.9. Reactions of the Pathway of Lipolysis. Enzyme abbreviations correspond with those in Figure 2.7. For each reaction, the full enzyme name and Enzyme Commission number is listed as well as the full reaction with all substrates, products and cofactors.

2.3.7 Ketogenesis

Just as fats are able to provide an alternate fuel source in a time of 'glucose drought', ketone bodies are also able to play this role. As Figure 2.8 shows, we see that ketogenesis consists of a few steps and is tightly connected to the end result of lipolysis. Whereas fats only provide energy to the tissue in which the breakdown of these fats occur, ketone bodies can be thought of as an extension of fat breakdown, an extension in that ketone bodies are transported to other tissues where they are oxidized and enter the TCA cycle making substrate for the respiratory chain and thus providing energy for those tissues. Only those cells with mitochondria are able to benefit from ketone bodies.

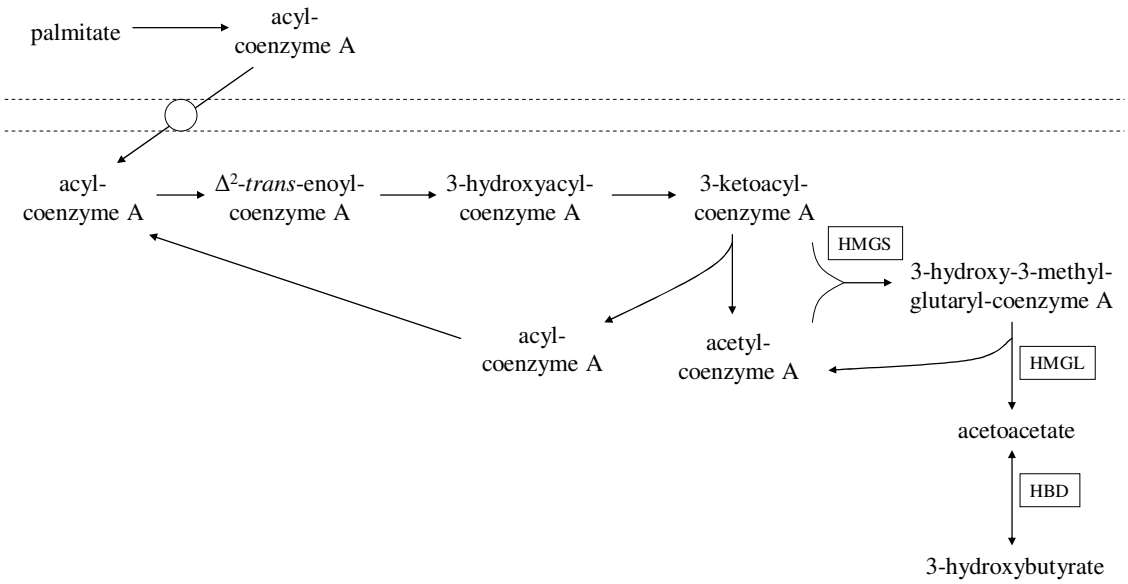

Figure 2.7. The Complete Pathway of Ketogenesis. Enzymes catalyzing specific reactions are denoted in boxes next to the arrow of each corresponding reaction. Abbreviations are as follows: ACS, acyl-coenzyme A synthetase; CT, carnitine transporter; ADH, acyl- coenzyme A dehydrogenase; ECH, Δ^2-trans-enoyl-coenzyme A hydratase; HDH, 3-hydraoxyacyl-coenzyme A dehydrogenase; TL, thiolase; FAO, fatty acid oxidase.

ENZYME (Enzyme Commission number and name) REACTION
HMGS (EC 2.3.3.10 HMG-CoA synthase) acetyl-CoA + H2O + acetoacetyl-CoA = 3-hydroxy-3-methylglutaryl-CoA + CoA
HMGL (EC 4.1.3.4 hydroxymethylglutaryl-CoA lyase) 3-hydroxy-3-methylglutaryl-CoA = acetyl-CoA + acetoacetate
HBD (EC 1.1.1.30 3-hydroxybutyrate dehydrogenase) acetoacetate + NADH + H+ = 3-hydroxybutanoate + NAD+

Table 2.10. Reactions of the Pathway of Ketogenesis. Enzyme abbreviations correspond with those in Figure 2.8. For each reaction, the full enzyme name and Enzyme Commission number is listed as well as the full reaction with all substrates, products and cofactors.

2.4 Regulation of the Metabolic System

The types of regulation currently in the model are allosteric regulation, or the physical modification of an enzyme which affects its level of activity, and hormonal regulation, in which signal transduction resulting from the binding of hormones to cell surface receptors affects the rate of a biochemical reaction. Transcriptional regulation affects the level of enzyme present thus affecting the rate of activity of the corresponding enzyme. This regulation is not currently present in this model but is discussed more in the section of future direction for this model.

2.4.1 Allosteric Regulation

Enzymes initiate allosteric regulation by binding to a protein and increasing or decreasing the activity of a certain reaction involving that protein. The modeling of this type of regulation is discussed in Chapter 4.

2.4.2 Hormonal Regulation

Insulin and glucagon are two hormones secreted from the pancreas that are vital for functional regulation of the metabolic system. Many published mathematical models describe the relationship between glucose, insulin and glucagon [5-8]. While demonstrating the dependency of glucose and these two hormones, these models provide a limited inclusion of the mechanisms but which this dependency exists. My proposed model includes many mechanisms for which hormonal regulation stabilizes blood glucose levels such as insulin-dependent glucose transporters and hormonal-dependent

regulation of glycogen. To compensate for the lack of a pancreatic component in my model, glucose directly regulates insulin and glucagon within the blood. Glucose increases the rate of insulin secretion while increasing the rate of glucagon degradation [14, 15].

$$\frac{d[B\_ins]}{dt} = k_{ins} + \frac{k_{1ins}\,[B\_gluc]^{ni}}{k_{mIns}{}^{ni} + [B\_gluc]^{ni}} - k_{d\_Bins}\,[B\_ins]$$

$$\frac{d[B\_glucgn]}{dt} = k_{glucgn} - \frac{k_{1glucgn}\,[B\_gluc]^{ng}}{k_{mGlgn}{}^{ng} + [B\_gluc]^{ng}} - k_{d\_Bglucgn}\,[B\_glucgn]$$

Insulin and glucagon were each given a level of basal secretion as well as a rate of decay. The blood insulin concentration within the model, [*B_Ins*], stays between .7 * 10^{-6} mM and 1.3 * 10^{-6} mM (refs) while the blood glucagon concentration, [*B_Glucgn*], stays between 3 * 10^{-8} mM and 5 * 10^{-8} mM [16, 17]. By making parameters k_{mIns} = 8 and $k_{mGlucgn}$ = 8, hormone concentrations approach their half max average value ([*B_Ins*] = 1 * 10^{-6} mM and [*B_Glucgn*] = 5 * 10^{-8} mM) as blood glucose levels approach 8 mM. Hill coefficients, *ni* and *ng*, were added to increase switch-like behavior.

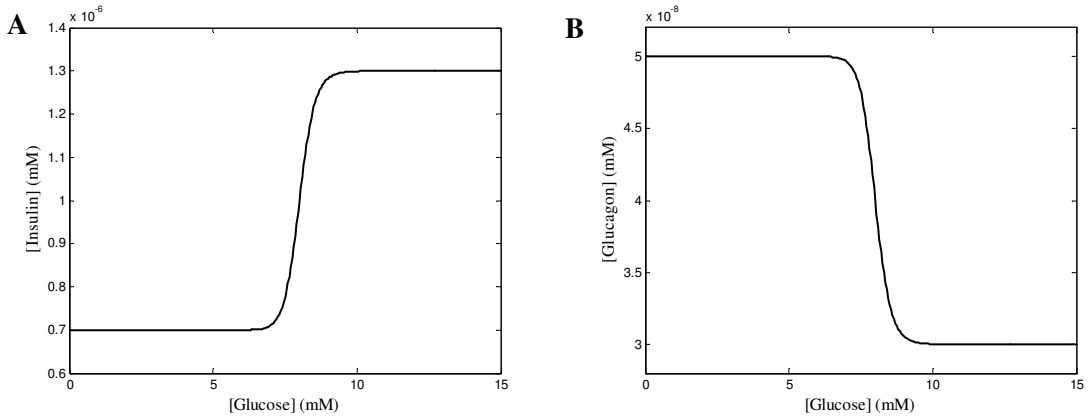

Figure 2.8. Insulin and Glucagon in Relation to Glucose. Blood insulin levels as a function of glucose is shown in **A** while blood glucose levels as a function of glucose is shown in **B**.

Rates affected by the presence of insulin or glucagon are multiplied by factors. The values of these factors for insulin regulation in the model range between 0 and 1 and most are set to reach a value of $\frac{1}{2}$ when [*B_Ins*] reaches 1 * 10^{-6} mM (model parameter k_{Dins}) while the remaining multiplicative factors reach a value of $\frac{1}{2}$ when [B_Ins] reaches 0.75 * 10^{-6} mM (model parameter k_{Dins2}). Values of multiplicative factors for glucagon regulation in the model also range between 0 and 1 and all are set to reach a value of $\frac{1}{2}$ when [B_Glucgn] reaches 4 * 10^{-8} mM (model parameter $k_{Dglucgn}$).

$$v_{L3} = \frac{k_{L3}\,[g6p]}{k_{mL3} + [g6p]} \left(1 + \frac{[B\_ins]^{ep2}}{k_{Dins}{}^{ep2} + [B\_ins]^{ep2}}\right) \left(\frac{k_{Dglucgn}{}^{en1}}{k_{Dglucgn}{}^{en1} + [B\_glucgn]^{en1}}\right)$$

The above rate (for conversion of glucose 6-phosphate to phosphoenolpyruvate) gives examples of both positive regulation by insulin and negative regulation by glucagon. This rate was designed so that in the absence of hormones ([*B_Ins*] = 0 and [*B_Glucgn*] = 0), the reaction will have a rate of:

$$v_{L3} = \frac{k_{L3}\,[g6p]}{k_{mL3} + [g6p]}$$

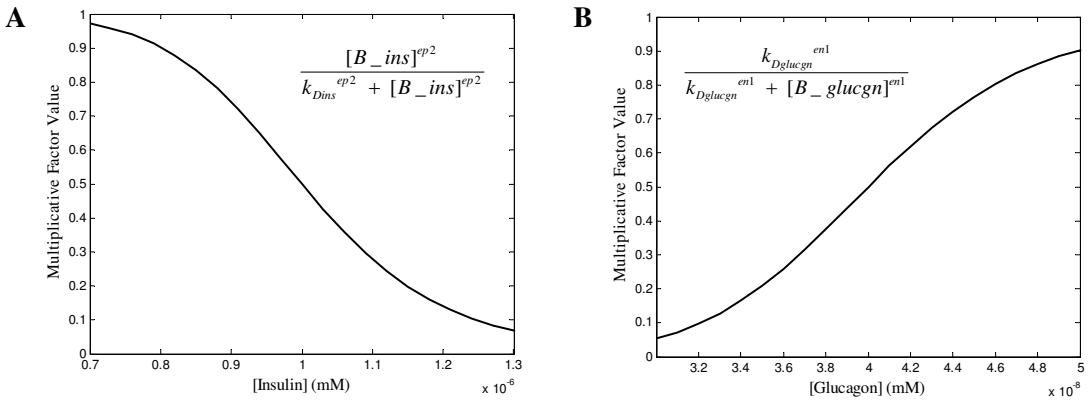

Figure 2.9. Regulatory Multiplicative Factors. The value of a negative regulatory multiplicative factor dependent on blood insulin levels is shown in **A**. Figure **B** shows the values of a multiplicative factor which determine negative regulation by blood glucagon levels. Both of these factors are present in the rate v_{L3}.

cAMP is a secondary signal for hormonal regulation. Through signal transduction, insulin increases the rate at which cAMP is degraded [10] thus having a negative affect on cAMP concentration levels. Conversely, through signaling glucagon increases the amount of cAMP present. For the model, concentration levels of cAMP were designed with similar features as insulin and glucagon growth and decay such as staying within a specified range and producing switch-like behavior for regulation

purposes as glucose levels reach 8 mM. cAMP is kept with the range of 2.4 * 10^{-6} mM and 4.3 * 10^{-6} mM [10, 16, 17] and the multiplicative factor of reactions regulated by cAMP equal $\frac{1}{2}$ when $[cAMP] = 1 * 10^{-5.5}$.

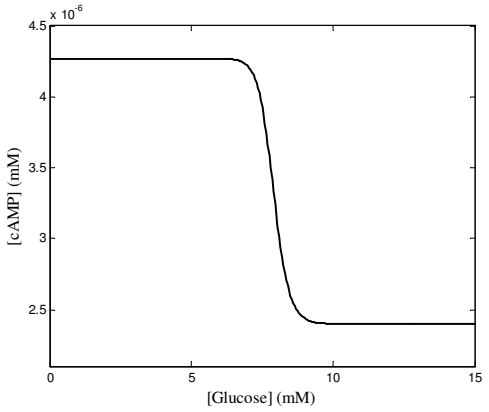

Figure 2.10. cAMP in Relation to Glucose. Liver cAMP concentration level as a function of glucose.

CHAPTER 3

Glycogen Regulatory Circuit

3.1 From Glucose to Glycogen and Back

As the main purpose of the regulation of glycogenesis and glycogenolysis is to maintain blood glucose levels, the pathway in which glucose is converted into glycogen and back should be outlined before detailing the structure of the glycogen regulatory circuit. While glycogen stores are found mainly in liver and muscle, the purpose and regulation of these stores differs. This thesis will focus on the regulation of hepatic glycogen as this store of glycogen is used to maintain blood glucose levels while muscle glycogen stores are used to provide immediate energy for the muscles in which the glycogen is stored. To simplify this system, the processes involved in creating and using glycogen stores will be considered for a single, well-mixed cell.

Glucose is passively transported across the hepatic cell membrane through the glucose transporter GLUT2 [9, 10]. Either hexokinase or glucokinase converts glucose to glucose 6-phosphate by adding a phosphate group to the sixth carbon molecule of glucose. This phosphate group is switched with another phosphate group in a bisphosphate molecule which is then attached to the first carbon molecule by phosphoglucomutase (EC 5.4.2.2) to form glucose 1-phosphate. Uridine diphosphoglucose pyrophosphorylase (EC 2.7.7.9) converts glucose 1-phosphate to uridine diphosphoglucose, UDP-glucose. Glycogen synthase (EC 2.4.1.11) then transfers

the glucose partition of UDP-glucose onto an existing structure of glycogen. The first enzyme in the pathway of glycogenolysis is glycogen phosphorylase (EC 2.4.1.1) which combines a glucose residue from glycogen with a phosphate group, forming glucose 1-phosphate. Phosphoglucomutase, the enzyme which converted glucose 6-phosphate to glucose 1-phosphate catalyzes a reversible reaction so that it also converts glucose 1-phosphate back to glucose 6-phosphate. Glucose 6-phosphatase (EC 3.1.3.9) then converts glucose 6-phosphate back to glucose which is transported from the liver through GLUT2. Figures portraying the pathways of glycogenesis and glycogenolysis pathways were shown in Figure 2.4 and Figure 2.5.

In order to study the regulatory circuit behind the activation of glycogen synthase and glycogen phosphorylase, this system has been slightly simplified by deleting three steps from these pathways. Glucose 1-phosphate and UDP-glucose have been removed and the levels of blood glucose and liver glucose are assumed to be indistinguishable. These changes are reasonable as glycogen synthase and phosphorylase are the rate limiting enzymes in the pathways between glucose 6-phosphate and glycogen. These changes leave three metabolites: glucose, glucose 6-phosphate and glycogen.

This is an open system since glucose enters through feeding and exits as the liver adapts to providing glucose during low blood glucose levels. Flux in and out of the glucose 6-phosphate occurs through the glycolytic and gluconeogenic pathways. Glycolysis is the pathway by which the cell, through a number of processes, converts glucose to form ATP, providing energy for cellular functions. Gluconeogenesis is the pathway in which amino acids are eventually used to make glucose and is fueled by the breakdown of free fatty acids.

It is known that glucose increases the rate at which insulin is secreted from the beta-cells in the pancreas and also acts as an inhibitor for the secretion of glucagons from the pancreatic alpha-cells [14, 15]. Insulin and glucagon both bind to respective receptors and initiate signal transduction to regulate metabolic activity within hepatocytes. Though the regulatory hormones insulin and glucagon originate from the pancreas, for simplification purposes, it will be assumed that these are solely located in the blood. A secondary signal which becomes a main regulator of glycogenic activity is cAMP. The production of this compound is increased by the signaling from glucagon while insulin signals an increase in the decay of cAMP [10].

3.2 Circuit Architecture

Glycogen synthase and glycogen phosphorylase both undergo covalent modification which determines whether each enzyme is in an active or inactive state. cAMP initiates phosphorylation of a number of enzymes structured in a cascade which eventually results in the phosphorylation, or the addition of a phosphate group, to glycogen synthase and glycogen phosphorylase. Unlike glycogen phosphorylase which is activated while in the phosphorylated state, glycogen synthase is activated while in the unphosphorylated state. By cAMP signaling the phosphorylation of these enzymes simultaneously, it results in a shifting of the net glycogenic flux by regulating two pathways, glycogenesis and glycogenolysis, through one cascade structure. This structure begins with cAMP binding to cAMP-dependent protein kinase, or protein kinase A, releasing the catalytic subunit of protein kinase A. This subunit phosphorylates phosphorylase kinase which activates this enzyme. When activated, this enzyme

catalyzes the phosphorylation of both glycogen synthase and glycogen phosphorylase. The catalytic subunit of protein kinase A also initiates phosphorylation of glycogen synthase but not of glycogen phosphorylase. Protein phosphatase 1 dephosphorylates glycogen synthase, glycogen phosphorylase and phosphorylase kinase. A diagram for this cascade is shown in Figure 3.1.

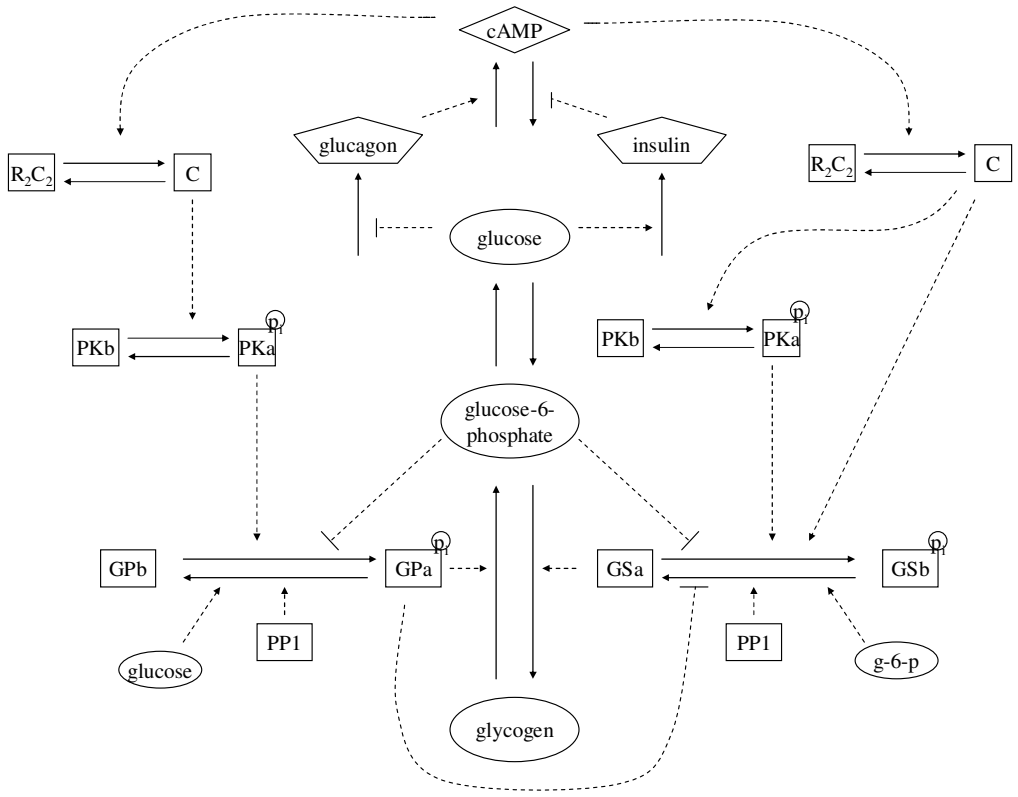

Figure 3.1. Glycogen Regulatory Circuit. The conversion between glucose, glucose-6-phosphate and glycogen is shown along with the cascade of enzymes that regulate this conversion. The hormones insulin and glucagon, regulated by glucose, are key regulators of this enzyme cascade. cAMP, cyclic adenosine monophosphate; R_2C_2, cAMP dependent protein kinase; C, R_2C_2 catalytic subunit; PKb, inactive phosphorylase kinase; PKa, active phosphorylase kinase; GPb, inactive glycogen phosphorylase; GPa, active glycogen phosphorylase; GSb, inactive glycogen phosphorylase; GSa, active glycogen phosphorylase; P, phosphate; g-6-p, glucose-6-phosphate; PP1, protein phosphatase 1.

CHAPTER 4

Mathematical Model

4.1 Enzyme Kinetics

Enzymes are proteins that act as catalysts for biochemical reactions. The rate of reaction is dependent on the amount of substrate present and the rate constant specific to that reaction. The value of a rate constant can sometimes be determined experimentally and often depends on multiple factors such as the pH level of the environment. The current model uses a combination of mass action kinetics and Michaelis-Menten kinetics [18] to mathematically describe the rates of the chemical reactions involved. This section outlines both types of kinetics.

4.1.1 Mass Action Kinetics

The theory of mass action kinetics is based on the concept that the rate of a chemical reaction is dependent on the probabilities of the molecules necessary for that reaction to occur to be present together in the same proximity. These probabilities are assumed to be independent and so the rate will be the product of the relevant concentrations for the reaction. As an example, for the basic conversion of molecule A to molecule B, $A \rightarrow B$, the rate can be approximated by a rate constant times the amount of

[A] present, or $v_1 = k_1 [A]$, where v_1 is the rate of the reaction and k_1 is a first order rate constant. Below are a few more examples of this theory:

1) $A + A \rightarrow B$, $v_1 = k_1 [A] [A] = k_1 [A]^2$, k_1 is second order

2) $A + B \rightarrow C$, $v_1 = k_1 [A] [B]$, k_1 is second order

In building an ODE model, these mathematical descriptions are then used to describe the rate of change of a concentration. For example, in the second reaction above, [A] and [B] change in a negative manner, each losing one unit of mass and while one unit of mass is being added to [C]. A system of ODEs to describe the change in mass of this reaction would be:

$$\frac{d[A]}{dt} = - k_1 [A] [B]$$

$$\frac{d[B]}{dt} = - k_1 [A] [B]$$

$$\frac{d[C]}{dt} = k_1 [A] [B]$$

4.1.2 Michaelis-Menten Kinetics

Mass action kinetics assumes that the rate is directly proportional to the probabilities that relevant concentrations will be present. In the late nineteenth century, Brown noted that enzyme catalyzed reactions did not follow second-order kinetics. A few years earlier, the formation of an enzyme-substrate complex during a reaction was

discovered by O'Sullivan and Tompson. While Brown did the initial work on describing the kinetics of this enzyme-substrate complex, Henri went on to describe these kinetics in a more mathematical sense and in 1913, Michaelis and Menten introduced their well-known equation [18]. Substrate *S* and enzyme *E* bind to form the substrate-enzyme complex *SE* before the enzyme dissociates and product *P* is released. The formation of *SE* is reversible while the dissociation of *E* and *P* is irreversible.

$$S + E \underset{k_{-1}}{\overset{k_1}{\rightleftharpoons}} SE \xrightarrow{k_2} E + P$$

Enzyme *E* is found either in free form or in the substrate-enzyme complex, *SE*. The total amount of enzyme *E* is:

$$[E]_T = [SE] + [E]$$

It is assumed that [*SE*] reaches steady state.

$$\frac{d[SE]}{dt} = k_1 [S] [E] - (k_{-1} + k_2) [SE] = 0,$$

By substituting $[E] = [E]_T - [SE]$,

$$k_1 [S] ([E]_T - [SE]) - (k_{-1} + k_2) [SE] = 0$$

Solving for [*SE*] yields

$$[SE] = \frac{k_1 [S] [E]_T}{k_1 [S] + k_{-1} + k_2}$$

Dividing the numerator and denominator by k_1 gives

$$[SE] = \frac{[S] [E]_T}{[S] + \frac{k_{-1} + k_2}{k_1}}$$

The rate limiting step for this process is the dissociation of the enzyme and release of product *P*. The rate of this reaction is given by:

$$v = k_2 [SE]$$

The rate of the irreversible reaction converting [*SE*] to [*E*] + [*P*] becomes

$$v = k_2[SE] = \frac{k_2 [E]_T[S]}{[S] + \frac{k_{-1} + k_2}{k_1}}$$

This method of modeling an enzyme-catalyzed reaction is more commonly written as:

$$v = \frac{V_{\max}[S]}{K_m + [S]}$$

where $K_m = \frac{k_{-1} + k_2}{k_1}$ is known as the Michaelis-Menten constant and $V_{\max} = k_2 [E]_T$ is the maximum reaction rate using the total amount of enzyme. This equation provides an approximation for the initial rates of biochemical reactions. As [*S*] goes to zero, the velocity also goes to zero. As [*S*] grows, *v* approaches an asymptotic value of $v = k_2 [E]_T$., or V_{max}. If $K_{eq} = [S]$, then $v_2 = \frac{1}{2} V_{max}$.

4.2 Literature Review

While many mathematical models exist for various structures and pathways within the metabolic system, these models have been studied in isolation from the rest of this system. As technology has allowed us to collect vast data on specific reactions, we have been able to look more closely at these pathways but need to be careful to not neglect the big picture that enfolds from metabolism. While a whole physiological model

of metabolism has yet to be offered, two papers propose models for the glycogen regulatory circuit, one determining steady state behavior and the other time dependent behavior.

Steady state properties were studied comparing results of this local system in the liver and in the muscle [19]. Though this circuit is very similar in both tissues, there are important differences that allow for separate function of the glycogen stores. This paper does not detail the differential equations used to model this system but does offer the resulting equations used for steady state analysis. The behavior of glycogen synthase and phosphorylase activation was found to be extremely switch-like in response to changing cAMP levels. Glycogen synthase was more sensitive than glycogen phosphorylase in the liver but the opposite was true for the muscle. Futile cycling was observed during a starved state but was not present while the system was in a fed state.

A 2-dimensional system of ordinary differential equations was introduced [20] to explore the dynamics of metabolic regulation of glycogen synthase and glycogen phosphorylase in response to particular levels of glucose concentration. During the fed state, a delayed effect on activation of glycogen synthase was found due to inhibition of synthase by activated glycogen phosphorylase. This inhibition by activated phosphorylase becomes insignificant when activated phosphorylase is below a certain threshold or where there is not a sufficient amount of glycogen as is the case with fasted animals (futile cycling is not mentioned in this paper). This model exhibits the need for an increase in glucose-6-phosphate and a decrease in glycogen synthase to activate 'glycogen synthase to significant levels'. It is the ratio of the synthase phosphatase to synthase kinase that determines the activation of glycogen synthase and this ratio is

controlled by levels of glucose-6-phosphate and activation glycogen phosphorylase. Although not observed thus far, the possibility of these enzymes exhibiting 'zero-order ultrasensitivity', operating in the domain where they are near saturation with respect to their substrate, was suggested.

4.3 Broad Contextual Model

Our first main goal for designing a contextual or whole-physiological model for the metabolic system was to capture the dynamical shift in concentration levels for the main metabolic fuels when the system is adapting to a fasted state from a fed state. The

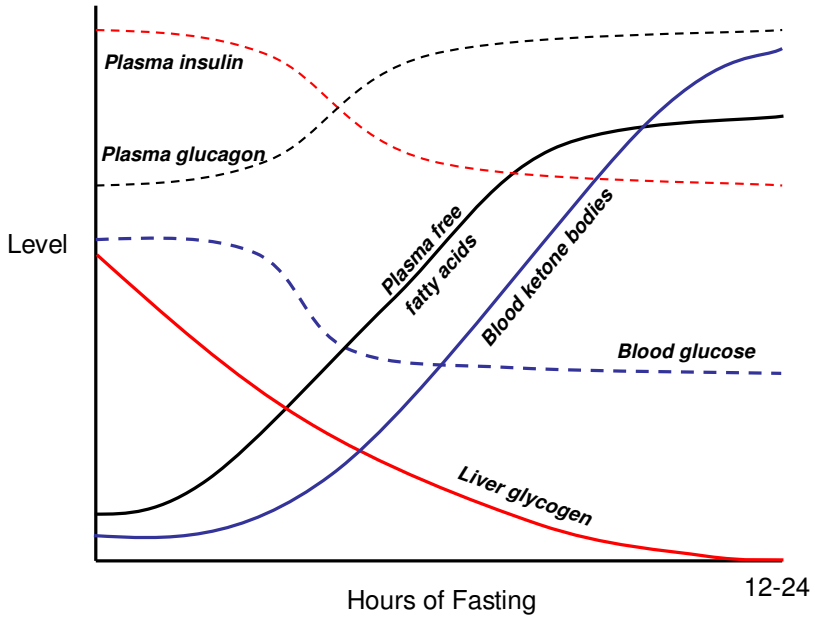

Figure 4.1. Effects of Fasting. Blood glucose, liver glycogen and plasma insulin levels drop as plasma glucagon, free fatty acids and blood ketone bodies levels increase in response to a fasted state.

relative change in levels of blood glucose, liver glycogen, plasma free fatty acids, blood ketone bodies, plasma insulin and plasma glucagon are shown in Figure 4.1 (recreated from [10]).

As the system enters into fasting, blood glucose levels are stabilized for a brief period before decreasing to the loss of glucose influx from digestion. Liver glycogen is depleted as it is being used to form glucose to stabilize the blood glucose levels. As the amount of hepatic glycogen decreases, plasma free fatty acid levels rise reflecting the breakdown of fats from fat tissue and transport of these fats in the bloodstream to the liver and other tissues to be an alternate metabolic fuel. There is also a rise in the level of ketone bodies in the blood as they are a byproduct of lipolysis. Ketone bodies are used by select tissues as a metabolic fuel but a high concentration of ketone bodies, resulting in ketoacidosis, is harmful for the body. Ketone bodies when present in large quantities can lower the pH level of the body, interrupting the normal function of many biochemical processes. The heart uses a large amount of free fatty acids and ketone bodies for fuel. The brain also relies on ketone bodies as extra fuel when glucose levels are low. Insulin and glucagon levels vary in response to glucose levels with insulin secretion from the pancreas being up-regulated by glucose and glucagon secretion from the pancreas being down-regulated by glucose. As mentioned earlier, pervious mathematical models have explored the effects of glucose on insulin and glucagon and the feedback of these hormones regulating blood glucose levels but have provided only a vague idea of how insulin and glucagon execute this regulation. The dynamical changes in concentration levels of the select metabolites in Figure 4.1 are a result of the levels of insulin and

glucagon and the purpose of our contextual model is to fill in more of the details of how this occurs.

4.3.1 Liver

The liver will contain the most detailed pathways for our model as the liver is the control center for metabolism partially due to the fact that it is able to process alternate metabolic fuels from within the liver as well as other tissues and form glucose and secrete it into the blood. The liver also is the place of ketogenesis thus providing alternate energy substrate as well as glucose. Table 4.1 lists the simplified metabolic pathways used in the model for the liver and Figure 4.2 organizes these pathways in a diagram.

glycolysis	gluc → g6p → pep → pyr
gluconeogenesis	alan → pyr → oa_m → malate → oa_c → pep → g6p → gluc
TCA cycle	oa_m → cit → aK → malate → oa_m
glycogenesis	gluc → g6p → glycgn
glycogenolysis	glycgn → g6p → gluc
lipogenesis	cit → acet_c → palm
lipolysis	palm → palmCoA → acet_m
ketogenesis	acet_m → ket

Table 4.1. Simplified Metabolic Pathways for the Liver. Gluc, glucose; g6p, glucose-6-phosphate; pep, phosphoenolpyruvate; alan, alanine; oa_m, mitochondrial oxaloacetate; oa_c, cytosolic oxaloacetate; cit, citrate; aK, alpha-ketoglutarate; glycgn, glycogen; acet_c, cytosolic acetyl Coenzyme A; palm, palmitate; palmCoA, palmitate Coenzyme A; ket, ketone bodies.

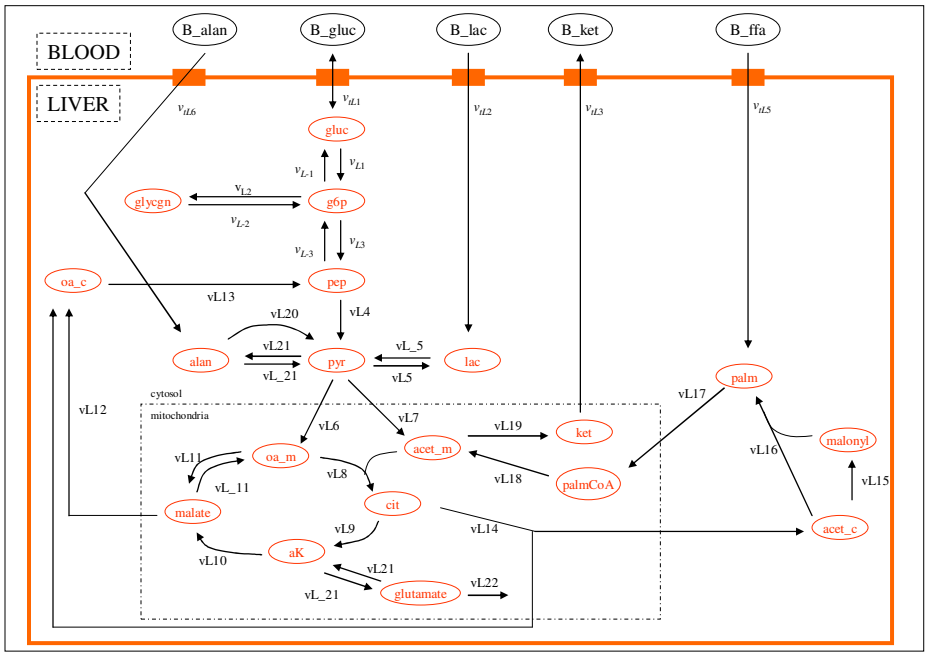

Figure 4.2. Reactions Included in Liver Component of the Model. The corresponding rate of each reaction is described in the text

A set of full equations is given in Appendix A. We will step through the model one reaction at a time to see how the dynamics of this system were captured mathematically. The first step of glycolysis is the conversion of glucose to glucose 6-phosphate, denoted by v_{L1}. While this reaction is catalyzed by both hexokinase and glucokinase, this reaction is simplified by assuming the presence of one enzyme. This reaction is up-regulated through insulin signaling. This reaction takes on a Michaelis-Menten form and is multiplied by a factor that allows for a flux independent of insulin and the up-regulation due to insulin signaling.

$$v_{L1} = \frac{k_{L1}\,[gluc]}{k_{mL1} + [gluc]} \left(1 + \frac{[B\_ins]^{ep1}}{k_{Dins}{}^{ep1} + [B\_ins]^{ep1}}\right)$$

The next step of simplified glycolysis is from glucose 6-phosphate to phosphoenolpyruvate. While v_{L3} combines a number of reactions within glycolysis, the enzyme of main importance is phosphofructokinase (see Figure 2.1) since this is the enzyme in glycolysis in which the direction of flow differs from gluconeogenesis. The form of this reaction is similar to the previous one except that the rate of this reaction decreases due to glucagon signaling. We see this effect in the last factor of this term.

$$v_{L3} = \frac{k_{L3}\,[g6p]}{k_{mL3} + [g6p]} \left(1 + \frac{[B\_ins]^{ep2}}{k_{Dins}{}^{ep2} + [B\_ins]^{ep2}}\right) \left(\frac{k_{Dglucgn}{}^{en1}}{k_{Dglucgn}{}^{en1} + [B\_glucgn]^{en1}}\right)$$

Phosphoenolpyruvate now gets converted to pyruvate by pyruvate kinase. The regulation of this reaction by hormones is similar to the previous step. An added factor is needed for v_{L4} to capture the negative feedback by alanine.

$$v_{L4} = k_{L4}\,[pep] \left(1 + \frac{[B\_ins]^{ep3}}{k_{Dins}{}^{ep3} + [B\_ins]^{ep3}}\right) \frac{k_{Dglucgn}{}^{en2}}{k_{Dglucgn}{}^{en2} + [B\_glucgn]^{en2}} \frac{k_{i13}}{k_{i13} + [alan]}$$

Pyruvate kinase catalyzes an irreversible reaction so pyruvate is unable to be converted directly back to phosphoenolpyruvate. The options for pyruvate in the model are to proceed through anaerobic glycolysis and be converted to lactate, be oxidized to oxaloacetate or to acetyl-CoA. Though the model does not take into consideration the spatial effects on the dynamics, it is worth keeping in mind that these options for pyruvate take place in the mitochondria whereas glycolysis takes place in the cytosol.

The conversion of pyruvate to lactate is a reversible reaction catalyzed by lactate dehydrogenase. Currently, these reactions are modeled with Michaelis-Menten dynamics.

$$v_{L5} = \frac{k_{L5}\,[pyr]}{k_{mL5} + [pyr]}$$

$$v_{-L5} = \frac{k_{-L5}\,[lac]}{k_{m\text{-}L5} + [lac]}$$

Pyruvate enters aerobic glycolysis by being converted to acetyl-CoA via pyruvate dehydrogenase and then entering the TCA cycle.

$$v_{L7} = \frac{k_{L7}\,[pyr]}{k_{mL7} + [pyr]} \; \frac{k_{i8}}{k_{i8} + [acet\_m]}$$

Pyruvate also plays a role in gluconeogenesis by being converted to oxaloacetate via pyruvate carboxylase. Within our model, gluconeogenesis begins with the transamination of amino acids so we will look at this step next. Instead of looking at all amino acids, we will just look at alanine and glutamine as these play a major role in the breakdown of proteins for gluconeogenesis and the metabolism of nitrogen, two areas of interest for this project. The reaction catalyzed by alanine aminotransferase is reversible and results in the transfer of an amino group from alanine to α-ketoglutarate to form glutamate with pyruvate being the result of the remains of alanine. Glutamate was at first not included within this model, however was later included to allow for the possibility of

the urea cycle which concerns nitrogen metabolism. Insulin signaling reduces the affects of this enzyme. Our model assumes Michaelis-Menten dynamics with respect to each substrate in these reactions.

$$v_{L21} = k_{L21} \frac{[pyr]}{k_{mL21p} + [pyr]} \frac{[glutamate]}{k_{mL21g} + [glutamate]} \frac{k_{Dins}^{en3}}{k_{Dins}^{en3} + [B\_ins]^{en3}}$$

$$v_{-L21} = k_{-L21} \frac{[alan]}{k_{m-L21a} + [alan]} \frac{[aK]}{k_{m-L21k} + [aK]} [acet\_m] \frac{k_{Dins}^{en3}}{k_{Dins}^{en3} + [B\_ins]^{en3}}$$

Pyruvate carboxylase activity, v_{L6}, which converts pyruvate to oxaloacetate in the mitochondria, is positively regulated by both mitochondrial acetyl-CoA and glucagon signaling.

$$v_{L6} = \frac{k_{L6}\,[pyr]}{k_{mL6} + [pyr]} \left(1 + \frac{p_2\,[acet\_m]}{k_{p2} + [acet\_m]}\right) \left(1 + \frac{[B\_glucgn]^{ep4}}{k_{Dglucgn}^{ep4} + [B\_glucgn]^{ep4}}\right)$$

From here, we have now entered the TCA cycle. To follow the shortest path of gluconeogenesis, we will only look at the step of the cycle involving conversion of mitochondrial oxaloacetate to malate as malate is shuttled out from the mitochondrial to leave the region in which gluconeogenesis has reactions in common with the TCA cycle. We will come back to look at the reactions in the TCA cycle. Malate dehydrogenase converts oxaloacetate to malate in both the cytosol and the mitochondria and this reaction is reversible. We will consider the reverse reaction for the mitochondrial portion when discussing the other TCA cycle reactions. The reaction from oxaloacetate to malate in

the mitochondria is positively regulated by glucagon signaling and has linear dynamics with respect to oxaloacetate.

$$v_{L11} = k_{L11}\,[oa\_m]\left(1 + \frac{[B\_glucgn]^{ep5}}{k_{Dglucgn}{}^{ep5} + [B\_glucgn]^{ep5}}\right)$$

Malate is transported through the mitochondrial membrane and converted back to oxaloacetate in the cytosol. Oxaloacetate is not able to be transported across the mitochondrial membrane so it must be converted to malate first.

$$v_{L12} = k_{L12}\,[malate]\,\frac{k_{Dins}{}^{en4}}{k_{Dins}{}^{en4} + [B\_ins]^{en4}}\left(1 + \frac{[B\_glucgn]^{ep6}}{k_{Dglucgn}{}^{ep6} + [B\_glucgn]^{ep6}}\right)$$

Phosphoenolpyruvate carboxylase converts oxaloacetate to phosphoenolpyruvate. Again, our model assumes linear dynamics with respect to oxaloacetate and is double regulating by insulin and glucagon, through a negative and a positive manner respectively.

$$v_{L13} = k_{L13}\,[oa\_c]\left(1 + \frac{[B\_glucgn]^{ep7}}{k_{Dglucgn}{}^{ep7} + [B\_glucgn]^{ep7}}\right)\frac{k_{Dins}{}^{en5}}{k_{Dins}{}^{en5} + [B\_ins]^{en5}}$$

We saw that although the pathway from glucose 6-phosphate to phosphoenolpyruvate had multiple steps, only one step was irreversible and so two different enzymes are required to complete this pathway. The reaction by one enzyme, phosphofructokinase (v_{L3}), is increased during glycolysis and the reaction by the other enzyme, fructose-1,6-

bisphosphatase ($v_{L\text{-}3}$), is increased during gluconeogenesis. We assume Michaelis-Menten kinetics in this reaction and account for positive regulation by glucagon signaling and negative regulation by insulin signaling.

$$v_{\text{-}L3} = \frac{k_{\text{-}L3}\,[pep]}{k_{m\text{-}L3} + [pep]} \left(1 + \frac{[B\_glucgn]^{ep8}}{k_{Dglucgn}{}^{ep8} + [B\_glucgn]^{ep8}}\right) \frac{k_{Dins2}{}^{en6}}{k_{Dins2}{}^{en6} + [B\_ins]^{en6}}$$

The last step of gluconeogenesis is the conversion of glucose 6-phosphate into glucose catalyzed by glucose 6-phosphatase and up-regulated by glucagon signaling.

$$v_{\text{-}L1} = \frac{k_{\text{-}L1}\,[g6p]}{k_{m\text{-}L1} + [g6p]} \left(1 + \frac{[B\_glucgn]^{ep9}}{k_{Dglucgn}{}^{ep9} + [B\_glucgn]^{ep9}}\right)$$

As for the reactions affecting the storage of glycogen, this is currently the only area in the model in which the amounts of enzymes present were explicitly modeled. The steps involving conversion of glucose to glucose 6-phosphate (v_{L1}) and back ($v_{L\text{-}1}$) were listed already. Our simplified process of glycogenesis involves glucose 6-phosphate being directly stored as glycogen and the main enzyme of this process is glycogen synthase. Michaelis-Menten kinetics are assumed.

$$v_{L2} = \frac{k_{L2}\,[GSa]\,[g6p]}{k_{mL2} + [g6p]}$$

The simplified conversion of glycogen to glucose 6-phosphate is catalyzed by glycogen phosphorylase.

$$v_{-L2} = \frac{k_{-L2}\,[GPa]\,[glycgn]}{k_{m\text{-}L2} + [glycgn]}$$

Going back to the TCA cycle, we have already discussed the entrance of pyruvate to the TCA cycle through either acetyl-CoA during glycolysis or oxaloacetate during gluconeogenesis. Citrate synthase combines oxaloacetate and acetyl-CoA to form citrate. This enzyme activity is reduced by the presence of palmitate-CoA.

$$v_{L8} = k_{L8}\,[oa\_m]\,[acet\_m]\,\frac{k_{i4}}{k_{i4} + [palmCoA]}$$

The model combines multiple steps to connect the pathway from citrate to α-ketoglutarate. Though these reactions are reversible, they are assumed irreversible in the model for simplification of pathways. Linear dynamics are assumed.

$$v_{L9} = k_{L9}\,[citrate]$$

Again multiple steps are combined into one when modeling the conversion of α-ketoglutarate to malate.

$$v_{L10} = k_{L10}\,[aK]$$

We now list the reversible reaction of malate dehydrogenase to convert malate to oxaloacetate completing the cycle.

$$v_{-L11} = k_{-L11}\,[malate]$$

We now leave the TCA cycle to look at the pathway of lipogenesis. Just as oxaloacetate and acetyl-CoA were combined to form citrate, citrate is transported to the cytosol where citrate lyase breaks down citrate to form acetyl-CoA and oxaloacetate. Due to the role of oxaloacetate and acetyl-CoA various pathways of different location in the cell, a separate concentration of each is considered in the model for the mitochondrial concentration and the cytosolic concentration. The activity of citrate lyase is increased due to insulin signaling but decreased due to glucagon signaling.

$$v_{L14} = k_{L14}\,[citrate]\left(1 + \frac{[B\_ins]^{ep10}}{k_{Dins}{}^{ep10} + [B\_ins]^{ep10}}\right)\frac{k_{Dglucgn}{}^{en7}}{k_{Dglucgn}{}^{en7} + [B\_glucgn]^{en7}}$$

Acetyl-CoA forms malonyl-CoA by acetyl-CoA carboxylase.

$$v_{L15} = k_{L15}\,[acet\_c]\left(1 + \frac{p_1\,[citrate]}{k_{p1} + [citrate]}\right)\frac{k_{i5}}{k_{i5} + [palmCoA]}$$

Acetyl-CoA and malonyl-CoA together enter a complicated process to form palmitate, a free fatty acid (see Figure 2.6). This process starts with one molecule of acetyl-CoA and one of malonyl-CoA and then forms a fatty acid complex which cycles

through a four enzyme process. The complex goes through this cycle seven times and each time picks up another molecule of malonyl-CoA producing a stoichiometry of 1:7:1 for acetyl-CoA to malonyl-CoA to palmitate.

$$v_{L16} = k_{L16} [acet\_c] [malonyl]^7$$

When blood glucose levels drop, the transport of free fatty acids from fat to blood and then from blood to the liver increases. These free fatty acids, restricted to palmitate in our model, break down in tissues to palmitate-CoA, also known as acyl-CoA. The breakdown of palmitate is negatively regulated by malonyl-CoA.

$$v_{L17} = k_{L17} \frac{k_{i1}}{k_{i1} + [malonyl]}$$

Acyl-CoA is transported across the mitochondrial membrane where it is converted to acetyl-CoA. This step is also down-regulated by malonyl-CoA. In order to differentiate between certain pathways, it was necessary in our model to consider which processes took place in the mitochondria and which in the cytosol. However, our model assumes passive transport and so we do not model the mitochondrial membrane mechanisms.

$$v_{L18} = k_{L18} [palmCoA] \frac{k_{i2}}{k_{i2} + [malonyl]}$$

The role of acetyl-CoA in the TCA cycle by forming citrate along with oxaloacetate was previously discussed. Forming mitochondrial acetyl-CoA is how free fatty acids are able to provide alternate fuel to cells. The liver also generates another metabolic fuel, ketone bodies, which are able to be transported to other cells. Though multiple tissues are capable of lipolysis, very few are capable of ketogenesis. The next reaction, up-regulated by cAMP but down-regulated by insulin signaling, is a combination of a multiple steps which convert two molecules of acetyl-CoA to a ketone body, namely acetoacetate and 3-hydroxybutyrate.

$$v_{L19} = k_{L19}\,[acet\_m]^2 \left(1 + \frac{[cAMP]^{ep11}}{k_{dcAMP}{}^{ep11} + [cAMP]^{ep11}}\right) \frac{k_{Dins}{}^{en8}}{k_{Dins}{}^{en8} + [B\_ins]^{en8}}$$

4.3.2 Blood

Although biochemical processes may take place in the blood, this is probably at an insignificant scale when compared to functional tissues. The blood component of our model has the primary purpose of a transport system between the metabolic tissues. The metabolites that are able to transport between tissues are glucose, lactate, free fatty acids, ketone bodies and alanine. The hormones insulin and glucagon reside only in the blood component in this model. Any effects due to the presence of insulin and glucagon are due to the inter-cell signaling of the binding of these hormones to cell surface receptors. Within the model, the blood concentrations of insulin and glucose directly affect the rate of certain reactions and also directly affect the synthesis and degradation of cAMP

although this process is also through inter-cell signaling. Figure 4.3 shows the transports of metabolites across the membranes of tissues in the model.

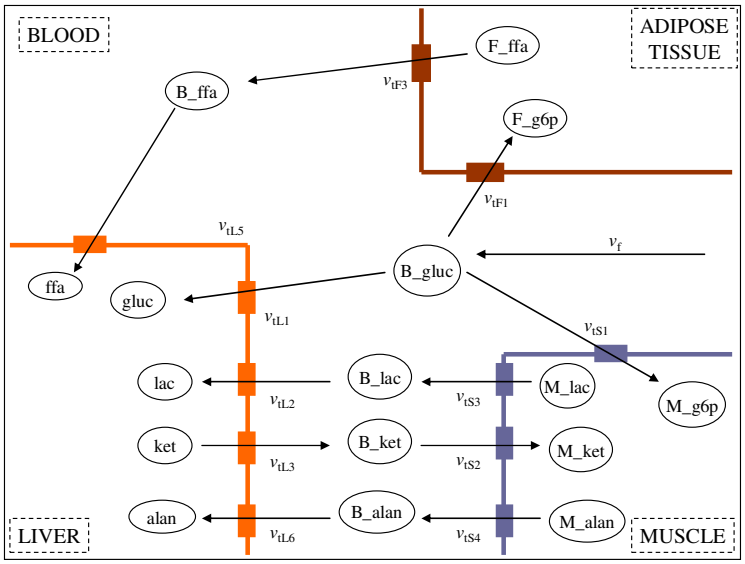

Figure 4.3. Reactions for Transport Across the Cell Membranes. The corresponding rate of each reaction is described in the text.

Glucose enters the system from the gut via the portal vein, bringing a supply of blood from the gut to the liver. The liver also receives another flow of blood through the hepatic artery. The blood that flows through the hepatic artery and hepatic vein is that which connects the liver to the rest of the metabolic system. As the portal vein only connect the liver with the gut, our model has only considered one type of blood, that which connects the liver with the muscle and fat tissue. This simplification requires an alternate method of bringing digested glucose into the system and so this glucose is introduced directly to the bloodstream.

This investigation of incorporating a detailed model of the glycogen regulatory circuit into a contextual metabolic framework focuses on the transition time from a feeding state to a post-absorptive, or fasted, state. The time-dependent variable providing

food to the system, v_{feed}, was designed with three objectives: 1) the system be brought to a fed steady state for $t < 0$ so that initial values of the simulation are that of a fed state, 2) the fasting state be reproduced by a gradual decline of feeding as seen with a gradual absorption of food from the gut during digestion, and 3) this function, v_{feed}, be continuous. To replicate a fed state, the system is brought to steady state with a constant flux of $v_{feed} = k_f$ where k_f is currently defined as 0.5 mM/min. To mimic the gradual decline of food intake during digestion, v_{feed} then follows a normal distribution curve with a mean of $t = 0$. A standard deviation such that $v_{feed} = 0.5$ mM/min when $t = 0$ will make this two piece function continuous. An absorption period of approximately 3 hours, or 180 minutes, was desired to correspond with previous studies on absorption rates of food products from the small intestine of a rat ([21], [22]). To achieve this, the quantity in the numerator of the exponent, $(t - \mu)$, was multiplied by a factor of 0.014 causing a stretch of the normal distribution function. This representation of the feeding function, v_{feed}, is as follows:

$$v_{feed}(t) = \begin{cases} k_f & for\ t < 0 \\ \dfrac{1}{\sigma\sqrt{2\pi}} e^{\frac{-(0.014(t-\mu))^2}{2\sigma^2}} & for\ t \geq 0 \end{cases} \qquad where\ \ \mu = 0\ and\ \sigma = \frac{1}{k_f\sqrt{2\pi}}$$

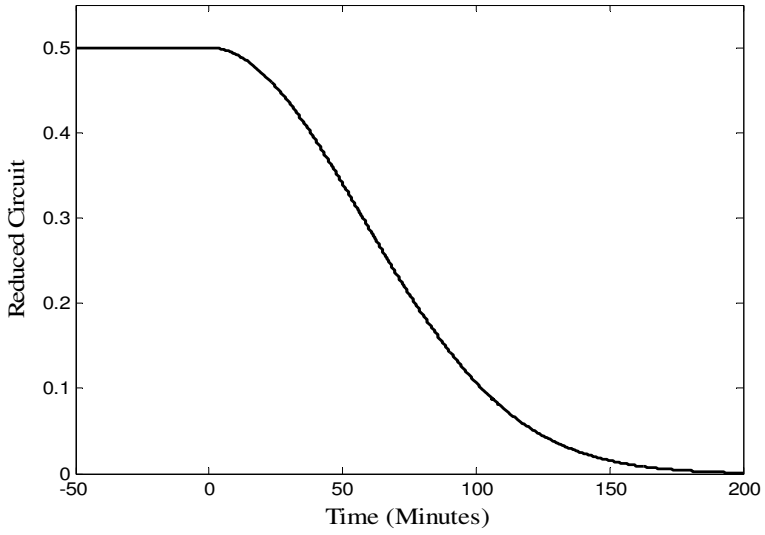

Figure 4.4. Feeding Flux, Fed to Fasted. The feeding function, v_{feed}, is a time-dependent, two-piece function to transition from a fed state with a constant flux for $t < 0$ and a gradual decline of flux for $t \geq 0$. Most absorption has taken place by approximately 3 hours.

While the liver membrane contains the insulin independent glucose transporter, GLUC2, fat and muscle tissue both contain GLUC4 transporters that are dependent on insulin. The transport of glucose across the liver membrane, v_{tL1}, is passive and so depends on the difference between the concentration of glucose inside and outside of the liver. The transport of glucose across the membranes of fat and muscle tissue, v_{tF1} and v_{tS1} respectively, is modeled linearly with respect to the amount of blood glucose and is up-regulated by blood insulin levels.

$$v_{tL1} = k_{tL1} ([B\_gluc] - [gluc])$$

$$v_{tF1} = k_{tF1} [B\_gluc] \left(1 + \frac{[B\_ins]^{ep12}}{k_{Dins}{}^{ep12} + [B\_ins]^{ep12}} \right)$$

$$v_{tS1} = k_{tS1}\,[B\_gluc]\left(1 + \frac{[B\_ins]^{ep13}}{k_{Dins}{}^{ep13} + [B\_ins]^{ep13}}\right)$$

The liver and muscle both contain lactate, the end product of anaerobic glycolysis. This metabolite participates in the Cori cycle, the process in which glucose from the liver enters the muscle, lactate is formed and transported back to the liver to enter gluconeogenesis and form glucose. As mentioned previously, the muscle is unable to produce glucose due to the lack of the enzyme glucose 6-phosphatase so the muscle assists in stabilizing glucose levels through the Cori cycle.

$$v_{tL2} = k_{tL2}\,[B\_lac]$$

$$v_{tS3} = k_{tS3}\,[M\_lac]$$

During fasting and starvation, ketone bodies are formed as free fatty acids are broken down. This occurs in the liver and these ketone bodies are transported to the muscle to be used as an alternate metabolic fuel so that the muscle does not require as much blood glucose and this glucose is reserved for other tissues unable to adapt to using alternate fuels.

$$v_{tL3} = k_{tL3}\,[ket]$$

$$v_{tS2} = k_{tS2}\,[B\_ket]$$

Also during fasting and starvation, fats are released from the fat tissue and transported to the liver and other tissues where they are used as an alternate fuel source. The model disregards the transport of fats to the muscle as this tissue is already taking the alternate fuel source of ketone bodies. Only fat transport into the liver is considered as fats also increase the rate at which amino acids are used as substrate for gluconeogenesis as well as providing an alternate fuel source for the TCA cycle. The release of fats from fat tissue takes on a more complicated form than other metabolite transport and is down-regulated by insulin.

$$v_{tL5} = k_{tL5}\,[B\_ffa]$$

$$v_{tF3} = k_{tF3}\,[F\_ffa]^{8}\,\frac{k_{Dins2}{}^{en9}}{k_{Dins2}{}^{en9} + [B\_ins]^{en9}}$$

Protein degradation is continuously occurs at all feeding levels but increases in response to the body's need of glucose. During fasting, this process is sped up to provide a source of substrate for gluconeogenesis. The model assumes proteins have already been broken down to the amino acid building blocks and considers alanine as the main amino acid in this process. Alanine is transported from the muscle to the liver and each transport is down-regulated by the presence of insulin.

$$v_{tL6} = k_{tL6}\,[B\_alan]\,\frac{k_{Dins}{}^{en10}}{k_{Dins}{}^{en10} + [B\_ins]^{en10}}$$

$$v_{tS4} = k_{tS4}\,[M\_alan]\,\frac{k_{Dins}{}^{en11}}{k_{Dins}{}^{en11} + [B\_ins]^{en11}}$$

The model assumes a linear rate of decay for each metabolite and hormone present in the blood.

$$v_{d\_Bgluc} = k_{d\_Bgluc}\ [B\_gluc]$$

$$v_{d\_Bffa} = k_{d\_Bffa}\ [B\_ffa]$$

$$v_{d\_Blac} = k_{d\_Blac}\ [B\_lac]$$

$$v_{d\_Bket} = k_{d\_Bket}\ [B\_ket]$$

$$v_{d\_Balan} = k_{d\_Balan}\ [B\_alan]$$

Insulin and glucagon

$$v_{Bins} = k_{ins} + \frac{k_{1ins}\ [B\_gluc]^{ni}}{(k_{mIns}^{\ ni} + [B\_gluc]^{ni})} - k_{d\_Bins}\ [B\_ins]$$

$$v_{Bglucgn} = k_{glucgn} - \frac{k_{1glucgn}\ [B\_gluc]^{ng}}{(k_{mG\lg n}^{\ ng} + [B\_gluc]^{ng})} - k_{d\_Bglucgn}\ [B\_glucgn]$$

4.3.3 Fat

Since our model is concentrated on the liver's role in metabolism, a brief sketch of the metabolic processes in the fat and muscle tissue are modeled. The important role of fat tissue is that glucose is taken up by fat in an insulin-dependent manner and is stored

as triacylglycerol within fat tissue until blood glucose levels drop and these glucose stores are needed. The transport of glucose into and free fatty acids from fat tissue were described in Section 4.3.2. The only metabolites modeled for fat tissue are glucose 6-phosphate, acyl-CoA, triacylglycercol and free fatty acids.

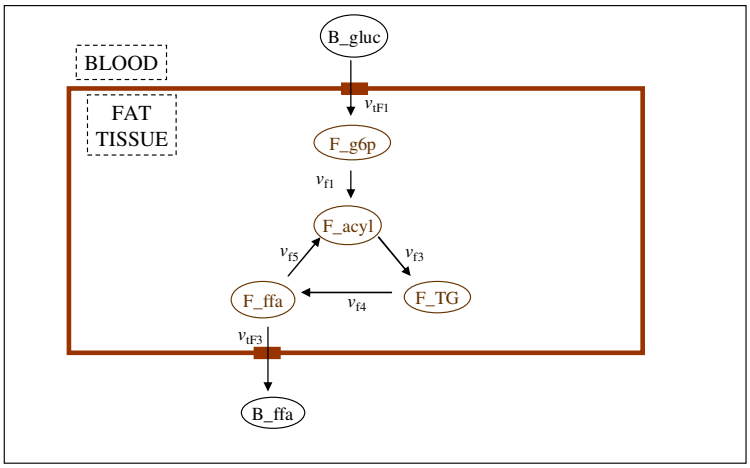

Figure 4.5. Reactions Included in the Fat Component of the Model. The corresponding rate of each reaction is described in the text.

Each reaction within the model for processes that take place in fat tissue are all approximated using linear dynamics with respect to the appropriate substrate for the reaction. As triacylglycerol is the storage form of glucose, each reaction increasing the formation of triacylglycerol is up-regulated by insulin signaling while the reaction that breaks down triacylglycerol, v_{f4}, is down-regulated by insulin signaling.

$$v_{F1} = k_{F1}\,[F\_g6p]\left(1 + \frac{[B\_ins]^{ep14}}{k_{Dins}{}^{ep14} + [B\_ins]^{ep14}}\right)$$

$$v_{F3} = k_{F3}\,[F\_acyl]\left(1 + \frac{[B\_ins]^{ep15}}{k_{Dins}{}^{ep15} + [B\_ins]^{ep15}}\right)$$

$$v_{F4} = k_{F4}\,[F\_TG]\,\frac{k_{Dins}{}^{en12}}{k_{Dins}{}^{en12} + [B\_ins]^{en12}}$$

$$v_{F5} = k_{F5}\,[F\_ffa]^3$$

4.3.4 Muscle

As with the fat tissue, the muscle component of the model contains a backbone of the metabolic processes that occur in normal muscle tissue and each reaction is modeled linearly with respect to corresponding substrate.

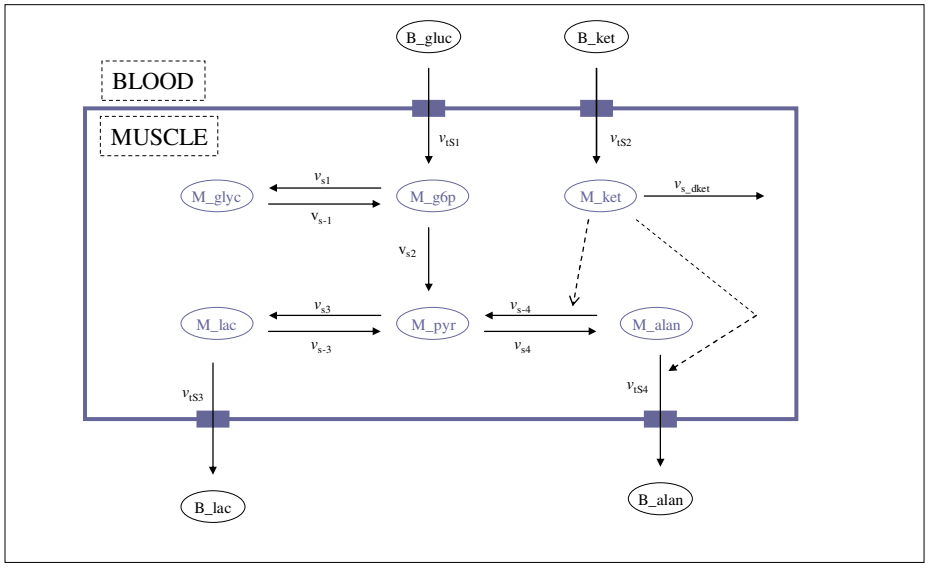

Figure 4.6. Reactions Included in the Muscle Component of the Model. The corresponding rate of each reaction is described in the text.

An abbreviated pathway of glycolysis is modeled in the muscle portion of the liver. This pathway, as is the glycogen regulatory circuit, in the muscle is very similar to that of the liver. The muscle is not capable of gluconeogenesis due to the absence of glucose 6-phosphatase. Because of this, the key metabolites of gluconeogenesis that were included in the liver were left out of the muscle model. Glucose 6-phosphate was included because of its options to either be converted to glycogen or to move through glycolysis with pyruvate as an end product.

$$v_{S1} = k_{S1}\,[M\_g6p]$$

$$v_{-S1} = k_{-S1}\,[M\_glycgn]$$

$$v_{S2} = k_{S2}\,[M\_g6p]$$

Pyruvate can either form lactate which can then be transported to the liver as part of the Cori cycle or form alanine, our representative of amino acids and proteins. Alanine is transported to the liver during fasting to provide substrate for gluconeogenesis.

$$v_{S3} = k_{S3}\,[M\_pyr]$$

$$v_{-S3} = k_{-S3}\,[M\_lac]$$

$$v_{S4} = k_{S4}\,[M\_pyr]$$

Ketone bodies enter the muscle to provide alternate fuel. In our model, these increase the rate at which alanine is degraded and transported from the liver.

$$v_{-S4} = k_{-S4}\,[M\_alan]\,[M\_ket]$$

$$v_{S\_dket} = k_{S\_dket}\,[M\_ket]$$

The roles of the muscle in our model include participation in the Cori cycle and protein degradation as well as a sink for alternate fuel in the form of ketone bodies. Greatly neglected is the use of glucose and these ketone bodies for energy through the TCA cycle.

4.4 Detailed Local Model

The localized section of metabolism chosen for a more detailed investigation encompasses the mechanisms behind the activation and deactivation of hepatic glycogen synthase and glycogen phosphorylase. Previously, it was mentioned that blood glucose levels regulate the amount of insulin and glucagon released into the bloodstream. Through binding to cell surface receptors and subsequent signal transduction, insulin and glucagon regulate cAMP levels with the cell. The reduced version of the glycogen regulation circuit has cAMP directly affecting the rate of phosphorylation of GS and GP while the full circuit includes the intermediate enzymes which create a cascade of phosphorylation to regulate the synthesis and degradation of glycogen.

4.4.1 Reduced Glycogen Regulatory Circuit

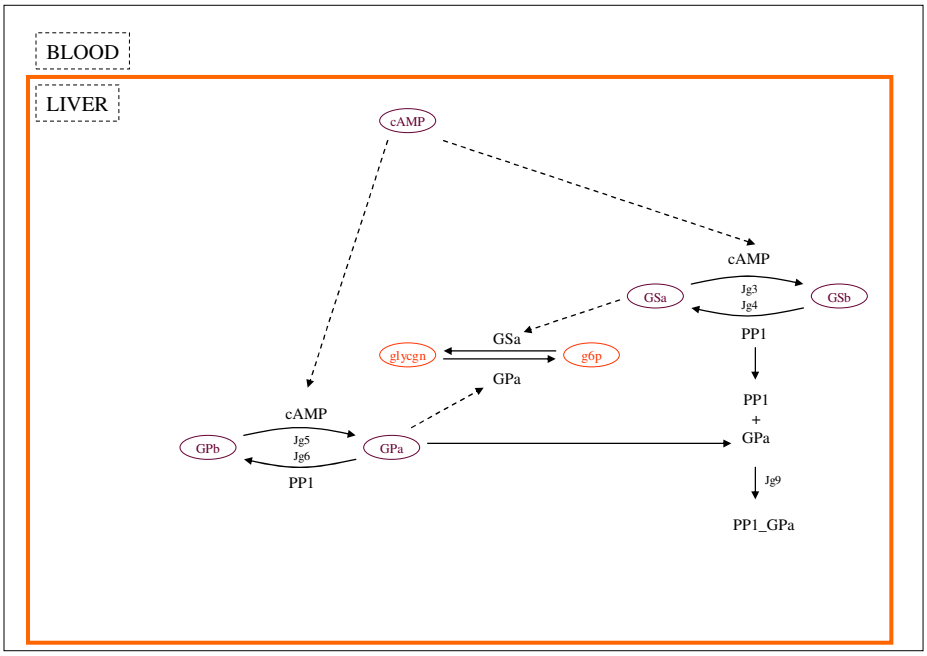

Figure 4.7. Reactions Included in the Reduced Glycogen Regulatory Circuit. The corresponding rate of each reaction is described in the text.

4.4.2 Full Glycogen Regulatory Circuit

At the center of figure 4.6, the metabolites within the model that are involved in glycogen synthesis and degradation are shown. Around these are the enzymes responsible for the regulation of the rate at which these processes occur. Figure 3.1 also gave us an idea of the enzyme cascade behind this regulatory circuit.

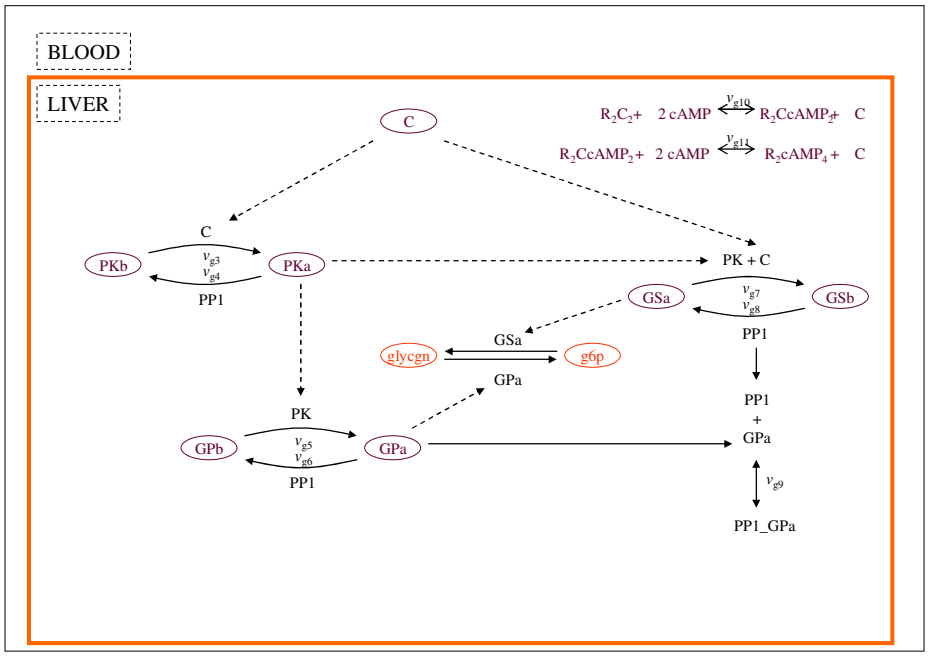

Figure 4.8. Reactions Included in the Full Glycogen Regulatory Circuit. The corresponding rate of each reaction is described in the text.

$$v_{g3} = \frac{k_{g3}\,[C]\,(kt - [PKa])}{k_{mg3} + (kt - [PKa])}$$

$$v_{g4} = \frac{k_{g4}\,([PP1] + [PP1\_GPa])\,[PKa]}{k_{mg4} + [PKa]}$$

$$v_{g5} = \frac{k_{g5}\,[PKa]\,(pt - GPa)}{k_{mg5}\,(1 + \frac{s_1\,[g6p]}{k_{g2}}) + (pt - [GPa])}$$

$$v_{g6} = \frac{k_{g6}\,([PP1] + [PP1\_GPa])\,[GPa]}{\frac{k_{mg6}}{\frac{1 + s_2\,[gluc]}{k_{gi}}} + [GPa]}$$

$$v_{g7} = \frac{k_{g7}\,([PKa] + [C])\,[GSa]}{k_{mg7}\,(1 + \frac{s_1\,[g6p]}{k_{g2}}) + [GSa]}$$

$$v_{g8} = \frac{k_{g8}\,([PP1] + [PP1\_GPa])\,(st - GSa)}{k_{mg8}\,(1 + \frac{s_1\,[g6p]}{k_{g2}}) + (st - [GSa])}$$

$$v_{g9} = k_a\,[PP1]\,[GPa] - k_{-a}\,[PP1\_GPa]$$

$$v_{g10} = k_{gc1}\,[R2C2]\,[cAMP]^2 - k_{-gc1}\,[R2\_C\_cAMP2]\,[C]$$

$$v_{g11} = k_{gc2}\,[R2\_C\_cAMP2]\,[cAMP]^2 - k_{-gc2}\,[R2\_cAMP4]\,[C]$$

To test the detailed model of the glycogen circuit, this model was run to steady state and compared with the results published in [19]. Here, the fractional modification, or the percentage of activation through either phosphorylation or dephosphorylation, of the enzymes is compared in the glycogen circuit under the conditions of a fed state and a fasted state. The variation between feeding states is depicted through the dissociation constant of GPa binding to glycogen synthase PP1. v_{g9}, which represents the net flux of the binding of GPa and PP1, equals zero at steady state. From the resulting equation, representation of the corresponding dissociation constant is found.

$$v_{g9} = k_a [PP1] [GPa] - k_{-a} [PP1\_GPa] = 0$$

$$k_d = \frac{[PP1] [GPa]}{[PP1\_GPa]} = \frac{k_{-a}}{k_a}$$

It has been shown that a significant amount of glycogen must be present for this binding to occur [23, 24]. To simulate a fed state in [19], a rate of $k_d = 0.002$ μM was used as there would be glycogen present to allow for PP1_GPa to accumulate at steady state. Glycogen would not be present in a fasted state so k_d is increased to $k_d = 2$ μM to reflect this.

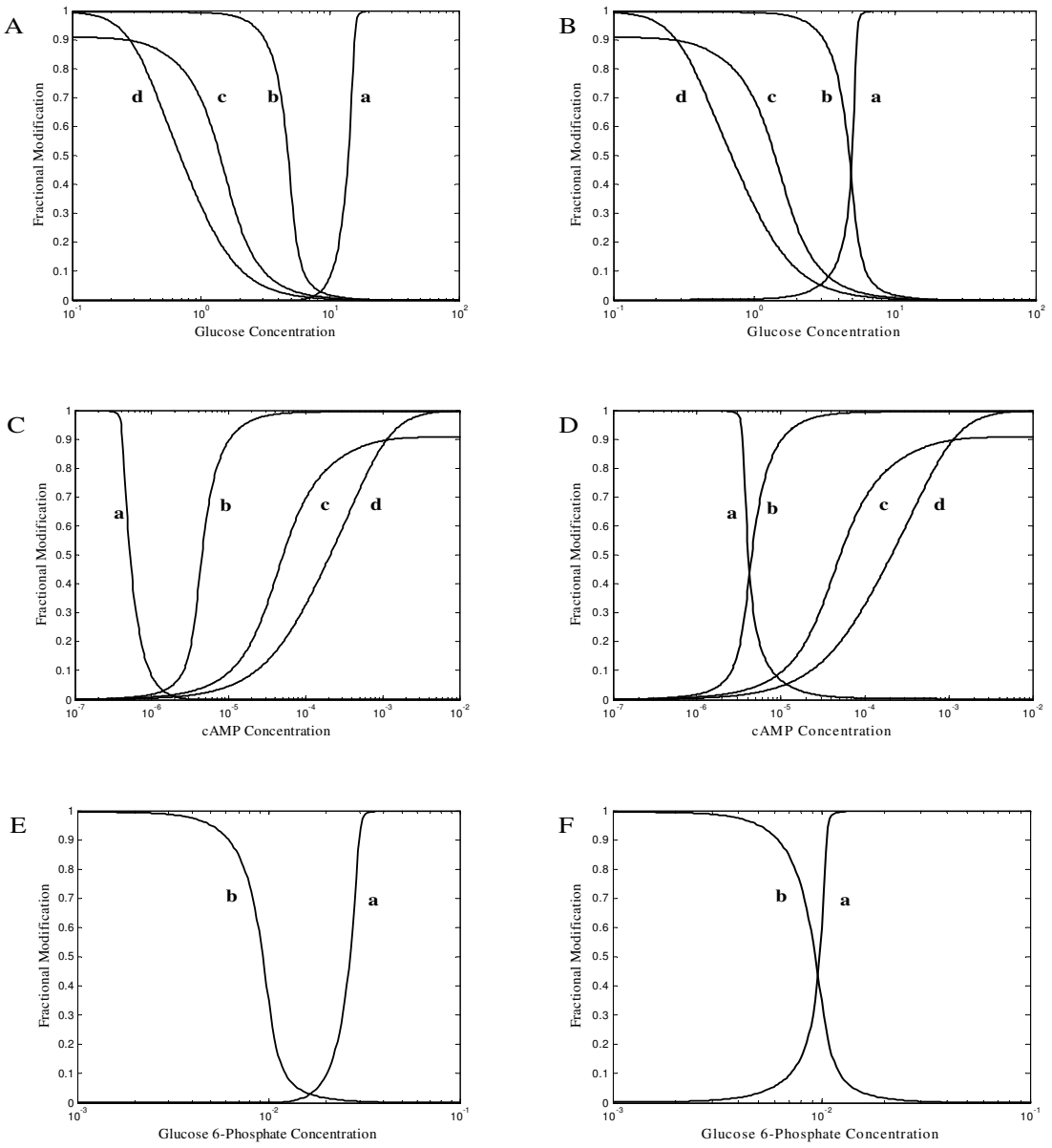

Figure 4.9. Steady State Results of the Glycogen Circuit Model. Figures in the left column (A, C, E) resulted from a simulation under fed conditions (k_d = 0.002 μM). Figures in the right column (B, D, F) resulted from simulations under fasted conditions (k_d = 2 μM). These replicate previously published results in which the presence of glycogen affects the activation of glycogen synthase (curve **a**) with respect to the dosage of glucose, cAMP, glucose 6-phosphate. Glycogen phosphorylase (curve **b**), phosphorylase kinase (curve **c**) and the catalytic subunit of cAMP dependent protein kinase (curve **d**) are unaffected by the presence or absence of glycogen.

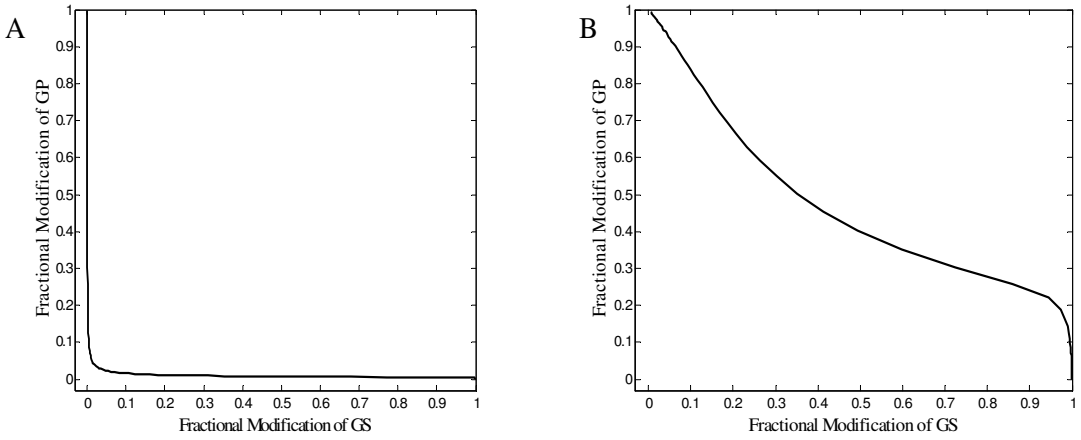

Figure 4.10. Futile Cycling at Steady State. These simulations also replicate previously published results in comparing the activation of GP, glycogen phosphorylase, with that of GS, glycogen synthase. A reciprocal regulation is observed during the fed state (A, k_d = 0.002 μM) while futile cycling occurs during fasting (B, k_d = 2 μM).

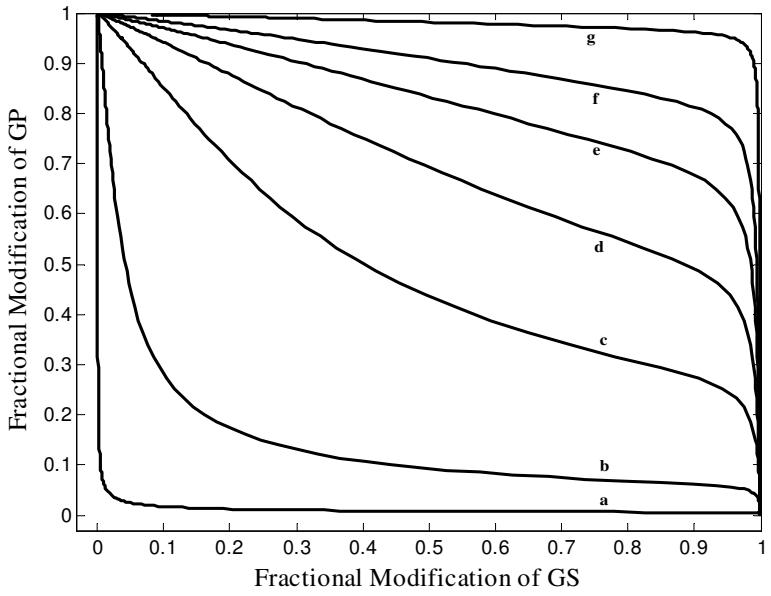

Figure 4.11. Futile Cycling at Various Levels of Feeding. **a** – fed, little futile cycling present, **g** – fasted, a lot of futile cycling present.

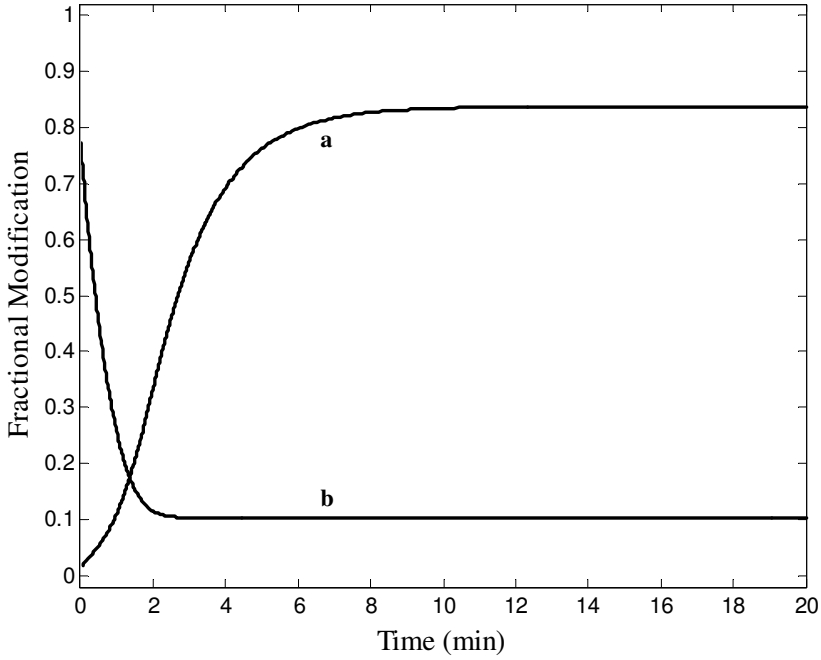

Figure 4.12. Fractional Modification of GS and GP Over Time. The initial conditions for this simulation were found by running the isolated model of the full regulatory circuit steady state with glucose = 5 mM and glucose 6-phosphate at 0.1 mM. At time = 0 minutes, glucose and glucose 6-phosphate were increased to 60 mM and .7 mM, respectively. With k_d = 0.2 μM, in a fasted state, the full regulatory circuit in isolation is able to replicate the results found in Cardenas that detail the effects of increased glucose on modification of GS and GP. Curve **a**, GSa; curve **b**, GPa.

4.5 Connecting the Models

Originally, cAMP was a direct regulator of the glycogen synthesis and degradation terms in the contextual model. This model was changed to include GPa and GSa concentrations in order to be able to easily connect the detailed regulatory model with the contextual model and to still run each model in isolation from the other. Recall

v_{L2} and v_{L-2} from section 4.3.1. When the detailed model is not connected to the contextual model, the 'whole-physiology' model can be run with a constant amount of GSa and GPa and the local model can be run with prescribed amounts of glucose, glucose 6-phosphate and cAMP. This format allows for easy manipulation of the regulatory circuit to 'cut out' enzymes within the cascade or to add new enzymes to create a more complicated cascade.

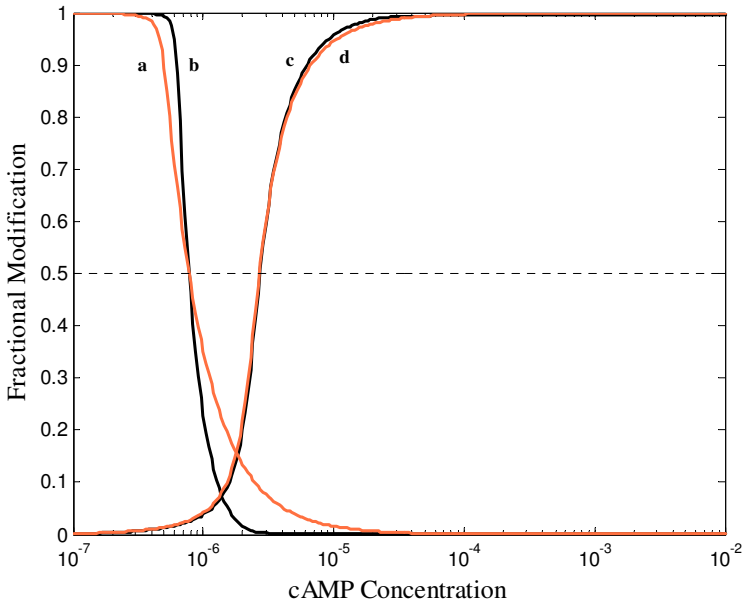

Figure 4.13. Steady State Comparison of Fractional Modification in Reduced and Full Circuits. By modifying the rate constants which affect the phosphorylation of GS and GP, the steady state switch-like behavior in the reduced model is comparable to that of the full model. Curve **a**, reduced model GS; curve **b**, full model GS; curve **c**, full model GP; curve **d**, reduced model GP.

CHAPTER 5

Results and Discussion:

Model Integration and Optimization

5.1 Overview

In isolation, the full glycogen regulatory circuit and the reduced glycogen regulatory circuit were comparable in response to glucose, glucose 6-phosphate and cAMP levels. These circuits were immersed into a 'whole'-physiology model to investigate the optimization of the effects of the full glycogen regulatory circuit on the metabolic system. The following model simulations will support the hypothesis that the architecture of the glycogen regulatory circuit stabilizes blood glucose levels by optimizing the combination of rates at which ingested glucose, glycogen and amino acids (with assistance from free fatty acids) are used as substrates for blood glucose.

To understand the various stages of feeding, simulations were produced in which the system had a constant intake of ingested glucose, producing a 'glucose-fed' stage. Ingested glucose was then removed and the system relied on the next source of glucose substrate, glycogen, putting the system in a 'glycogen-fed' stage. Next, glycogen was depleted and the system was put into a 'ffa/aa-fed' (free fatty acid/amino acid) stage of feeding in which alanine (an amino acid) was broken down to form glucose with free fatty acids used as an assisted energy source for this process. There were no significant

differences between the simulations involving the full glycogen regulatory circuit and the reduced circuit.

Time dependent simulations showed differences in select metabolite concentration levels during the transitional periods between feeding stages. The full circuit allowed for a quicker response time in which glycogen was able to be stored or utilized during high and low blood glucose levels respectively. This led to a more controlled balance among ingested glucose, glycogen and amino acids in stabilizing blood glucose levels.

5.2 Initial Fasting Simulation

The first objective of the contextual model was to mimic the observed behavior of key metabolites and regulators as was discussed in Section 4.3. The results of a fasting simulation are shown in Figure 5.1. This simulation started with initial conditions from a fed state. There are two periods of transition in this simulation, one at $t = 0$ in which the system shifts from relying on ingested glucose to use of hepatic glycogen stores accumulated during feeding. Blood glucose levels exhibit damped oscillations until about 400 minutes. We will discuss later how blood glucose levels for the fasted state are lower than those for the fed state. The second transition period occurs at about $t = 1700$ when liver glycogen is depleted. Here the system adapts again to increasingly rely on fat reserves to generate energy for glucose synthesis from amino acids through hepatic gluconeogenesis. We again see the adjusted level of blood glucose to be lower than that of a fed state and also a fasted state. Other metabolites exhibit a complex range of responses to the adaptive changes needed to maintain critical blood glucose levels during

these bioenergetic transitions. Glycogen is depleted during the fasting state while blood concentrations of free fatty acids and ketone bodies both rise during each period of transition. Insulin and glucagon levels change inversely, in response to and to maintain the observed changes in blood glucose concentrations. This simulation was run with the full glycogen regulatory circuit included. Figure 5.2 provides a comparison between a simulation run with the full glycogen regulatory circuit and one with the reduced regulatory circuit.

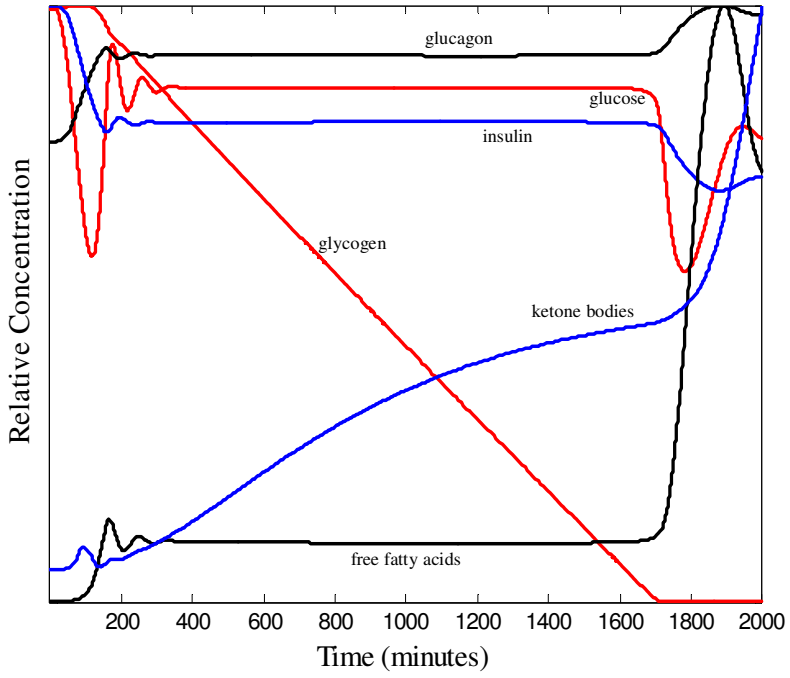

Figure 5.1. Initial Simulation of Relative Concentrations of Select Metabolites During Fasting. The model captures the dynamic behavior of selected metabolites and hormones during the fasting period. The system, initially in a fed state, began fasting at $t = 0$.

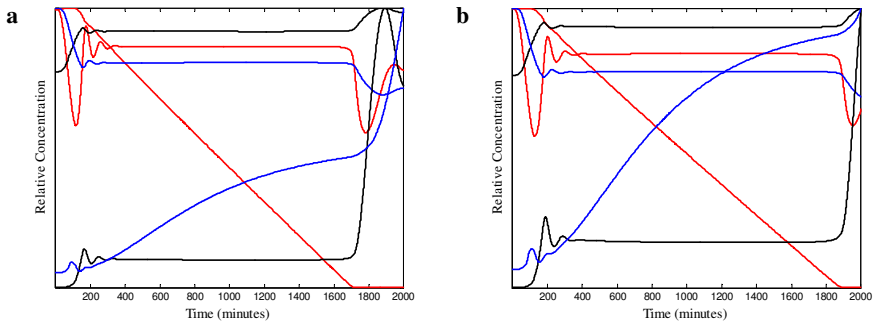

Figure 5.2. Comparison of System Responses to Fasting Using the Full or Reduced Circuits. (full, **a**; reduced, **b**) While some differences arise, the relative behavior of metabolites and hormones follow the observed behavior reported in the literature [10], as can be verified by comparing Figure 5.2 to Figure 4.1.

5.3 System Behavior During Various Feeding Stages

The model results support the hypothesis that glycogen regulatory circuitry is designed to efficiently store and utilize glycogen during transitory feeding states, particularly in the refeeding state. As the conversion of glucose to and from glycogen and amino acids is a continuous and intertwined process, it is unrealistic to consider separate situations in which glucose is solely converted from glycogen or solely converted from amino acids and fats. During fasting, the period of dependence on liver glycogen overlaps that of dependence on gluconeogenesis. In fact, these processes appear to approach their respective asymptotes, with some futile cycling occurring during the transitions. However, by looking at ingested glucose, glycogen and amino acids as independent substrates for glucose, one can determine the ability of the system to stabilize glucose levels from these individual sources.

For this investigation, the body was considered to be in one of three bioenergetic states: a fed state in which substrates for blood glucose are provided through digestion of food (glucose-fed); a fasted state in which digestion has ceased and the maintenance of blood glucose levels is dependent upon glycogen that has been stored in the liver (glycogen-fed); and a starvation state in which hepatic glycogen stores have been essentially depleted and amino acids are being broken down with the assistance of fats (as an energy source) and are the substrate for blood glucose (Free Fatty Acid/Amino Acid-fed or FFA/AA-fed). The steady state of the system for each feeding state was

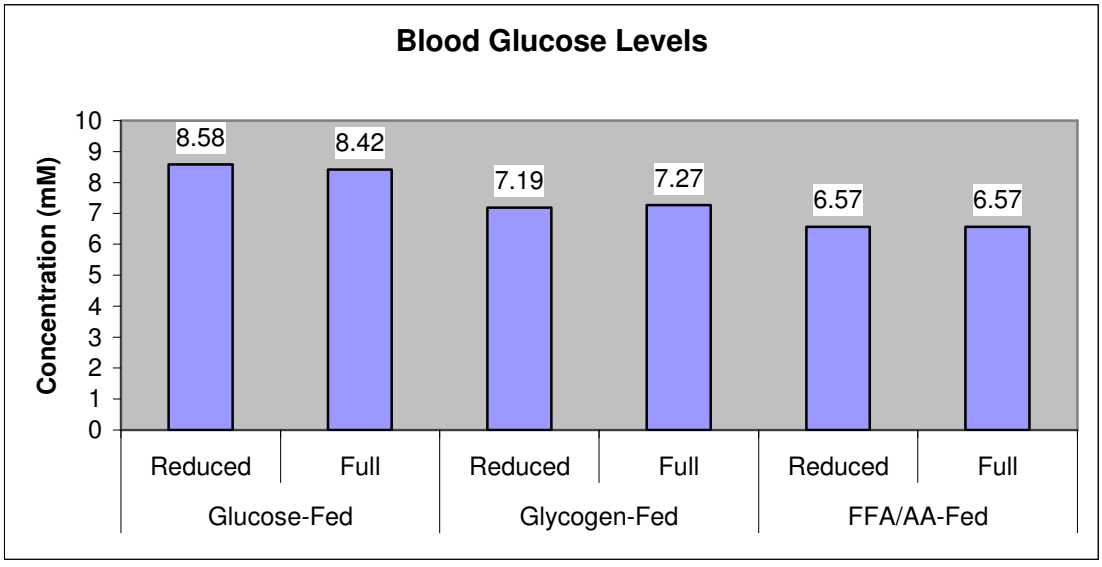

Figure 5.3. Simulation Results: Blood Glucose Levels During the Three Feeding States. These levels are highest when the system receives a constant intake of glucose through digestion and lowest when the system is in a state of starvation, relying on the FFA and AA stores to make glucose. Little difference is seen when comparing the simulations with the full glycogen circuit with those obtained with the reduced circuit.

investigated in order to yield insights into the behavior of the system as a whole, and the sensitivity of the system to modification of the glycogen control circuitry: full glycogen circuit and a reduced glycogen circuit.

An important feature of the metabolic system is its ability to maintain blood glucose levels. Figure 5.3 shows the blood glucose levels obtained from simulations of the three feeding stages. Blood glucose levels drop as the system progresses through the various stages. There is little difference between the simulations containing the full glycogen regulatory circuit and the reduced circuit with respect to the blood glucose concentrations achieved in the three states. There are, however, significant differences in the dynamics of the transitions through each of the states (see below) Furthermore, though differences predicted by the model are probably biologically insignificant, it is worth noting that the full glycogen regulatory circuit keeps blood glucose levels closer to the desired level of 8 mM. The insulin/glucagon switch in response to changing glucose levels is designed to occur at 8 mM ($k_{mins} = 8$, $k_{mGlgn} = 8$).

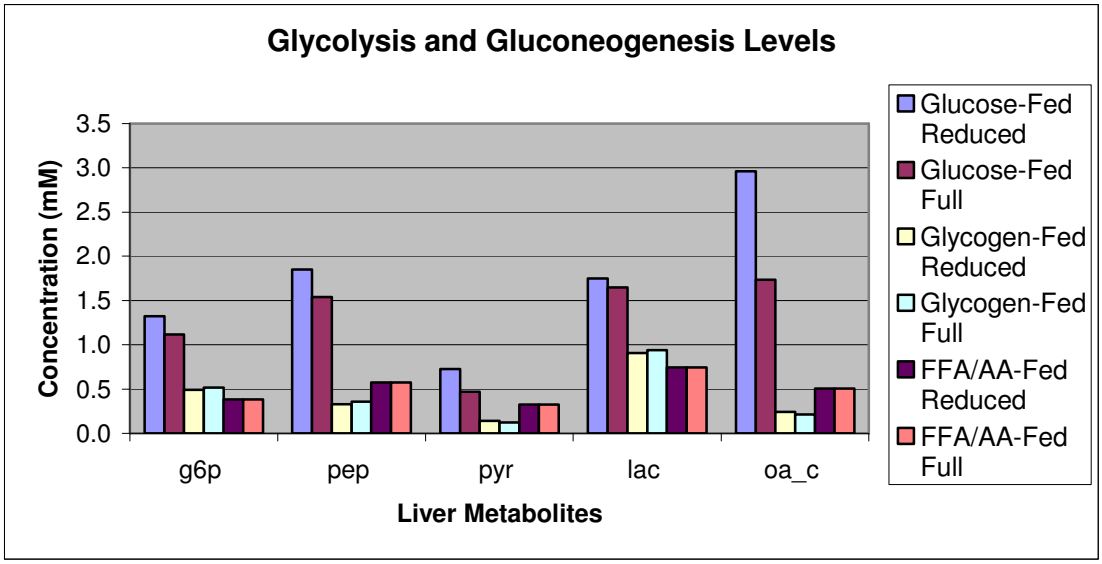

Figure 5.4. Simulation Results: Glycolytic and Gluconeogenic Intermediate Levels During the Three Feeding Stages. The blue and maroon bars represent a glucose-fed stage and are notably increased for the metabolites involved in both glycolysis and gluconeogenesis. Cytosolic oxaloacetate (oa_c), the only metabolite here involved in gluconeogenesis but not glycolysis, is increased in the glucose-fed stage due to excess glucose cycling back. The main difference between the two models is that the level of oxaloacetate is controlled by the model with the full glycogen regulatory circuit. This is due to the excess glucose being stored as glycogen rather leaking through the system. (g6p, glucose 6-phosphate; pep, phosphoenolpyruvate; pyr, pyruvate; lac, lactate; oa_c, oxaloacetate)

During the glucose-fed state (blue and maroon bars in Figure 5.4), the concentrations of metabolites involved in glycolysis, specifically glucose-6-phosphate (g6p), phosphoenolpyruvate (pep), pyruvate (pyr) and lactate (lac), are raised due to the excess of glucose in the system. While cytosolic oxaloacetate (oa_c) is not involved in glycolysis, its level is also increased during a glucose-fed state due to the excess glucose fed into the TCA cycle and then distributed back through the gluconeogenic pathway. The levels of cytosolic oxaloacetate are higher in the simulation with the reduced

glycogen regulatory circuit than the full circuit, most likely due to the ability of the system with the full circuit to store glycogen at a faster rate. This will be discussed more later.

Metabolites in the gluconeogenic pathway, phosphoenolpyruvate (pep), pyruvate (pyr) and cytosolic oxaloacetate (oa_c) are slightly raised in the FFA/AA-fed state as glucose is being synthesized through this pathway from amino acids.

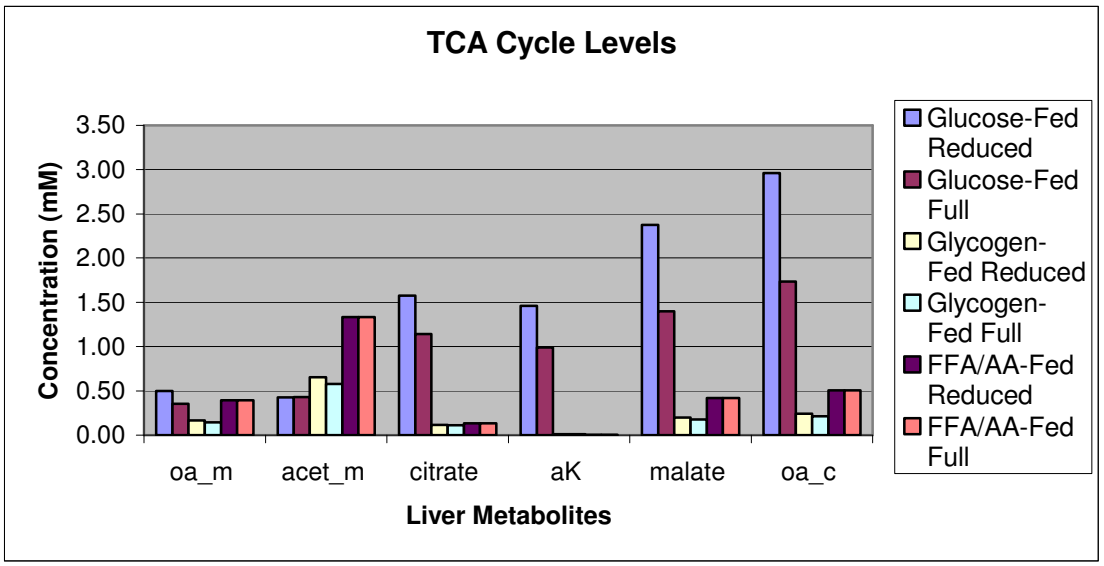

Figure 5.5. Simulation Results: TCA Cycle Intermediate Levels During the Three Feeding States. The behavior in Figure 5.4 is supported here by examining the levels of the metabolites found in the TCA cycle. In the glucose fed stage (the blue and maroon bars) citrate, alpha-ketoglutarate (aK) and malate have lower concentration levels in the model with the full glycogen regulatory circuit due to excess glucose being funneled into storage as glycogen. The concentration levels of mitochondrial acetyl-CoA (acet_m) are raised in the FFA/AA fed stage due to its involvement in the ketogenesis pathway.

The differences observed in Figures 5.4 and 5.5 are caused by the different amounts of glycogen and blood glucose present. The difference in these concentration levels are initiated by the glycogen regulatory circuit and the reaction time in which glycogen synthase is activated. This reaction time will be discussed further with a time-dependent simulation. While the system is in a state of high blood glucose levels, the full glycogen regulatory circuit fully activates glycogen synthase while the reduced circuit only partially activates glycogen synthase (Figure 5.6).

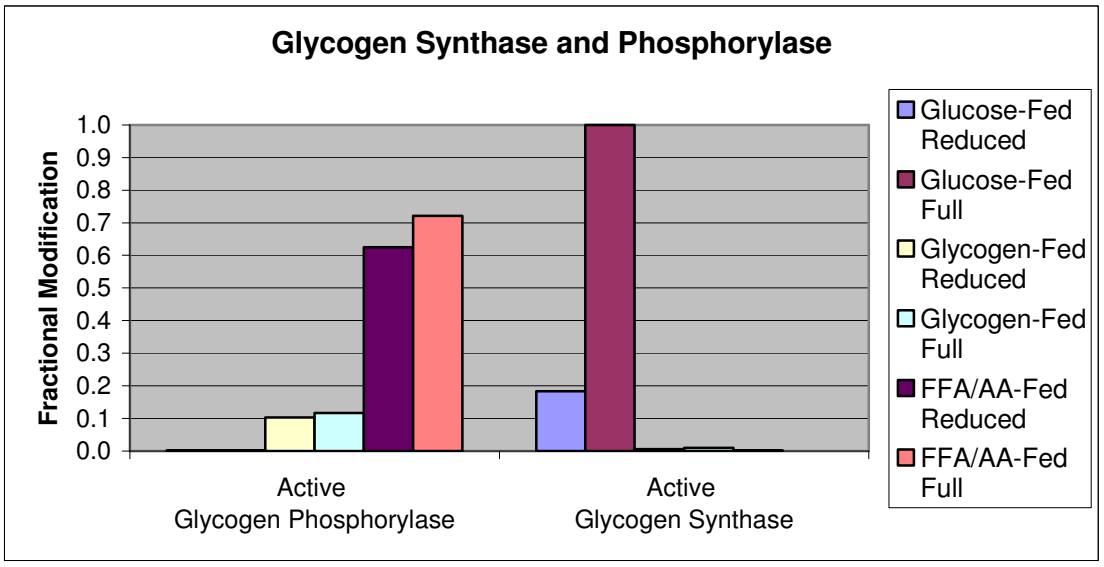

Figure 5.6. Simulation Results: Fractional Modification of Glycogen Synthase and Glycogen Phosphorylase During the Three Feeding States. Many of the differences in concentration levels seen in previous figures are a result of the amount of active glycogen synthase present in the models. For the glucose-fed stage, glycogen synthase is fully activated by the full glycogen regulatory circuit which accounts for the increased production of glycogen in the system with the full circuit.

The purpose of muscle tissue in this model is to utilize blood glucose and act purely as a sink. Further development of this model will capture the processes by which amino acids are extracted from the muscle and transported to the liver to make glucose. Fat tissue in this model utilizes and stores glucose and releases fats when blood glucose levels are low that will be transported to the liver to undergo lipolysis. As the pathways of these tissues are simplified, Figure 5.7 shows that the metabolic concentration levels mimic the levels of blood glucose. Figure 5.8 verifies that in spite of this simplification, expected behavior of an inverse relationship between blood glucose levels and the levels of fats and ketones is captured by this model.

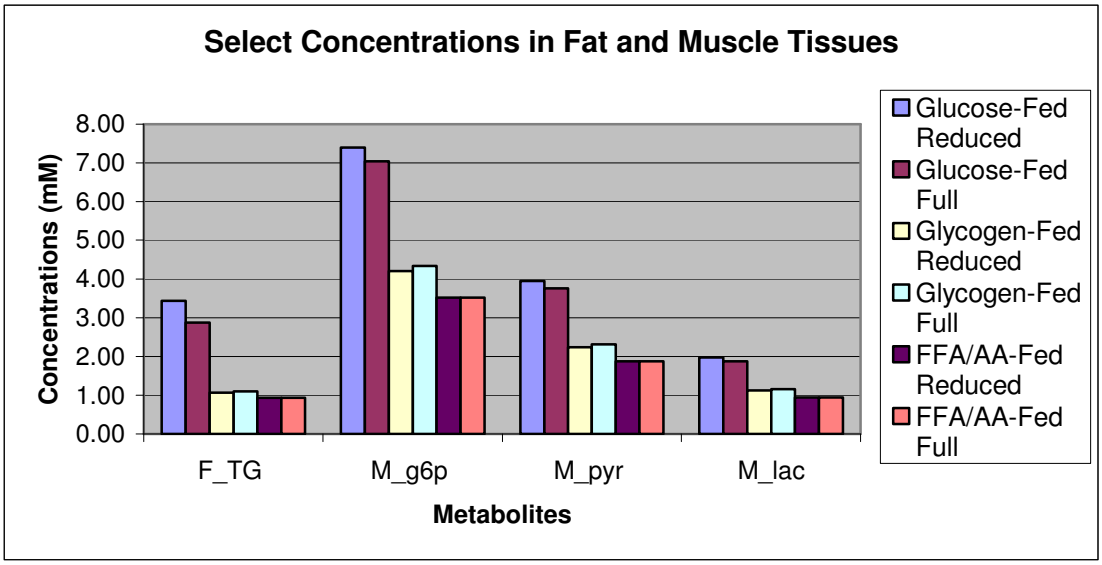

Figure 5.7. Simulation Results: Select Concentrations in Fat and Muscle Tissues During the Three Feeding States. Highest levels are observed in the glucose-fed system due to excess glucose. These mimic the levels of blood glucose as they all are results of blood glucose being transport into respective tissues.

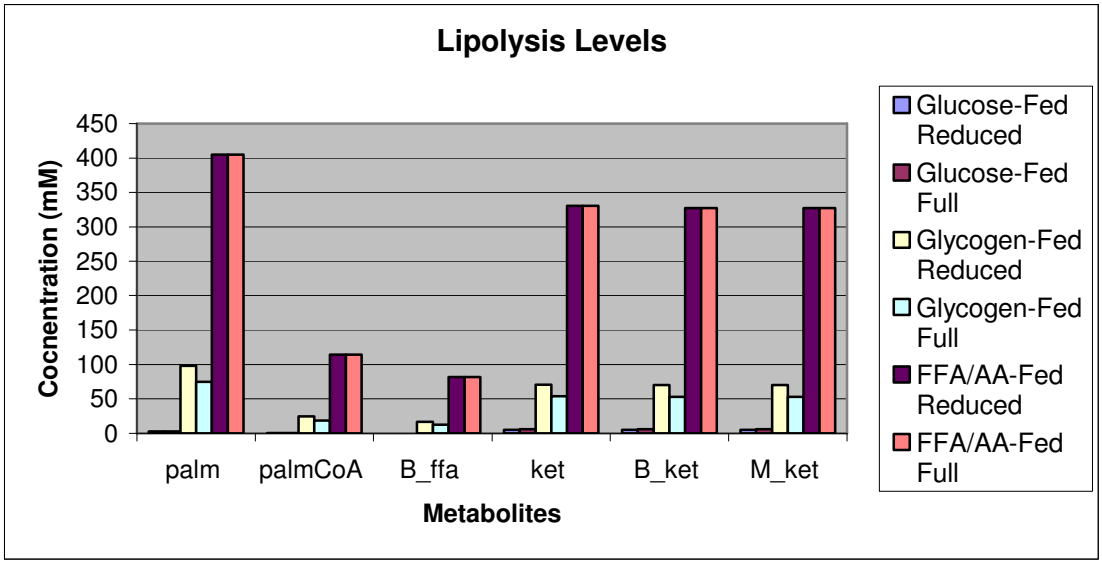

Figure 5.8. Simulation Results: Lipolysis Levels During the Three Feeding States. Fats assist in regulating blood glucose levels but have the dangerous side affect of higher ketone body levels. The activity of lipolysis increases as the system transitions from one feeding stage to another. (palm, palmitate; palmCoA, palmitate-CoA; B_ffa, blood free fatty acids; ket, ketone bodies; B_ket, blood ketone bodies; M_ket, muscle ketone bodies)

A look at the time-dependent behavior of glycogen as the system is reaching a steady state (Figure 5.5 **B**) in a glucose-fed environment shows that a steady state is not reached for the glycogen concentration. A time series for the net flux of glycogen synthesis (Figure 5.5 **D**) revealed that this reaction has reached equilibrium and that the net flux is positive resulting in a growing concentration of glycogen Other variables were observed and glycogen was the only one for which a steady state was not reached. For the fasted simulations, the initial condition of glycogen is chosen arbitrarily and is the same for both the full and reduced models. It is important to note that the full model (*black*) stores glycogen at a higher rate than the reduced model (*orange*). This is a direct

result of the elevated levels of active glycogen synthase in the model with the full regulatory circuit.

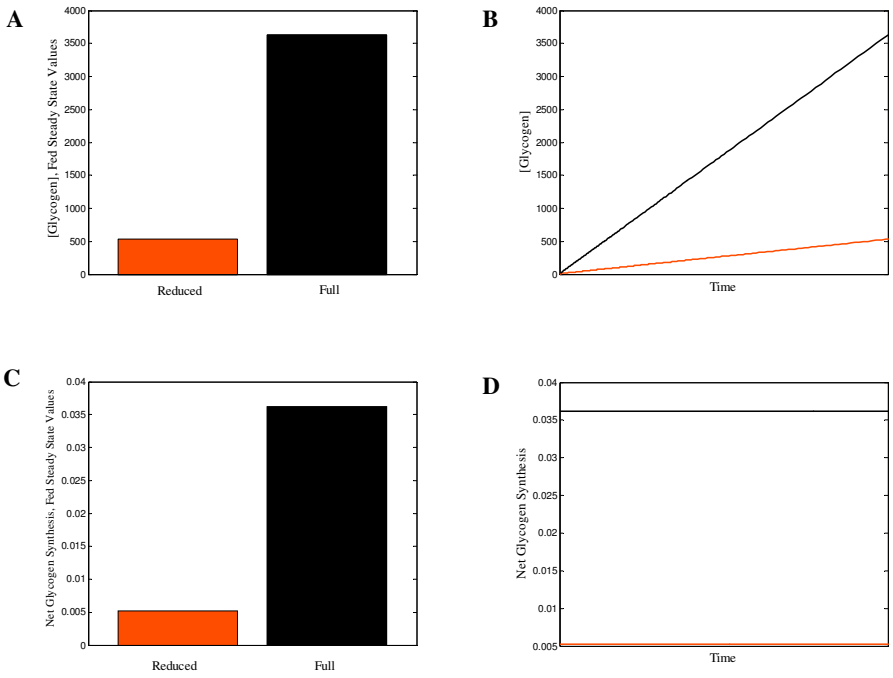

Figure 5.9. Values of Glycogen and Net Glycogen Synthesis for a Glucose-Fed Steady State. The amount of glycogen is significantly higher in the full model than in the reduced in the fed steady state, figure **A**. However, observation of glycogen levels over time, figure **B**, reveal that glycogen is not in a true steady state. Figures **C** and D show the levels of net glycogen synthesis, respectively. Figure **C** shows that net glycogen synthesis is increased in the model with the full circuit and Figure **D** shows that this flux is at equilibrium. Thus, the glucose-fed system is at a quasi-steady state.

5.4 Time-Dependent Simulations: Monotonically Increasing Blood Glucose Levels

The main difference between the full and reduced glycogen regulatory circuits discovered through the investigation above was that the model with the full regulatory circuit was capable of storing more glycogen. A system efficient in storing glycogen as a source of glucose substrate while in a fed stage can be beneficial to a system by providing the means of stabilizing blood glucose levels during a post-fed or post-absorption stage. To investigate this difference of the amount of glycogen storage, time-dependent simulations were run. First, the transition of the system from a starved state to a fed state was simulated by starting blood glucose at a low level and forcing this concentration to increase over time. This was done in the model by bring the system to a fed quasi-steady state while initializing blood glucose to have a concentration of 0 mM. The rate at which blood glucose increased was kept constant at $\frac{d[Bgluc]}{dt} = 0.01$. This behavior for blood glucose is seen in Figure 5.10 **a** while the resulting behavior of glycogen levels is seen in Figure 5.10 **b**. The glycogen is quickly used up in both simulations as blood glucose levels are detrimentally low. Once blood glucose levels have (artificially) increased and surpassed the critical concentration level of 8 mM, the system shifts from utilizing glycogen to storing glycogen. Once again, the simulation with the full glycogen regulatory circuit stores more glycogen and it appears that this is due to the system switching to a glycogen-storing state more quickly than the other model.

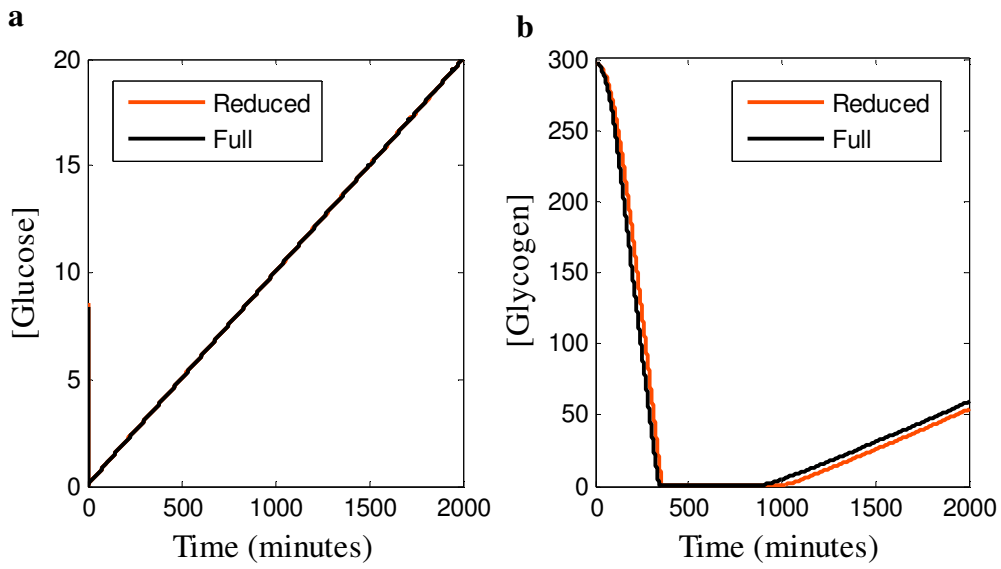

Figure 5.10. Time-Dependent Simulation: Glucose and Glycogen Levels. Glucose has a constant feeding rate. Glycogen is depleted and then starts to build after glucose reaches a critical level (8 mM) at which the insulin/glucagon switch is activated. The model with the full circuit stores more glucose as it initiated glycogen storage more rapidly.

This glycogen utilizing/storing switch that occurs in the system, as a result of the glucagon/insulin switch discussed earlier, affects the amount of glycogen stored by controlling the rates of glycogen synthesis and degradation. It is shown in Figure 5.11 that the behavior of insulin and glucagon blood levels (**a** and **b** respectively) are very similar when comparison the simulations with the full glycogen regulatory circuit and the reduced circuit. This switch-like behavior of insulin and glucose is shown in relative comparison to blood glucose levels (**c**) which reach 8mM at around $t = 800$. While there is minimal difference in the responsive behavior of insulin and glucagon, there is a significant difference in the timing at which glycogen synthase is activated. Figure 5.11 **d** compares the relative levels (magnified 15x) of active glycogen synthase (GSa) for

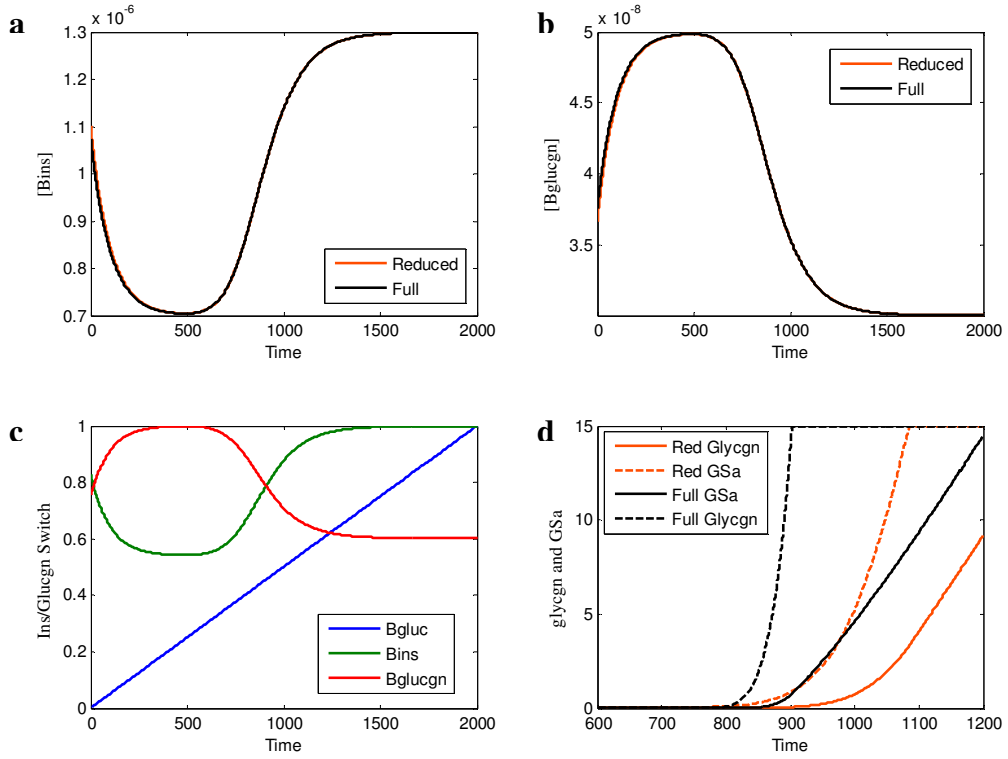

Figure 5.11. Simulation Results: Insulin and Glucagon Levels Compared to Glycogen Synthase Activation. Figures **a** and **b** compare levels of insulin and glucagon respectively between the models with the full regulatory circuit and the reduced circuit. Results are shown from the model with the full regulatory circuit in figure **c** demonstrating the switch-like behavior of these two hormones occurring in response to blood glucose levels increasing. Though insulin and glucagon levels are similar in each model, figure **d** shows a significant difference in the activation of glycogen synthase resulting in the greater buildup of glycogen in the model with the full regulatory circuit. The activation switch for glycogen synthase is quicker causing a higher initial rate of glycogen synthesis.

each circuit along with the corresponding glycogen levels. Though both models appear to activate glycogen synthase and thus build glycogen at approximately the same time (t = 800), the activation of glycogen synthase with the full circuit is much faster than that of

the reduced circuit resulting in more glycogen stored. This difference in the rate of synthesis is evident between t = 800 and t = 1100 where the rate of synthesis appears to become equal. This lends support to the idea that the glycogen regulatory circuit is vital to maintaining precise transition for the system during perturbation.

Heatmaps will be used to investigate this difference in the rate of glycogen synthesis as well as other rates of select processes in the system. Heatmaps are generated using an array of colors to correspond to the various levels of flux in the system. The assigned colors for these heatmaps are specified in Figure 5.12 with blue corresponding to a value of -5, orange corresponding to a value of 0 and red corresponding to a value of 2. While some heatmaps will show the actual level of flux for a reaction, some heatmaps will be used to compare fluxes between two simulations.

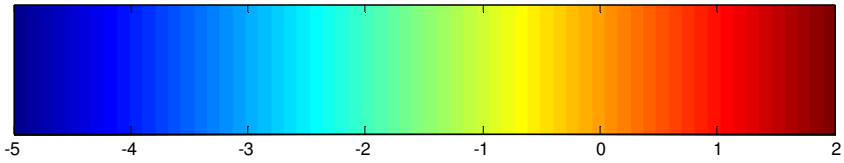

Figure 5.12. Color Bar Scale for Flux Heatmaps. A series of heatmaps will be presented in which the amount of flux for select processes throughout the system are graphically represented by a color coded map. The color bar above gives the scaling used in most color maps, or heatmaps, with orange corresponding to a value of 0, red corresponding to a value of 2 and blue corresponding to a value of -5.

The first heatmap, shown in Figure 5.13, displays the various fluxes involving glucose 6-phosphate. This metabolite is involved in many processes and acts as an intersection connecting various metabolic pathways. Glucose 6-phosphate is also the

only metabolite from which glycogen can be synthesized. As seen earlier, this occurs through other intermediate metabolites (glucose 1-phosphate and UDP-glucose) which were left out for simplification purposes. Row 1 of the heatmap show the overall rate of

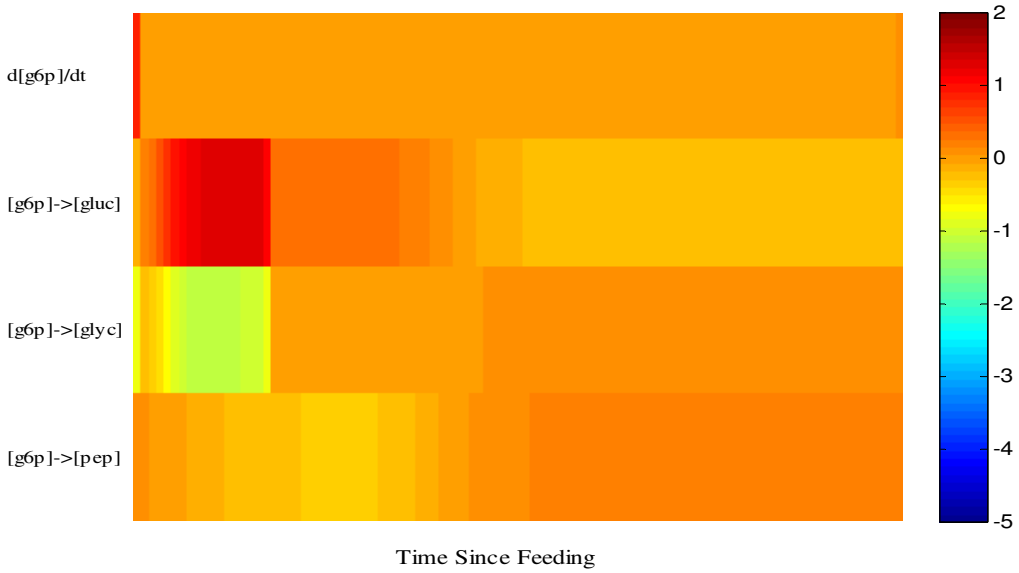

Figure 5.13. Simulation Results: Heatmap for Glucose 6-Phosphate Flow. Glucose 6-phosphate is involved in multiple pathways in the system. This heatmap is a result of a simulation for the model with the full glycogen regulatory circuit and compares the total rate of change for glucose 6-phosphate (row 1) with the net rates of change for the separate pathways of glycogen synthesis (row 2), glucose production (row 3) and gluconeogenesis/glycolysis (row 4). It is easily seen that in the beginning of the simulation, where blood glucose levels are low but rising and glycogen is still present, the dominate direction of flow is from glycogen to glucose 6-phosphtate to glucose. In the latter stages of this simulation, the system has settled into a pattern of glucose 6-phosphate being formed from glucose and then being processed into glycogen.

change for glucose 6-phosphate ($\frac{d[g6p]}{dt} = v_{L1} + v_{-L2} + v_{-L3} - v_{-L1} - v_{L2} - v_{L3}$) while the remaining rows show the net rate of change for the three bidirectional pathways ($[g6p] \rightarrow [gluc]$: $v_{-L1} - v_{L1}$; $[g6p] \rightarrow [glycgn]$: $v_{L2} - v_{-L2}$; $[g6p] \rightarrow [pep]$: $v_{L3} - v_{-L3}$).

Extending this investigation to the entire fluxome (collection of fluxes) of the liver allows for a more complete understanding of the dynamics of the system during a transitional feeding stage. The processes for the liver are detailed in Table 5.1 and the fluxes for these processes are portrayed in a heatmap in Figure 5.14. Like the previous figure for the flow of glucose 6-phosphate, this figure is taken from simulation results for the model with the full glycogen regulatory circuit. Two major shifts occur, the first being at the beginning of the simulation and the other at around t = 800. The first shift is due to the adjustment of the system to current feeding condition. The initial conditions were determined from a running the system to a quasi-steady state. The second major shift, around t = 800, occurs after glucose has reached the critical value of 8 mM and the insulin/glucagon switch has occurred. A detailed description follows of the information this fluxome heatmap contains.

When glycogen is still present in the system (t < 350), the rates of glycogen degradation and the conversion of glucose 6-phosphate to glucose are increased as glycogen is being used as a source of glucose substrate. Glycogen is nearly depleted for 350 < t < 800 and the system displays many signs of being in a low glucose state. During this time, glycogen synthase is almost entirely in the inactive state while glycogen phosphorylase is in an active state, as seen in Figure 5.15. The rates of glycogen synthese (v_{L2}) and degradation (v_{-L2}) are both low as little active GS is present and little glycogen is present for active GP to convert to glucose 6-phosphate. While some futile

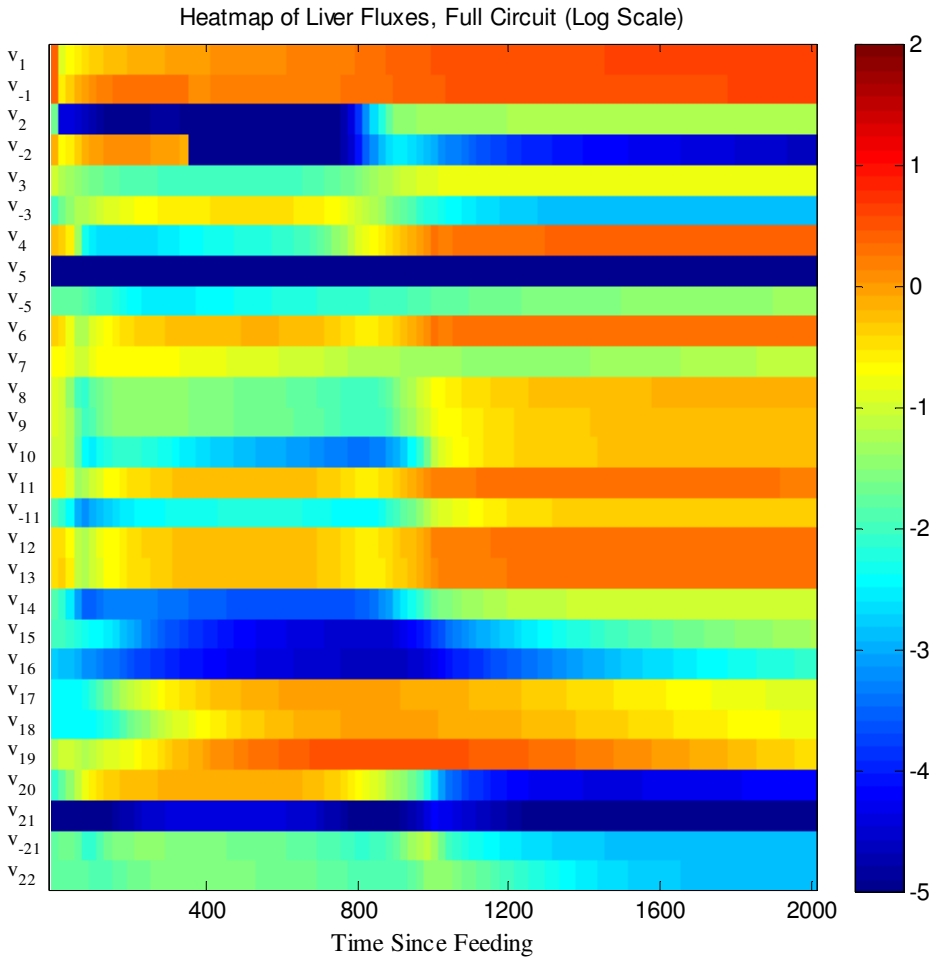

Figure 5.14. Time-Dependent Simulation: Heatmap for Liver Fluxes, Full Circuit. This heatmap detailed the fluxome for the liver during a transition from low blood glucose levels to high blood glucose levels. Two major shifts are seen in the fluxome, the first due to an adjustment of the system to low blood glucose levels, the second due to glucose reaching a critical level of 8 mM causing the system to shift into a well-fed state. The text gives a detailed description of the fluxome behavior for the system. The corresponding rate of each reaction is described in the text and also can be found in the appendix.

cycling occurs, it is kept to a minimum, conserving energy, as little glycogen is being made due to this low level of active glycogen synthase. A bidirectional flow occurs

between glucose 6-phosphate and phosphoenolpyruvate and from the heatmap it is clearly seen that the dominant direction of this flow is from phosphonenolpyruvate to glucose 6-phosphate as v-L3 is greater than v_{L3}. These metabolites are in both pathways of glycolysis (converting glucose to energy) and gluconeogenesis (converting amino acids to glucose with the assistance of fats). The conversion of phosphoenolpyruvate to glucose 6-phosphate being more prominent indicates that the level of gluconeogenesis is greater that that of glycolysis while the system is in a state of low glucose levels. The fluxes for other process involved in gluconeogenesis (v_{L11}, v_{LI2}, v_{L13}, v_{L20} and $v_{\text{-}L21}$) are active during this time. Fluxes for process involved in the TCA cycle (v_{L8}, v_{L9}, v_{L10}, $v_{\text{-}L11}$) are decreased during a time of low glucose levels as there is little substrate for this cycle provided from glucose. The rates of lipolysis (v_{L17}, v_{LI8}) and ketogenesis (v_{L19}) are also increased in the simulation corresponding with the increased breakdown of fats that occurs in order to provide the necessary energy to convert amino acids to glucose via gluconeogenesis. Two interesting questions that arise are why are fats unable to be used in place of glucose to provide energy for the cell and why are fats themselves unable to be converted to glucose? While this thesis does not answer these questions, this model could be used in an attempt to do so.

This heatmap displays the major shift in the fluxome as the system transitions from a low glucose state to a fed state (approximately $t = 800$). Conversion between glucose and glucose 6-phosphate appears to occur at comparable rates. With glucose levels above 8 mM, more glucose should be converted to glucose 6-phosphate rather than from glucose 6-phosphate. Futile cycling for the synthesis and degradation of glycogen increases as

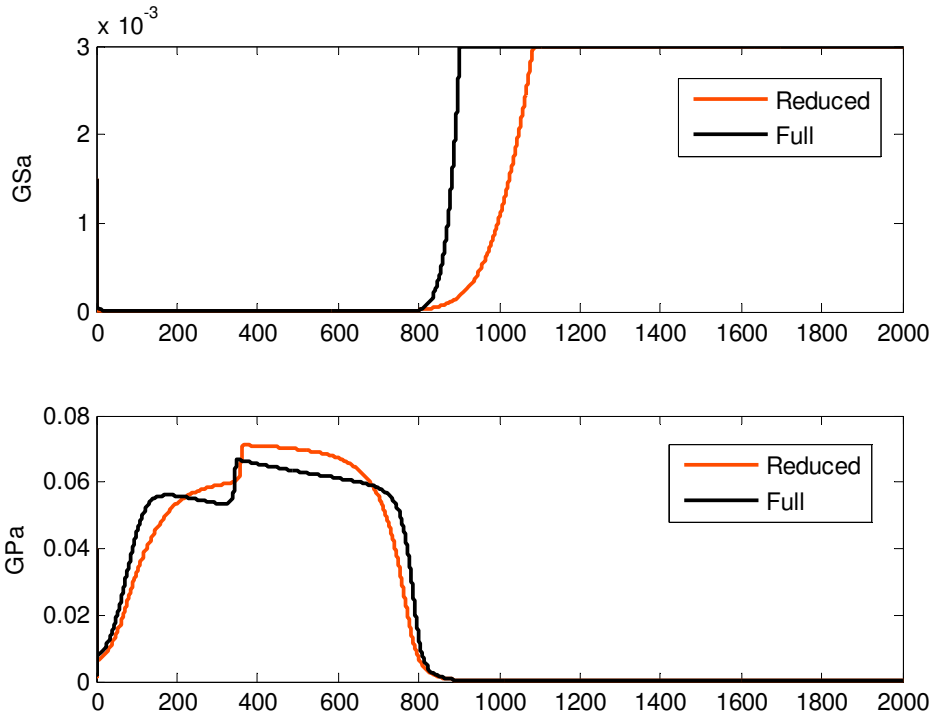

Figure 5.15. Time-Dependent Simulation: Active Glycogen Synthase and Active Glycogen Phosphorylase Levels. While active glycogen phosphorylase levels are similar between the two simulations, there is a significant difference in timing for which glycogen synthase becomes activated. The switch reacts more quickly for the model with the full glycogen regulatory circuit, allowing for glycogen to be made more efficiently when glucose levels reach the critical point of 8 mM.

both fluxes increase (v_{L2} and $v_{\text{-}L2}$). The synthesis of glycogen clearly occurs at a greater rate indicating a positive net storage of glycogen. Glycolysis rates have increased (v_{L3}, v_{L4}, v_{L5}) as well as activity of the TCA cycle (v_{L6}, v_{L8}, v_{L9}, and v_{L10}) and lipogenesis (v_{L14}, v_{L15}, v_{L16}). The only questionable shift for fluxes in this simulation is for the fluxes involved in gluconeogenesis (v_{L11}, v_{L12}, v_{L13}, v_{L20} and $v_{\text{-}L21}$). While those pertaining to the breakdown of amino acid alanine (v_{L20} and $v_{\text{-}L21}$) for the carbon substrate in gluconeogenesis are decreased during a state of high glucose levels, the remaining fluxes

(v_{L11}, v_{L12}, and v_{L13}) have increased. Some of this subtrate is cycled back through the TCA cycle via v_{L4} but some is also converted back to glucose and accounts for why v_{L1}, and v_{-L1} are approximately equal and the net synthesis of glucose from glucose 6-phosphate is approximately 0 during a time of high glucose levels. While this appears to be inconsistent with known behavior of metabolism for a system with high blood glucose levels, this should not have an affect on the activity of glycogen storage and degradation.

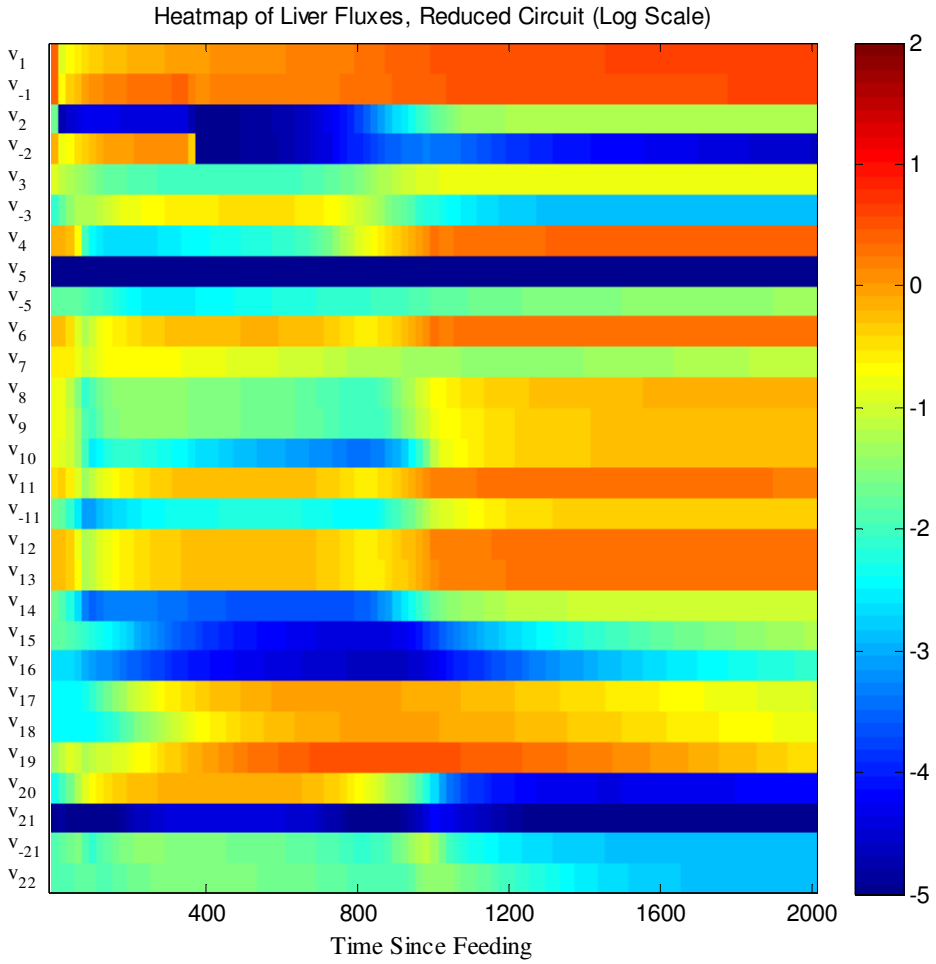

Figure 5.16. Time-Dependent Simulation: Heatmap for Liver Fluxes, Reduced Circuit. This heatmap is very similar to that in Figure 5.14 for the simulation with the full glycogen regulatory circuit. See text for a full description.

This simulation was repeated with the reduced glycogen regulatory circuit. The resulting heatmap for the hepatic fluxome is shown in Figure 5.16 and is nearly indistinguishable from the heatmap for the fluxome with the full regulatory circuit. In order to compare the fluxomes from these simulations, a ratio was created of the fluxome from the full circuit model to the fluxome of the reduced circuit model and displayed using a logarithmic scale, resulting in Figure 5.17. Values of 0 in this heatmap correspond to ratios of 1 meaning that there is no difference between the fluxome level of that process in the full circuit model and the reduced circuit model. In the beginning, many flux levels are lower in the full circuit model than in the reduced circuit model as evident by the lighter shades of orange in the heatmap for $t < 200$. This could be accounted for by the glycogen being depleted at a slightly faster rate in the reduced circuit model (see Figure 5.10) providing more substrate for these processes. The other (quite) notable difference in these fluxomes is the rates of glycogen synthesis and degradation. For $t < 800$, the rate of glycogen degradation is comparable but the rate of glycogen synthesis is greater in the reduced circuit model than in the full circuit model suggesting a greater amount of futile cycling in the former. If an extreme deficit of blood glucose exists, futile cycling could be detrimental to the system by using unnecessary energy. When glycogen is nearly depleted ($400 < t < 800$) both rates are lower in the full circuit model than in the reduced circuit model. As these processes are never fully stopped, some futile cycling occurs at all times but for $t < 800$ this futile cycling occurs at a greater (and possibly non-optimal) rate for the reduced circuit model. Once blood glucose levels reach the optimal value of 8 mM (at approximately $t = 800$), the full circuit now shifts to having a greater level of futile cycling as both rates of glycogen synthesis

and degradation are greater than those in the reduced circuit model seen by a darker shade of red corresponding to a positive value. The increase of the glycogen synthesis flux is due to the activation of glycogen synthase (which occurs earlier in the full circuit model). Glycogen phosphorylase is still activated around t = 800 (see Figure 5.15, note the glycogen phosphorylase is active for a longer period in the full circuit model simulation) resulting in this increase in futile cycling.

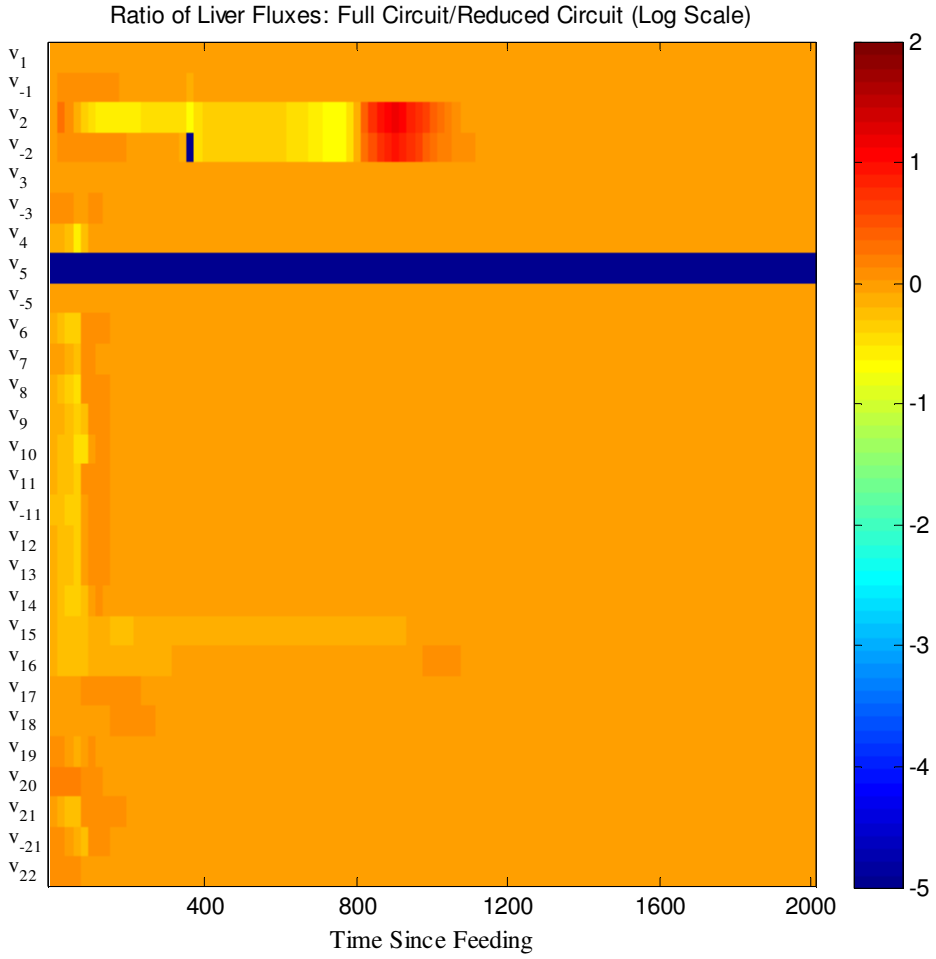

Figure 5.17. Heatmap of the Ratio of Liver Fluxes, Full to Reduced. The largest difference observed in the liver fluxes is between glycogen synthesis and glycogen phosphorylase. Activity for both fluxes increased in model with full circuit. Introduce the presence of futile cycling.

5.5 Time-Dependent Simulations: Oscillatory Feeding Pattern

Previous simulations have shown that the architecture of the physiological glycogen regulatory circuit decreases response time in the activation/deactivation switch for glycogen synthase and glycogen phosphorylase during transitory feeding periods. The typical human experiences a periodic feeding function by digesting three meals

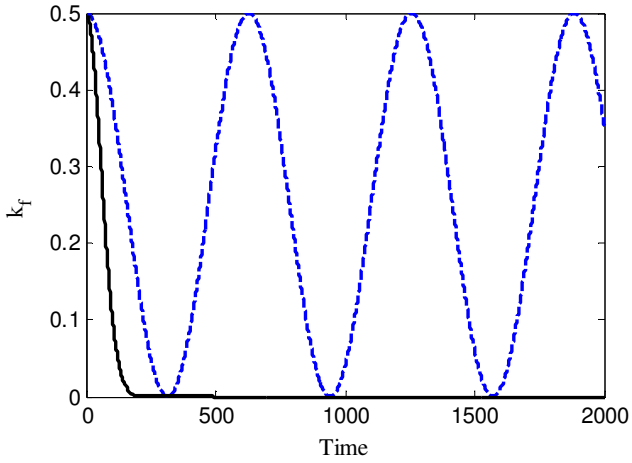

Figure 5.18. Oscillatory Feeding Function. To model a periodic feeding pattern the rate at which glucose is ingested is set to $k_{feed} = .25\cos(.01t) + .25$, shown by the blue dashed line. This feeding function is shown in comparison to the feeding function used to model a fasting period (see figure 5.1) in which ingested glucose decreases (kf based on a normal distribution of $k_{feed} = \frac{e^{\frac{-(.014t-\mu)^2}{2\sigma^2}}}{\sigma\sqrt{2\pi}}$ with $\mu = 0$, $\sigma = \frac{1}{k_f\sqrt{2\pi}}$ and $k_f = 0.5$.

spaced throughout a day. This next simulation uses an oscillatory feeding function ($k_{feed} = .25\cos(.01t) + .25$) to mimic this behavior of a periodic ingestion of glucose. Figure 5.18 gives a plot of this feeding function.

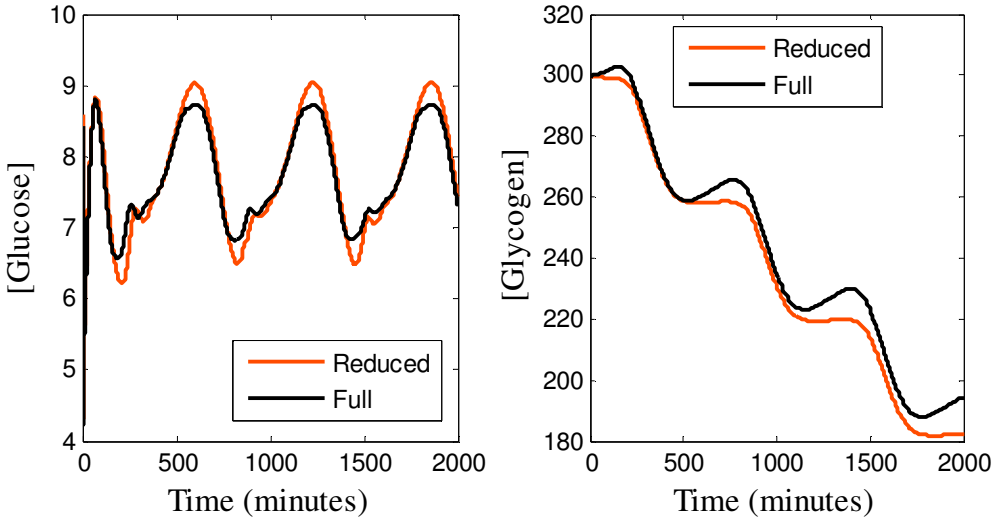

Figure 5.19. Oscillatory Feeding Simulation: Glucose and Glycogen Levels. The full regulatory circuit keeps glucose levels closer to desired 8 mM level (**a**). Glycogen is seemingly preserved in model with full circuit (**b**).

The differences in blood glucose levels in Figure 5.3 (steady state blood glucose values for the three feeding stages) were not considered to vary greatly between the two models. Creating a pattern of oscillatory feeding for the system suggests that these differences observed throughout the system may enable a better stabilization of blood glucose levels by regulating the level remain near the value of 8 mM (see Figure 5.19 **a**). In figure **b**, there is a similarity in the rate of glycogen degradation for the two models but an obvious increase of glycogen synthesis for the model with the full circuit.

Figure 5.20 shows blood glucose levels along with a heatmap for liver fluxes corresponding to the glucose levels for oscillatory feeding for the model with the full glycogen regulatory circuit. It is again verified that this system is driven by glucose in that most reactions are reduced when blood glucose levels are low with the exception of glycogen degradation, to stabilize glucose levels, and the breakdown of amino acids for making glucose via gluconeogenesis.

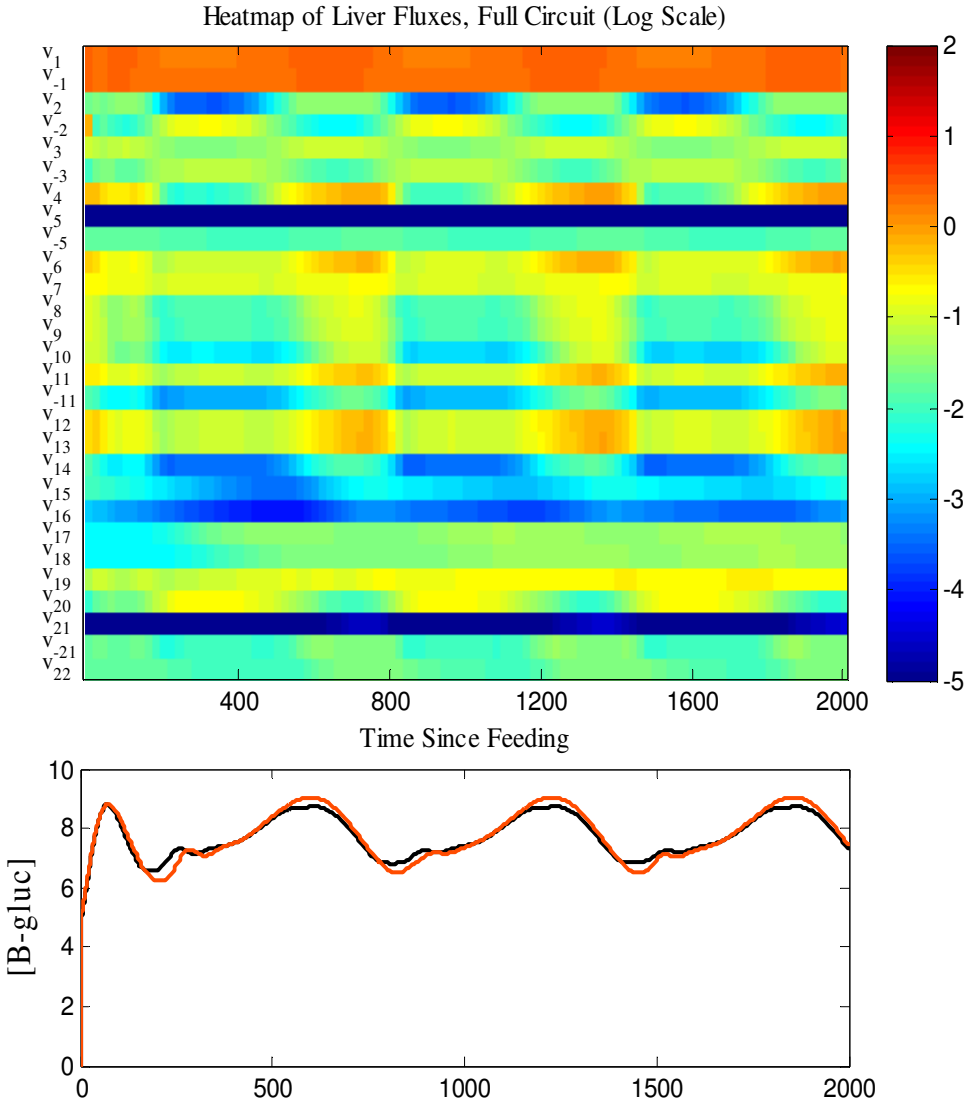

Figure 5.20. Oscillatory Feeding Simulation: Heatmap for Liver Fluxes, Full Circuit, With Glucose. Fluxes are shown (**a**) in relation to blood glucose levels (**b**). During times when blood glucose is less than 8 mM, most reactions are reduced with the exception of glycogen degradation (v_{-2}) and the breakdown of amino acids for gluconeogenesis (v_{20}).

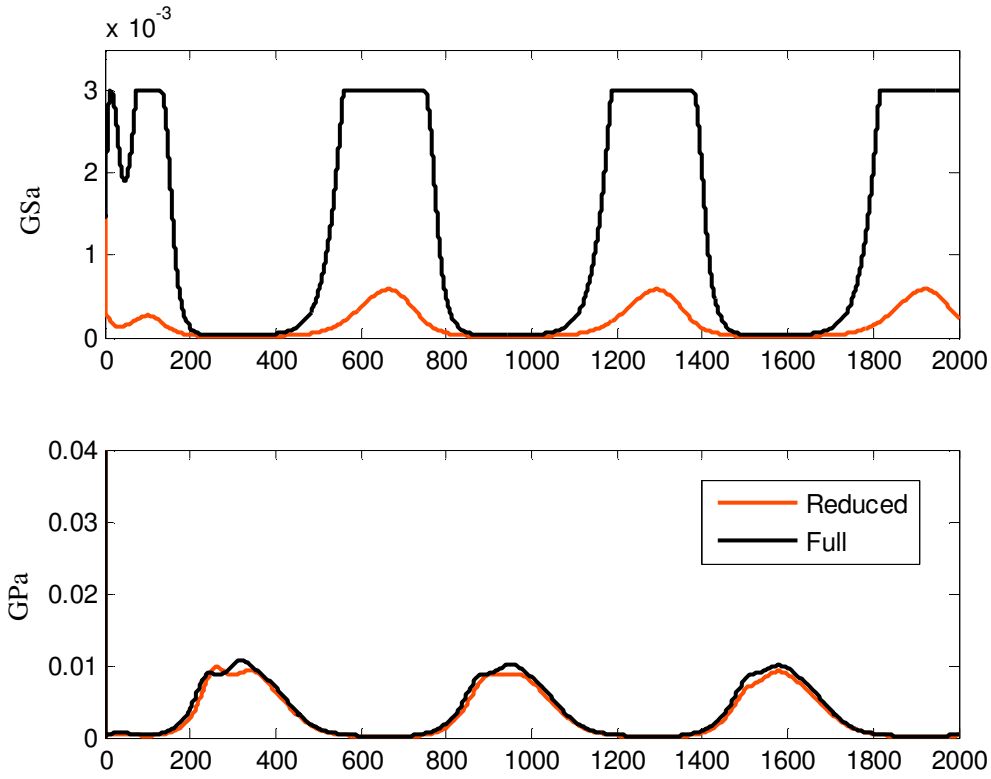

Figure 5.21. Oscillatory Feeding Simulation: Glycogen Synthase and Glycogen Phosphorylase Activity. As with the previous feeding pattern, little difference is seen in the glycogen phosphorylase levels (**b**) between the two regulatory circuits. Glycogen synthase, however (**a**) varies in both the reaction time of activation and also the level of activation.

The levels of activated glycogen synthase were observed to be grossly different between the model with the full circuit and that with the reduced circuit during the steady state simulations for the various feeding stages (Figure 5.6). The previous time-dependent simulation showed that the reaction time of activation was quicker in the model with the full glycogen regulatory circuit but the levels of activated glycogen synthase were comparable. In this simulation with an oscillatory feeding pattern, both

the quicker reaction time of activation and the higher level of active glycogen synthase are observed in the model with the full circuit (Figure 5.21). As before, glycogen phosphorylase shows little difference between the two models.

The heatmap in Figure 5.22 shows that the level of fat transport from fat tissue to the liver is greater in the model with the full glycogen regulatory circuit (v_{tF3} and v_{tL5}). It would seem reasonable to think that the model with the more active fat transport would also have a greater rate of ketone transport from the liver to the blood. However, Figure 5.23 shows this is not the case as ketone transport from the liver to the blood (v_{tL3}) is lower in the model with the full circuit. Figure 5.23 also shows that ketone body levels in the blood are higher in the model with the reduced circuit. This suggests that the model with the full regulatory glycogen circuit is able to utilize more fats and amino acids while keeping ketone body levels at a lower, more controlled level.

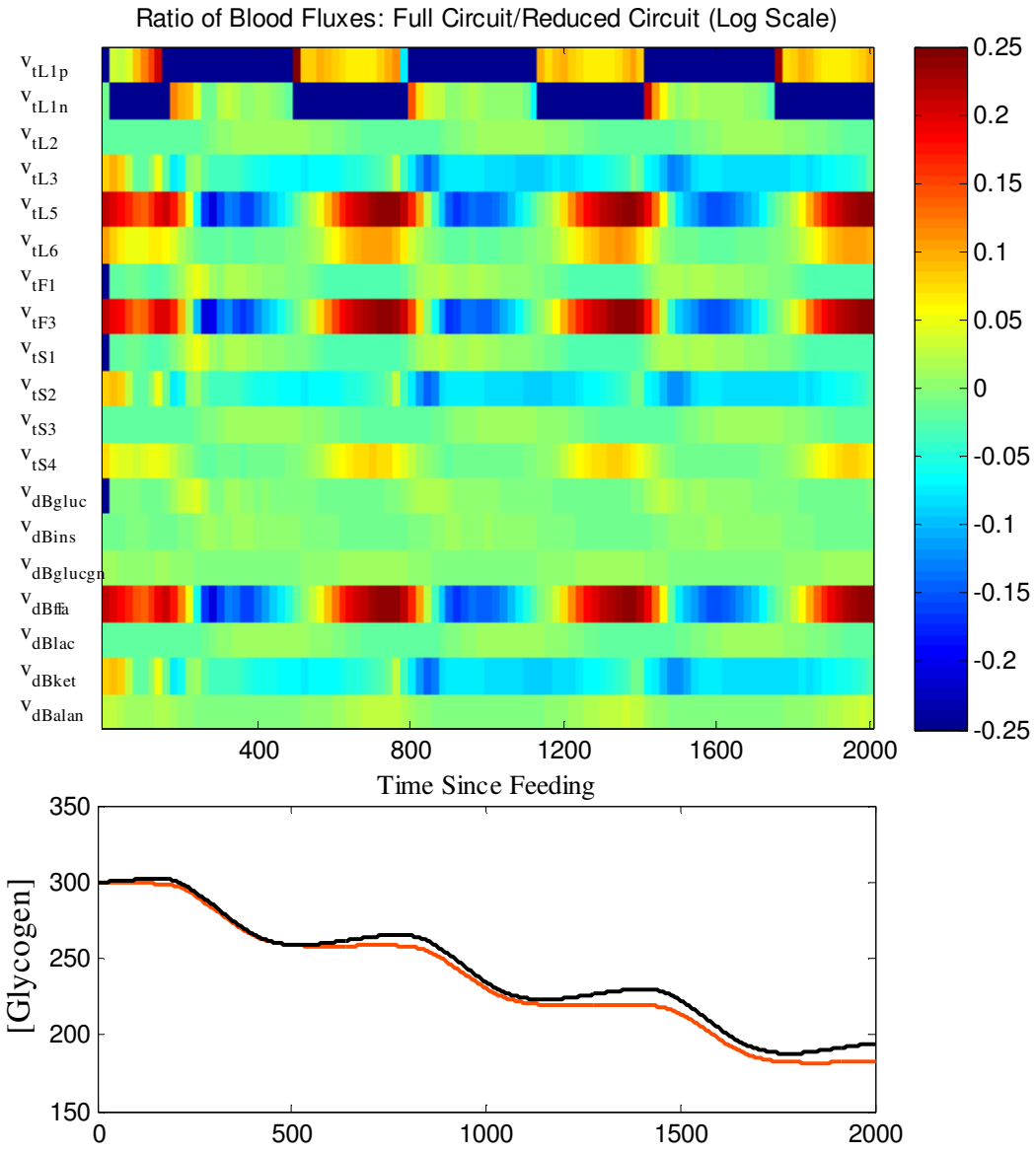

Figure 5.22. Oscillatory Feeding Simulation: Heatmap of the Ratio of Blood Fluxes, Full to Reduced, With Glycogen. Glucose direction switching (flux=0 when blue). Fat transport is higher in the model with the full glycogen circuit (v_{tF3} and v_{tL5}) while ketone body transport from the liver to the blood is lower (v_{tL3}).

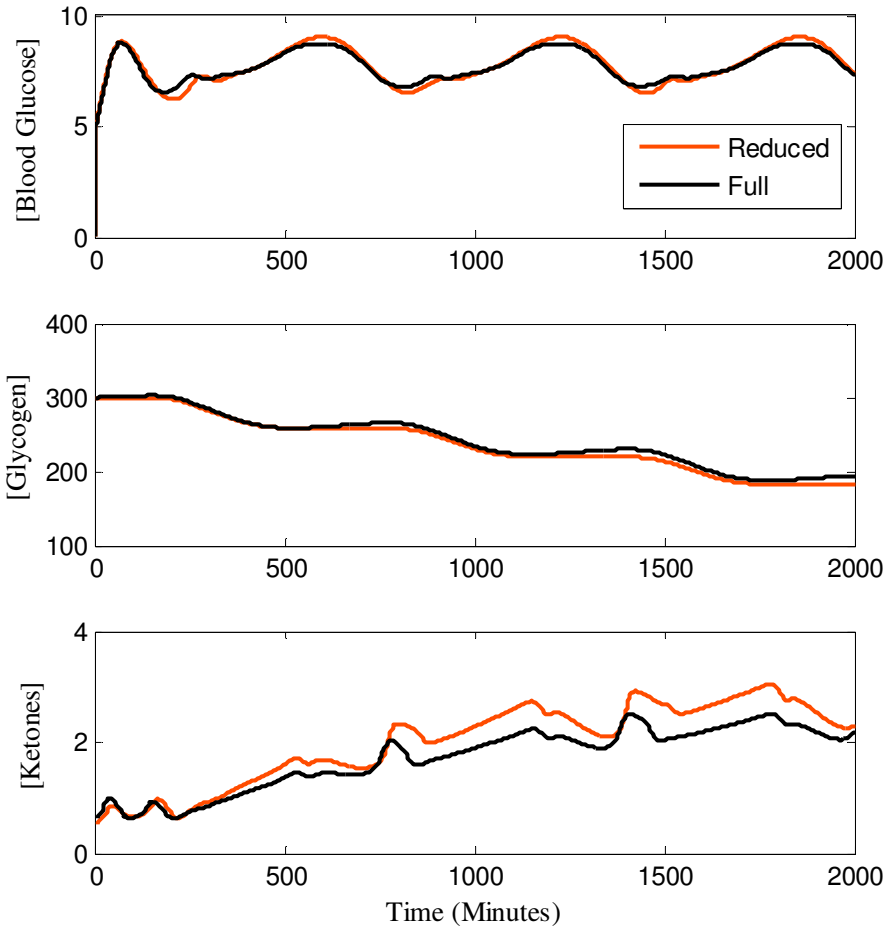

Figure 5.23. Oscillatory Feeding Simulation: Blood Glucose, Glycogen and Ketone Bodies. While the full glycogen regulatory circuit somewhat preserves glycogen and more tightly regulates glucose near the desired level of 8 mM, it also regulates the release of ketone bodies into the bloodstream.

CHAPTER 6

Future Work

6.1 Meal Variation

To reduce the complexity of whole metabolism, this model focused on the intake of a strictly glucose meal. A glucose meal provided an ideal environment to investigate the switching of glycogen regulatory enzymes as the activation of these enzymes is a result of regulation associated with blood glucose levels. As previously mentioned, meals are a combination of carbohydrates, fats and proteins which are digested to glucose, free fatty acids and amino acids, respectively. The current model includes concentrations of glucose, free fatty acids and amino acids in the blood so is capable of easily being modified to investigate a meal composed as a mixture of these digestive products. As this model was built with a purpose of investigating a fasted state, certain transport mechanisms with the model would need modified to more accurately depict the switching of feeding states. For example, the fat tissue component within the model allows uptake of glucose from and free fatty acid release to the blood but neither of these processes are reversible. To accurately model the uptake of free fatty acids from a meal, the transport mechanism of free fatty acids across the fat tissue membrane will need to be made bidirectional.

Only one size of meal was considered in this investigation when bringing the system to a fed steady state. With a strictly glucose meal, the size of meal can easily be modified within the function v_{feed}. Timing of meals is another variable to be considered when looking at glucose metabolism. This investigation focused on having initial conditions from a fed state and looking at the fasting period after this one meal in order to increase understand of the transition from a fed to fasted state. Another transition period of interest is that of moving from the fasted state to a fed state. The mechanisms necessary to stabilize blood glucose levels during this type of transition may vary depending on the size and timing of the second meal. With some modification, this model can be used to investigate variations of meals such as meal composition, meal size and timing of meals

6.2 Connecting More Subsystems

This thesis introduces the inclusion of a detailed model of the glycogen regulatory circuit into a whole-physiology, contextual model. Numerous mathematical models of specific pathways within the metabolic system have been proposed in the literature. Continuing with this model by including more detailed models of specific pathways can lead to a more accurate model depicting the role of various pathways and metabolites within the whole metabolic system.

6.3 Transcriptional Regulation

Regulation mechanisms included in this model were allosteric and hormonal in nature. The only enzymes explicitly modeled were those of the glycogen regulatory

circuit. These enzymes provided a protein layer to this model. mRNA transcripts regulate the amount of proteins, in this case enzymes, formed thus regulating the level of enzyme activity. The technology of today allows for the mass collection of data from experiments measuring the level of mRNA transcripts under specific conditions, such as fed and fasted conditions. With slight modification, this model can be used to investigate the role of transcriptional regulation in the glycogen regulatory circuit as well as the allosteric regulation that occurs in activating the enzymes.

6.4 Fluxomics

The technological advances of the day also allow for the collection of *in vivo* data about fluxes within the system. This has been done using nuclear magnetic resonance (NMR). As shown with the heatmaps depicting the various fluxes within the model, observing the fluxome, the collections of fluxes of a system, can provide important information not observed by looking at concentrations alone. This model can be further enhanced by comparing the fluxes from the model with experimental data in the literature for metabolic fluxes. This experimental data may be helpful in suggesting a more accurate parameter set. This model and NMR experimentation may be useful in identifying certain metabolic conditions through the fluxome.

6.5 Liver Glycogen and Muscle Glycogen

Though the regulatory circuits for activation of glycogen synthase and glycogen phosphorylase are very similar between liver and muscle, some important functional differences exist. Protein phosphatase-1 (PP1) dephosphorylates phosphorylase kinase,

glycogen synthase and glycogen phosphorylase in both the liver and the muscle (Fong). While other phospatases are capable of catalyzing these reactions, only PP1 was taken into consideration in the model for simplification purposes. Studies have shown that an inhibition of PP1 activity on hepatic glycogen synthase is due to the presence of glycogen phosphorylase [24]. This mechanism is modeled by the binding of GPa and PP1 in the liver, inactivating this PP1 in relation to glycogen synthase. While this inhibition has not been seen in the muscle, a different mechanism of inhibition has been identified. In the muscle, inhibitor-1 inactivates PP1 which affects the dephosphorylation rate of all enzymes in the cascade. The current model contains muscle glycogen but the synthesis and degradation of this glycogen has been turned off while investigating liver glycogen. Further study of this model can easily include the differences in behavior of synthesis and degradation of both liver and muscle glycogen during fed and fasted states.

APPENDIX A

Model Equations

A.1 Rates and Equations for Contextual Model

LIVER RATES:

$$v_{L1} = \frac{k_{L1}\,[gluc]}{k_{mL1} + [gluc]} \left(1 + \frac{[B\_ins]^{ep1}}{k_{Dins}{}^{ep1} + [B\_ins]^{ep1}}\right)$$

$$v_{\text{-}L1} = \frac{k_{\text{-}L1}\,[g6p]}{k_{m\text{-}L1} + [g6p]} \left(1 + \frac{[B\_glucgn]^{ep9}}{k_{Dglucgn}{}^{ep9} + [B\_glucgn]^{ep9}}\right)$$

$$v_{L2} = \frac{k_{L2}\,[GSa]\,[g6p]}{k_{mL2} + [g6p]}$$

$$v_{\text{-}L2} = \frac{k_{\text{-}L2}\,[GPa]\,[glycgn]}{k_{m\text{-}L2} + [glycgn]}$$

$$v_{L3} = \frac{k_{L3}\,[g6p]}{k_{mL3} + [g6p]} \left(1 + \frac{[B\_ins]^{ep2}}{k_{Dins}{}^{ep2} + [B\_ins]^{ep2}}\right) \left(\frac{k_{Dglucgn}{}^{en1}}{k_{Dglucgn}{}^{en1} + [B\_glucgn]^{en1}}\right)$$

$$v_{\text{-}L3} = \frac{k_{\text{-}L3}\,[pep]}{k_{m\text{-}L3} + [pep]} \left(1 + \frac{[B\_glucgn]^{ep8}}{k_{Dglucgn}{}^{ep8} + [B\_glucgn]^{ep8}}\right) \frac{k_{Dins2}{}^{en6}}{k_{Dins2}{}^{en6} + [B\_ins]^{en6}}$$

$$v_{L4} = k_{L4}\,\frac{[pep]}{k_{mL4} + [pep]} \left(1 + \frac{[B\_ins]^{ep3}}{k_{Dins}{}^{ep3} + [B\_ins]^{ep3}}\right) \frac{k_{Dglucgn}{}^{en2}}{k_{Dglucgn}{}^{en2} + [B\_glucgn]^{en2}}\, \frac{k_{i13}}{k_{i13} + [alan]}$$

$$v_{L5} = \frac{k_{L5}\,[pyr]}{k_{mL5} + [pyr]}$$

$$v_{\text{-}L5} = \frac{k_{\text{-}L5}\,[lac]}{k_{m\text{-}L5} + [lac]}$$

$$v_{L6} = \frac{k_{L6}\,[pyr]}{k_{mL6} + [pyr]} \left(1 + \frac{p_2\,[acet\_m]}{k_{p2} + [acet\_m]}\right) \left(1 + \frac{[B\_glucgn]^{ep4}}{k_{Dglucgn}{}^{ep4} + [B\_glucgn]^{ep4}}\right)$$

$$v_{L7} = \frac{k_{L7}\,[pyr]}{k_{mL7} + [pyr]} \frac{k_{i8}}{k_{i8} + [acet\_m]}$$

$$v_{L8} = k_{L8}\,[oa\_m]\,[acet\_m] \frac{k_{i4}}{k_{i4} + [palmCoA]}$$

$$v_{L9} = k_{L9}\,[citrate]$$

$$v_{L10} = k_{L10}\,[aK]$$

$$v_{L11} = k_{L11}\,[oa\_m] \left(1 + \frac{[B\_glucgn]^{ep5}}{k_{Dglucgn}{}^{ep5} + [B\_glucgn]^{ep5}}\right)$$

$$v_{-L11} = k_{-L11}\,[malate]$$

$$v_{L12} = k_{L12}\,[malate] \frac{k_{Dins}{}^{en4}}{k_{Dins}{}^{en4} + [B\_ins]^{en4}} \left(1 + \frac{[B\_glucgn]^{ep6}}{k_{Dglucgn}{}^{ep6} + [B\_glucgn]^{ep6}}\right)$$

$$v_{L13} = k_{L13}\,[oa\_c] \left(1 + \frac{[B\_glucgn]^{ep7}}{k_{Dglucgn}{}^{ep7} + [B\_glucgn]^{ep7}}\right) \frac{k_{Dins}{}^{en5}}{k_{Dins}{}^{en5} + [B\_ins]^{en5}}$$

$$v_{L14} = k_{L14}\,[citrate] \left(1 + \frac{[B\_ins]^{ep10}}{k_{Dins}{}^{ep10} + [B\_ins]^{ep10}}\right) \frac{k_{Dglucgn}{}^{en7}}{k_{Dglucgn}{}^{en7} + [B\_glucgn]^{en7}}$$

$$v_{L15} = k_{L15}\,[acet\_c] \left(1 + \frac{p_1\,[citrate]}{k_{p1} + [citrate]}\right) \frac{k_{i5}}{k_{i5} + [palmCoA]}$$

$$v_{L16} = k_{L16}\,[acet\_c]\,[malonyl]^7$$

$$v_{L17} = k_{L17} \frac{k_{i1}}{k_{i1} + [malonyl]}$$

$$v_{L18} = k_{L18}\,[palmCoA] \frac{k_{i2}}{k_{i2} + [malonyl]}$$

$$v_{L19} = k_{L19}\,[acet\_m]^2\left(1 + \frac{[cAMP]^{ep11}}{k_{dcAMP}{}^{ep11} + [cAMP]^{ep11}}\right)\frac{k_{Dins}{}^{en8}}{k_{Dins}{}^{en8} + [B\_ins]^{en8}}$$

$$v_{L20} = k_{L20}\,[alan]\,\frac{k_{Dins2}{}^{en3}}{k_{Dins2}{}^{en3} + [B\_ins]^{en3}}$$

$$v_{L21} = k_{L21}\,\frac{[pyr]}{k_{mL21p} + [pyr]}\,\frac{[glutamate]}{k_{mL21g} + [glutamate]}\,\frac{k_{Dins}{}^{en3}}{k_{Dins}{}^{en3} + [B\_ins]^{en3}}$$

$$v_{-L21} = k_{-L21}\,\frac{[alan]}{k_{m-L21a} + [alan]}\,\frac{[aK]}{k_{m-L21k} + [aK]}\,[acet\_m]\,\frac{k_{Dins}{}^{en3}}{k_{Dins}{}^{en3} + [B\_ins]^{en3}}$$

$$v_{L22} = k_{L22}\,[glutamate]$$

BLOOD RATES (Transport and Decay):

$$v_{tL1} = k_{tL1}\,([B\_gluc] - [gluc])$$

$$v_{tL2} = k_{tL2}\,[B\_lac]$$

$$v_{tL3} = k_{tL3}\,[ket]$$

$$v_{tL5} = k_{tL5}\,[B\_ffa]$$

$$v_{tL6} = k_{tL6}\,[B\_alan]\,\frac{k_{Dins}{}^{en10}}{k_{Dins}{}^{en10} + [B\_ins]^{en10}}$$

$$v_{tF1} = k_{tF1}\,[B\_gluc]\left(1 + \frac{[B\_ins]^{ep12}}{k_{Dins}{}^{ep12} + [B\_ins]^{ep12}}\right)$$

$$v_{tF3} = k_{tF3}\,[F\_ffa]^8\,\frac{k_{Dins2}{}^{en9}}{k_{Dins2}{}^{en9} + [B\_ins]^{en9}}$$

$$v_{tS1} = k_{tS1}\,[B\_gluc]\left(1 + \frac{[B\_ins]^{ep13}}{k_{Dins}{}^{ep13} + [B\_ins]^{ep13}}\right)$$

$$v_{tS2} = k_{tS2}\,[B\_ket]$$

$$v_{tS3} = k_{tS3}\,[M\_lac]$$

$$v_{tS4} = k_{tS4}\,[M\_alan]\ \frac{k_{Dins}^{\ en11}}{k_{Dins}^{\ en11} + [B\_ins]^{en11}}$$

$$v_{d\_Bgluc} = k_{d\_Bgluc}\,[B\_gluc]$$

$$v_{d\_Bins} = k_{d\_Bins}\,[B\_ins]$$

$$v_{d\_Bglucgn} = k_{d\_Bglucgn}\,[B\_glucgn]$$

$$v_{d\_Bffa} = k_{d\_Bffa}\,[B\_ffa]$$

$$v_{d\_Blac} = k_{d\_Blac}\,[B\_lac]$$

$$v_{d\_Bket} = k_{d\_Bket}\,[B\_ket]$$

$$v_{d\_Balan} = k_{d\_Balan}\,[B\_alan]$$

FAT RATES:

$$v_{F1} = k_{F1}\,[F\_g6p]\left(1 + \frac{[B\_ins]^{ep14}}{k_{Dins}^{\ ep14} + [B\_ins]^{ep14}}\right)$$

$$v_{F3} = k_{F3}\,[F\_acyl]\left(1 + \frac{[B\_ins]^{ep15}}{k_{Dins}^{\ ep15} + [B\_ins]^{ep15}}\right)$$

$$v_{F4} = k_{F4}\,[F\_TG]\ \frac{k_{Dins}^{\ en12}}{k_{Dins}^{\ en12} + [B\_ins]^{en12}}$$

$$v_{F5} = k_{F5}\,[F\_ffa]^3$$

MUSCLE RATES:

$$v_{S1} = k_{S1}\,[M\_g6p]$$

$$v_{\text{-}S1} = k_{\text{-}S1}\,[M\_glycgn]$$

$$v_{S2} = k_{S2}\,[M\_g6p]$$

$$v_{S3} = k_{S3}\,[M\_pyr]$$

$$v_{-S3} = k_{-S3}\,[M\_lac]$$

$$v_{S4} = k_{S4}\,[M\_pyr]$$

$$v_{-S4} = k_{-S4}\,[M\_alan]\,[M\_ket]$$

$$v_{S\_dket} = k_{S\_dket}\,[M\_ket]$$

HORMONAL GROWTH RATES:

$$v_{ins} = k_{ins}$$

$$v_{Igluc} = \frac{k_{1ins}\,[B\_gluc]^{ni}}{k_{mIns}{}^{ni} + [B\_gluc]^{ni}}$$

$$v_{glucgn} = k_{glucgn}$$

$$v_{Ggluc} = \frac{k_{1glucgn}\,[B\_gluc]^{ng}}{k_{mGlgn}{}^{ng} + [B\_gluc]^{ng}}$$

MODEL EQUATIONS:

$$\frac{d[gluc]}{dt} = v_{tL1} - v_{L1} + v_{-L1}$$

$$\frac{d[g6p]}{dt} = v_{L1} - v_{-L1} - v_{L2} + v_{-L2} - v_{L3} + v_{-L3}$$

$$\frac{d[glycgn]}{dt} = v_{L2} - v_{-L2}$$

$$\frac{d[pep]}{dt} = 2\,v_{L3} - 2\,v_{-L3} - v_{L4} + v_{L13}$$

$$\frac{d[pyr]}{dt} = v_{L4} - v_{L5} + v_{-L5} - v_{L6} - v_{L7} - v_{L21} + v_{-L21} + v_{L20}$$

$$\frac{d[lac]}{dt} = v_{L5} - v_{-L5} + v_{tL2}$$

$$\frac{d[oa\_m]}{dt} = v_{L6} - v_{L8} - v_{L11} + v_{-L11}$$

$$\frac{d[acet\_m]}{dt} = v_{L7} - v_{L8} + 8\, v_{L18} - 2\, v_{L19}$$

$$\frac{d[citrate]}{dt} = v_{L8} - v_{L9} - v_{L14}$$

$$\frac{d[aK]}{dt} = v_{L9} - v_{L10} + v_{L21} - v_{-L21}$$

$$\frac{d[malate]}{dt} = v_{L10} + v_{L11} - v_{-L11} - v_{L12}$$

$$\frac{d[oa\_c]}{dt} = v_{L12} - v_{L13} + v_{L14}$$

$$\frac{d[acet\_c]}{dt} = v_{L14} - v_{L15} - v_{L16}$$

$$\frac{d[malonyl]}{dt} = v_{L15} - 7\, v_{L16}$$

$$\frac{d[palm]}{dt} = v_{L16} - v_{L17} + v_{tL5}$$

$$\frac{d[palmCoA]}{dt} = v_{L17} - v_{L18}$$

$$\frac{d[ket]}{dt} = v_{L19} - v_{tL3}$$

$$\frac{d[alan]}{dt} = v_{tL6} + v_{L21} - v_{-L21} - v_{L20}$$

$$\frac{d[glutamate]}{dt} = - v_{L21} + v_{-L21} - v_{L22}$$

$$\frac{d[B\_gluc]}{dt} = v_{feed} - v_{tL1} - v_{tF1} - v_{tS1} - v_{d\_Bgluc}$$

$$\frac{d[B\_ffa]}{dt} = - v_{tL5} + v_{tF3} - v_{d\_Bffa}$$

$$\frac{d[B\_lac]}{dt} = v_{tS3} - v_{tL2} - v_{d\_Blac}$$

$$\frac{d[B\_ket]}{dt} = v_{tL3} - v_{tS2} - v_{d\_Bket}$$

$$\frac{d[B\_alan]}{dt} = v_{tS4} - v_{tL6} - v_{d\_Balan}$$

$$\frac{d[F\_g6p]}{dt} = v_{tF1} - v_{F1}$$

$$\frac{d[F\_acyl]}{dt} = v_{F1} - v_{F3} + v_{F5}$$

$$\frac{d[F\_TG]}{dt} = v_{F3} - v_{F4}$$

$$\frac{d[F\_ffa]}{dt} = 0$$

$$\frac{d[M\_g6p]}{dt} = v_{tS1} - v_{S1} + v_{-S1} - v_{S2}$$

$$\frac{d[M\_glycgn]}{dt} = v_{S1} - v_{-S1}$$

$$\frac{d[M\_pyr]}{dt} = 2\,v_{S2} - v_{S3} + v_{-S3} - v_{S4} + v_{-S4}$$

$$\frac{d[M\_lac]}{dt} = v_{S3} - v_{-S3} - v_{tS3}$$

$$\frac{d[M\_ket]}{dt} = v_{tS2} - v_{S\_dket}$$

$$\frac{d[M\_alan]}{dt} = 0$$

$$\frac{d[B\_ins]}{dt} = v_{ins} + v_{Igluc} - v_{d\_Bins}$$

$$\frac{d[B\_glucgn]}{dt} = v_{glucgn} - v_{Ggluc} - v_{d\_Bglucgn}$$

A.2 Rates and Equations for Glycogen Regulatory Circuit Model

REDUCED GLYCOGEN REGULATORY CIRCUIT:

$$\frac{d[cAMP]}{dt} = \frac{k_{c1}\,[B\_glucgn]^{ng}}{k_{cm1}{}^{ng} + [B\_glucgn]^{ng}} - \frac{k_{c2}\,[B\_ins]^{ni}}{k_{cm2}{}^{ni} + [B\_ins]^{ni}}\,[cAMP]$$

$$\frac{d[GPa]}{dt} = \frac{k_{g5}\,[cAMP]\,(pt - [GPa])}{k_{mg5}\left(1 + \frac{s_1\,[g6p]}{k_{g2}}\right) + pt - [GPa]} - \frac{k_{g6}\,(PP1 + PP1\_GPa)\,[GPa]}{\frac{k_{mg6}}{1 + \frac{s_2\,[gluc]}{k_{gi}}} + [GPa]}$$

$$- k_a\,[PP1]\,[GPa] + k_{-a}\,[PP1\_GPa]$$

$$\frac{d[GSa]}{dt} = \frac{k_{g8}\,([PP1])\,(st - [GSa])}{\frac{k_{mg8}}{1 + \frac{s_1\,[g6p]}{k_{g2}}} + st - [GSa]} - \frac{k_{g7}\,([cAMP])\,[GSa]}{k_{mg7}\left(1 + \frac{s_1\,[g6p]}{k_{g2}}\right) + [GSa]}$$

$$\frac{d[PP1]}{dt} = 0$$

$$\frac{d[PP1\_GPa]}{dt} = 0$$

$$\frac{d[PKa]}{dt} = 0$$

$$\frac{d[R_2C_2]}{dt} = 0$$

$$\frac{d[C]}{dt} = 0$$

$$\frac{d[R_2CcAMP_2]}{dt} = 0$$

$$\frac{d[R_2cAMP_4]}{dt} = 0$$

FULL GLYCOGEN REGULATORY CIRCUIT:

$$\frac{d[cAMP]}{dt} = \frac{k_{c1}\,[B\_glucgn]^{ng}}{k_{cm1}{}^{ng} + [B\_glucgn]^{ng}} - \frac{k_{c2}\,[B\_ins]^{ni}}{k_{cm2}{}^{ni} + [B\_ins]^{ni}}\,[cAMP] - 2\,k_{gc1}\,[R_2C_2]\,[cAMP]^2 + 2\,k_{\_gc1}\,[R_2CcAMP_2]\,[C] + 2\,k_{gc2}\,[R_2CcAMP_2]\,[cAMP]^2 - 2\,k_{\_gc2}\,[R_2cAMP_4]\,[C]$$

$$\frac{d[GPa]}{dt} = \frac{k_{g5}\,[PKa]\,(pt - [GPa])}{k_{mg5}\left(1 + \frac{s_1\,[g6p]}{k_{g2}}\right) + pt - [GPa]} - \frac{k_{g6}\,(PP1 + PP1\_GPa)\,[GPa]}{\frac{k_{mg6}}{1 + \frac{s_2\,[gluc]}{k_{gi}}} + [GPa]} - k_a\,[PP1]\,[GPa] + k_{-a}\,[PP1\_GPa]$$

$$\frac{d[GSa]}{dt} = \frac{k_{g8}\,([PP1])\,(st - [GSa])}{\frac{k_{mg8}}{1 + \frac{s_1\,[g6p]}{k_{g2}}} + st - [GSa]} - \frac{k_{g7}\,([PKa] + [C])\,[GSa]}{k_{mg7}\left(1 + \frac{s_1\,[g6p]}{k_{g2}}\right) + [GSa]}$$

$$\frac{d[PP1]}{dt} = - k_a\,[PP1]\,[GPa] + k_{-a}\,[PP1\_GPa]$$

$$\frac{d[PP1\_GPa]}{dt} = k_a\,[PP1]\,[GPa] - k_{-a}\,[PP1\_GPa]$$

$$\frac{d[PKa]}{dt} = \frac{k_{g3}\,[C]\,(kt - [PKa])}{k_{mg3} + kt - [PKa]} - \frac{k_{g4}\,([PP1] + [PP1\_GPa])\,[PKa]}{k_{mg4} + [PKa]}$$

$$\frac{d[R_2C_2]}{dt} = -k_{gc1}\,[R_2C_2]\,[cAMP]^2 + k_{\_gc1}\,[R_2CcAMP_2]\,[C]$$

$$\frac{d[C]}{dt} = k_{gc1}\,[R2C2]\,[cAMP]^2 - k_{\_gc1}\,[R_2CcAMP_2]\,[C] + k_{gc2}\,[R_2CcAMP_2]\,[cAMP]^2 - k_{\_gc2}\,[R_2cAMP_4]\,[C]$$

$$\frac{d[R_2CcAMP_2]}{dt} = k_{gc1}\,[R_2C_2]\,[cAMP]^2 - k_{\_gc1}\,[R_2CcAMP_2]\,[C] - k_{gc2}\,[R_2CcAMP_2]\,[cAMP]^2 + k_{\_gc2}\,[R_2cAMP_4]\,[C]$$

$$\frac{d[R_2cAMP_4]}{dt} = k_{gc2}\,[R_2CcAMP_2]\,[cAMP]^2 - k_{\_gc2}\,[R_2cAMP_4]\,[C]$$

APPENDIX B

Parameter Values

B.1 Parameter Values for Liver Reactions

Reaction	*Parameters*
v_{L1}	$k_{L1} = 3$ $k_{mL1} = 7.7$ [25] $ep1 = 10$
v_{-L1}	$k_{-L1} = 4$ $k_{m-L1} = 1.3$ [27] $ep9 = 10$
v_{L2}	$k_{L2} = 20$ $k_{mL2} = .57$ [29]
v_{-L2}	$k_{-L2} = 20$ $k_{m-L2} = 1.4$ [30]
v_{L3}	$k_{L3} = 0.1$ $k_{mL3} = .01$ [31] $ep2 = 10$ en1 = 10
v_{-L3}	$k_{-L3} = .1$ $k_{m-L3} = 0.0034$ [32] $ep8 = 10$ $en6 = 10$
v_{L4}	$k_{L4} = 2$, $k_{mL4} = 0.18$ [33] $k_{i13} = 2$, $ep3 = 10$, $en2 = 10$
v_{L5}	$k_{L5} = 0$ $k_{mL5} = .03$ [34]
v_{-L5}	$k_{-L5} = 0.1$ $k_{m-L5} = 0.8$ [35]

Reaction	*Parameters*
v_{L6}	$k_{L6} = 1$ $k_{mL6} = 0.22$ [26] $p_2 = 1$ $k_{p2} = 2$ $ep4 = 10$
v_{L7}	$k_{L7} = 1$ $k_{mL7} = 0.0204$ [28] $k_{i8} = 2$
v_{L8}	$k_{L8} = 0.1$ $k_{i4} = 3$
v_{L9}	$k_{L9} = 0.1$
v_{L10}	$k_{L10} = 0.1$
v_{L11}	$k_{L11} = 0.6$ $ep5 = 10$
v_{-L11}	$k_{-L11} = 0.01$
v_{L12}	$k_{L12} = 0.6$ $ep6 = 10$ $en4 = 10$
v_{L13}	$k_{L13} = 0.5$ $ep7 = 10$ $en5 = 10$

v_{L14}	$k_{L14} = 0.01$ $ep10 = 10$ $en7 = 10$
v_{L15}	$k_{L15} = 0.01$ $p_1 = 1$ $k_{p1} = 0.5$ $k_{i5} = 1$
v_{L16}	$k_{L16} = 0.01$
v_{L17}	$k_{L17} = 0.01$ $k_{i1} = 0.1$
v_{L18}	$k_{L18} = 0.01$ $k_{i2} = 1$

v_{L19}	$k_{L19} = 0.01$ $ep11 = 10$ $en8 = 10$
v_{L20}	$k_{L20} = 0.2$
v_{L21}	$k_{L21} = 0.001$ $en3 = 10$ $k_{mL21p} = 0.4$ [36, 37] $k_{mL21g} = 4.3$ [36, 38]
v_{-L21}	$k_{-L21} = 0.2$ $en3 = 10$ $k_{m-L21a} = 21$ [39] $k_{m-L21k} = 0.22$ [39]
v_{L22}	$k_{L22} = 0.01$

B.2 Parameter Values for Blood Reactions (Transport, Decay and Feed)

Reaction	*Parameters*
v_{tL1}	$k_{tL1} = 100$
v_{tL2}	$k_{tL2} = 0.1$
v_{tL3}	$k_{tL3} = 0.1$
v_{tL4}	$k_{tL4} = 0.1$
v_{tL5}	$k_{tL5} = 0.1$
v_{tL6}	$k_{tL6} = 1$ $en10 = 10$
v_{d_Bgluc}	$k_{d\_Bgluc} = 0.01$
v_{d_Bins}	$k_{d\_Bins} = 0.01$
$v_{d\_Bglucgn}$	$k_{d\_Bglucgn} = 0.01$
v_{d_Bffa}	$k_{d\_Bffa} = 0.01$

Reaction	*Parameters*
v_{tF1}	$k_{tF1} = 0.01$ $ep12 = 10$
v_{tF3}	$k_{tF3} = 0.01$ $en9 = 20$
v_{tS1}	$k_{tS1} = 0.01$ $ep13 = 10$
v_{tS2}	$k_{tS2} = 1$
v_{tS3}	$k_{tS3} = 0.01$
v_{tS4}	$k_{tS4} = 3$ $en11 = 10$
v_{d_Blac}	$k_{d\_Blac} = 0.01$
v_{d_Bket}	$k_{d\_Bket} = 0.01$
v_{d_Balan}	$k_{d\_Balan} = 0.01$
v_{feed}	$k_{feed} = 0.5$

B.3 Parameter Values for Fat Reactions

Reaction	*Parameters*
v_{F1}	$k_{F1} = 0.1$ $ep14 = 10$
v_{F3}	$k_{F3} = 0.2$ $ep15 = 10$

Reaction	*Parameters*
v_{F4}	$k_{F4} = 0.1$ $en12 = 10$
v_{F5}	$k_{F5} = 0.1$

B.4 Parameter Values for Muscle Reactions

Reaction	*Parameters*
v_{S1}	$k_{S1} = 0$
v_{-S1}	$k_{-S1} = 0$
v_{S2}	$k_{S2} = 0.02$
v_{S3}	$k_{S3} = 0.01$
v_{-S3}	$k_{-S3} = 0.01$

Reaction	*Parameters*
v_{S4}	$k_{S4} = 0.07$
v_{-S4}	$k_{-S4} = 0$
v_{S5}	$k_{S5} = 0.5$
v_{S_dket}	$k_{S\_dket} = 0.01$

B.5 Parameter Values for Glycogen Regulatory Circuit Reactions

Reaction	*Parameters*
v_{g3}	k_{g3} = 1200 [19] k_{mg3} = 0.0004 [19]
v_{g4}	k_{g4} = 300 [19] k_{mg4} = 0.0011 [19, 42]
v_{g5}	k_{g5} = 1200 [19, 43] k_{mg5} = 0.01 [19, 44]
$v_{g5,}$ $v_{g7,}$ v_{g8}	s_1 = 100 [19] k_{g2} = 0.5 [19]

Reaction	*Parameters*
v_{g6}	k_{g6} = 300 [19, 40] k_{mg6} = 0.005 [19, 41] s_2 = .001 [19]) k_{gi} = 10 [19]
v_{g7}	k_{g7} = 1200 [19] k_{mg7} = 0.015 [19]
v_{g8}	k_{g8} = 3 [19] k_{mg8} = 0.00012 [19, 45]

B.6 Additional Parameter Values for Glycogen Regulatory Circuit in Isolation ([19, 46-48])

Parameters
capkt = 0.00025 mM
It = 0.0018 mM
kt = 0.0025 mM
pt = 0.07 mM
st = 0.003 mM
PP1 = 0.00025 mM

Parameters
PP2A = 0.000025 mM
k11 = 0.000043 mM
k22 = 0.0007 mM
ki = 0.1 mM
campt = 0.01 mM
kg = 349.5 mM

	Parameters
	g6pt = 0.7 mM
	kgi = 10 mM
	s1 = 100
	kg2 = 0.5 mM
	s2 = 0.001

B.7 Parameter Values Pertaining to Non-Metabolite Regulators (Insulin, Glucagon and cAMP)

Reaction	*Parameters*
v_{L1}, v_{L3}, v_{L4}, v_{L12}, v_{L13}, v_{L14}, v_{L19}, v_{L21}, v_{-L21}, v_{tL6}, v_{tF1}, v_{tS1}, v_{tS4}, v_{F1}, v_{F3}, v_{F4}	$k_{Dins} = 1 * 10^{-6}$
v_{-L3}, v_{L20}, v_{tF3}	$k_{Dins2} = 0.75 * 10^{-6}$
v_{-L1}, v_{L3}, v_{-L3}, v_{L4}, v_{L6}, v_{L11}, v_{L12}, v_{L13}, v_{L14}	$k_{Dglucgn} = 4 * 10^{-8}$
v_{L19}	$k_{DcAMP} = 1 * 10^{-5.5}$
v_{ins}	$k_{ins} = 7 * 10^{-4}$
v_{Igluc}	$k_{1ins} = 6 * 10^{-4}$ $k_{mins} = 8$ $ni = 10$
v_{Ggluc}	$k_{1glucgn} = 5 * 10^{-9}$ $k_{mGlgn} = 8$ $ng = 10$

Reaction	*Parameters*
v_{glucgn}	$k_{glucgn} = 2 * 10^{-9}$
v_{c1}	$k_{c1} = 1$ $k_{mc1} = 4 * 10^{-8}$
v_{c2}	$k_{c2} = 1 * 10^{-5.5}$ $k_{mc2} = 1 * 10^{-6}$
v_{gc1}	$k_{gc1} = 6 * 10^{10}$ $k_{-gc1} = 1.3953 * 10^{15}$
v_{gc2}	$k_{gc2} = 6 * 10^{10}$ $k_{-gc2} = 8.5714 * 10^{13}$
v_{Igluc}, v_{c1}	$ni = 10$
v_{Ggluc}, v_{c2}	$ng = 10$

APPENDIX C

Matlab Simulation Code

C.1 Main Function Code (main.m)

```
function main
clear; clc;

% which_loop = 'trnscrpt';      % compares 2 simulations, with different transcriptional
regulation patterns (see par_transcripts.m)
which_loop = 'circuits';
number_runs = 2;                % number of simulations to compare (only 1 or 2),
norm_method = 0;
run1_transcripts = 0;   % input which transcript data to use IF comparing transcripts
run2_transcripts = 0;   % see transcript_vectors.m (let run2_transcripts=[3]
reg_ko1 = 0;            %    and reg_ko2=2 in order to knockout GPa
reg_ko2 = 0;

%  LOOP for 1 or 2 simulations
for num_simulation = 1:number_runs

   % initialize 'trans' vector if comparing transcrpt reg. or initialize
   %   which glycogen regulatory circuits to compare ('mut')
   if which_loop == 'trnscrpt'
      trans =
transcript_vectors(run1_transcripts,run2_transcripts,reg_ko1,reg_ko2,num_simulation);
   elseif which_loop == 'circuits'
      trans = zeros(1,15);    % no transcriptional regulation
      if num_simulation == 1
         mut = 'red';         % Reduced circuit (orange output)
```

```
    elseif num_simulation == 2
        mut = 'ful';          % Full circuit (black output)
    end
end

y0 = init_main;     % load initial conditions from init_main.m

% 1st run -- to steady state under constant feeding
tmax = 100000;
run=1;      % determines what feeding level will be (see ode_blood.m)
options = odeset('AbsTol',10^-12,'RelTol',10^-12);
[t,y] = ode15s(@ode_main,[0 tmax],y0,options,run,trans,mut);
num_simulation

% 2nd run -- see ode_blood.m for feeding pattern (~line 30 to 44)
y0 = y(end,:);      % save output from last run as updated init conds
y0(3)=300;    %glycgn, start at same glycgn concentration
tmax = 2000;2000;       % max time point
run=2;              % determines what feeding level will be (see ode_blood.m)
[t,y] = ode15s(@ode_main,[0 tmax],y0,options,run,trans,mut);

% 3rd run -- REFEED with constant feeding
y0 = y(end,:);      % save output from last run as updated init conds
tmax = 500;
run=1;              % determines what feeding level will be (see ode_blood.m)
%[t,y] = ode15s(@ode_main,[0 tmax],y0,options,run,trans,mut);

if num_simulation==1        % save output for graphing
    y1 = y;       t1 = t;
else
    y2 = y;       t2 = t;
```

```
   end
end

%    GRAPHS

% plot first run output
[v_matLIVER1,v_matBLOOD1,v_matFAT1,v_matMUSCLE1] =
plot_main(t1,y1,1,number_runs,trans);
if number_runs==1       % close figures only used to compare 2 runs
   figure(301);close;figure(302);close;figure(303);close;
end

% plot second run output and comparison graphs
if number_runs==2
   [v_matLIVER2,v_matBLOOD2,v_matFAT2,v_matMUSCLE2] =
plot_main(t2,y2,2,number_runs,trans);
   plot_compare_run(v_matLIVER1,v_matLIVER2,1);
   plot_compare_run(v_matBLOOD1,v_matBLOOD2,2);
   plot_compare_run(v_matFAT1,v_matFAT2,3);
   plot_compare_run(v_matMUSCLE1,v_matMUSCLE2,4);

end

display('End of program')
return
```

C.2 Code for Initial Conditions (init_main.m, init_liver.m, init_glycogen.m, init_blood.m, init_fat.m, init_muscle.m)

init_main.m

```
% init_main.m
```

```
% Called by main.m
% Initial conditions are grouped by tissue in separate init_*.m files and
% brought together here to be loaded into one main intial condition vector

function y0 = init_main()

y0_liver = init_liver();
y0_blood = init_blood();
y0_fat = init_fat();
y0_muscle = init_muscle();
y0_glycogen = init_glycogen();
y0 = [y0_liver; y0_blood; y0_fat; y0_muscle; y0_glycogen];
return
```

init_liver.m

```
% init_liver.m
% Called by init_main.m

function y0 = init_liver()

gluc = 5; g6p = 10; glycgn = 10; pep = .001; pyr = 3; lac = 1; oa_m = .0002;
acet_m = 7; citrate = .5; aK = 1; malate = 3; oa_c = .0004; acet_c = 6;
malonyl = .3; palm = .3; palmCoA = .3; ket = .08; alan = .1;
cAMP = 10^(-5.5); glutamate = .1; co2 = 0;

y0 = [gluc; g6p; glycgn; pep; pyr; lac; oa_m; acet_m; citrate; aK;
   malate; oa_c; acet_c; malonyl; palm; palmCoA; ket; alan; cAMP;
   glutamate; co2];
return
```

init_glycogen.m

```
% init_glycogen.m
% Called by init_main.m

function y0=init_glycogen()

par=par_glycogen();
capkt = par(27); kt = par(28); pt = par(29);
st = par(30); PP1t = par(31);

PP1 = 1*PP1t; PP1_GPa = .0*PP1t;
PKb = kt; PKa = 0;
GPa = 1*pt; GSa = st;
R2C2 = capkt; C = 0; R2_C_cAMP2 = 0; R2_cAMP4 = 0;

y0 = [PP1; PP1_GPa; PKa; GPa; GSa; R2C2; C; R2_C_cAMP2; R2_cAMP4];
return
```

init_blood.m

```
% init_blood.m
% Called by init_main.m

function y0 = init_blood()

B_gluc = 4; B_ins = 1 * 10^(-6); B_glucgn = 40 * 10^(-9);
B_ffa = .3; B_lac = .2; B_ket = .08; B_alan = .1; sink = 0;

y0 = [B_gluc; B_ins; B_glucgn; B_ffa; B_lac; B_ket; B_alan; sink];
return
```

init_fat.m

```
% init_fat.m
```

```
% Called by init_main.m

function y0 = init_fat()

F_g6p = 0; F_acyl = 0; F_TG = 0; F_ffa = 2;

y0 = [F_g6p; F_acyl; F_TG; F_ffa];
return
```

init_muscle.m

```
% init_muscle.m
% Called by init_main.m

function y0 = init_muscle()

M_g6p = 8; M_glyc = 100; M_pyr = .2; M_lac = .2;
M_ket = .1; M_alan = .4;

y0 = [M_g6p; M_glyc; M_pyr; M_lac; M_ket; M_alan];
return
```

C.3 Code for Parameter Values (par_liver.m, par_glycogen.m, par_blood.m, par_fat.m, par_muscle.m, par_transcripts.m, par_flux.m)

par_liver.m

```
% par_liver.m
% called by ode_liver.m

function par = par_liver()

k1 = 3;.2;        % GK, gluc -> g6p
```

```
km1 = 7.7;      %   k1 * gluc /(km1 + gluc) * (1 + (B_ins/kDins)^ep1)
ep1 = 10;
k_1 = 4;.2;.1;.2;       % G6Pase, g6p -> gluc
km_1 = 1.3;     %   k_1 * g6p /(km_1 + g6p) * (1 + (B_glucgn/kDglucgn)^ep9)
ep9 = 10;
k2 = 20;        % GS, g6p -> glyc
km2 = .57;        %   k2 * GSa * g6p / (km2 + g6p)
k_2 = 20;     % GP, glyc -> g6p
km_2 = 1.4;       %   k_2 * GPa * glycgn / (km_2 + glycgn)
k3 = .1;.05;.1;    % g6p -> pep
km3   =   .01;          %          k3   *   g6p/(km3+g6p)   *   (1   +   (B_ins/kDins)^ep2)   *
kDglucgn^en1/(kDglucgn^en1 + B_glucgn^en1)
ep2 = 10;
en1 = 10;
k_3 = .3;   % pep -> g6p
km_3   =   .0034;       %      k_3   *   pep/(km_3+pep)   *   (1   +   (B_glucgn/kDglucgn)^ep8)   *
kDins^en6/(kDins^en6 + B_ins^en6)
ep8 = 10;
en6 = 10;
k4 = 2;    % pep -> pyr
km4 = .18;   %    k4 * pep   * (1 + (B_ins/kDins)^ep3) * kDglucgn^en2/(kDglucgn^en2 +
B_glucgn^en2) * ki13/(ki13 + alan)
ki13 = 2;
ep3 = 10;
en2 = 10;
k5 = .0;    % LDH, pyr -> lac
km5 = .03;       % k5 * pyr / (km5 + pyr)
k_5 = .1;   % LDH, lac -> pyr
km_5 = .8;       % k_5 * lac / (km_5 + lac)
k6 = 1;    % PC, pyr -> oa_m
km6 = 0.22;
```

```
p2 = 1;        %     k6 * pyr /(km6+pyr)* (1 + p2*acet_m/(kp2 + acet_m)) * (1 + (B_glucgn/kDglucgn)^ep4)
kp2 = 2;
p7 = 10;
ep4 = 10;
k7 = 1;    % PDH, pyr -> acet_m
ki8 = 2;    %   k7 * pyr / (km7 + pyr) * ki8/(ki8 + acet_m)
km7 = .0204;
k8 = .1;    % oa_m, acet_m -> cit
ki4 = 3;    %   k8 * oa_m * acet_m * ki4/(ki4 + palmCoA)
k9 = .1;    % cit -> aK
k10 = .1;   % aK -> malate
k11 = .6;   % oa_m -> malate
ep5 = 10;        % k11 * oa_m * (1 + (B_glucgn/kDglucgn)^ep5)
k_11 = .01;   % malate -> oa_m
k12 = .6;   % malate -> oa_c
ep6 = 10;              % k12 * malate * kDins^en4/(kDins^en4 + B_ins^en4)* (1 + (B_glucgn/kDglucgn)^ep6)
en4 = 10;
k13 = .5;   % PEPCK, oa_c -> pep
ep7 = 10;    %   k13 * oa_c * (1 + (B_glucgn/kDglucgn)^ep7) * kDins^en5/(kDins^en5 + B_ins^en5)
en5 = 10;
k14 = .01;   % cit -> acet_c, oa_c
ep10 = 10;              %      k14 * citrate * (1 + (B_ins/kDins)^ep10) * kDglucgn^en7/(kDglucgn^en7 + B_glucgn^en7)
en7 = 10;
k15 = .01;   % acet_c -> malonyl
p1 = 1;     %   k15 * acet_c * (1 + p1*citrate/(kp1 + citrate)) * ki5/(ki5 + palmCoA)
kp1 = .5;
ki5 = 1;
```

```
k16 = .01;   % acet_c, malonyl -> palm
             % k16 * acet_c * malonyl^7
k17 = .01;   % palm -> palmCoA
ki1 = .1;   %   k17 * palm * ki1/(ki1 + malonyl)
k18 = .01;   % palmCoA -> acet_m
ki2 = 1;    %   k18 * palmCoA * ki2/(ki2 + malonyl)
k19 = .01;   % acet_m -> ket
ep11   =   10;              %        k19   *   acet_m^2   *   (1   +   (cAMP/kdcAMP)^ep11)   *
kDins^en8/(kDins^en8 + B_ins^en8)
en8 = 10;
k20 = .2;   % alan -> pyr, non-ALT pathway
k21 = .001;    % pyr,glutamate -> alan,aK
en3 = 10;               % k21 * pyr * glutamate * kDins^en3/(kDins^en3 + B_ins^en3)
km21p = .4;
km21g = 4.3;
k_21 = .2;   % alan,aK -> pyr,glutamate
             %  k_21 * alan * aK * acet_m * kDins^en3/(kDins^en3 + B_ins^en3)
km_21a = 21;
km_21k = .22;
k22 = .01;  % glutamate sink
kc1 = 1;   % cAMP growth due to B_glucgn
kcm1 = 40*10^(-9); % kc1 * B_glucgn/(kcm1 + B_glucgn)
kc2 = kc1 * 10^(5.5);   % cAMP decay due to B_ins
kcm2 = 1*10^(-6);
% dcAMP = kc1 * B_glucgn/(kcm1 + B_glucgn) ...
%       - kc2 * B_ins/(kcm2 + B_ins) * cAMP;
kDins = 1 * 10^(-6);
kDins2 = .75*10^(-6);
kDglucgn = 40 * 10^(-9);
kdcAMP = 1*10^(-5.5);
```

```
par=[k1; km1; k_1; km_1; k2; km2; k_2; km_2; k3; km3; k_3; km_3;
   k4; km4; k5; km5; k_5; km_5; k6; k7; km7; k8; k9; k10;
   k11; k_11; k12; k13; k14; k15; k16; k17; k18; k19; k21; k_21;
   ki1; ki2; ki4; ki5; ki8; ki13; p1; p2; p7;
   kc1; kc2; kcm1; kcm2; kDins; kDglucgn; kdcAMP; kp1; kp2;
   ep1; ep2; ep3; ep4; ep5; ep6; ep7; ep8; ep9; ep10; ep11;
   en1; en2; en3; en4; en5; en6; en7; en8; kDins2; k20; k22; km6; km21p;
   km21g; km_21a; km_21k];
return
```

par_glycogen.m

```
% par_glycogen.m
% called by ode_glycogen.m

function par=par_glycogen()

k1 = 1.4 *60; % min-1 rate constant for phosphorylation of inhibitor
k2 = 0.01 *60; % min-1 rate constant for dephosphorylation of inhibitor
k3 = 20 *60; % min-1 rate constant for phosphorylation of phosphorylase kinase
k4 = 5 *60; % min-1 rate constant for dephosphorylation of phosphorylase kinase
k5 = 20 *60; % min-1 rate constant for phosphorylation of Phosphorylase
k6 = 5 *60; % min-1 rate constant for dephosphorylation of Phosphorylase
k7 = 20 *60; % min-1 rate constant for phosphorylation of glycogen synthase
k8 = 0.05 *60; % min-1 rate constant for dephosphorylation of glycogen synthase
km1 = 5 /1000; % mM for inhibitor phosphorylation
km2 = 0.7 /1000; % mM for dephosphorylation of Inhibitor-1
km3 = 0.4 /1000; % mM for Phosphorylation of phosphorylase kinase
km4 = 1.1 /1000; % mM for dephosphorylation of phosphorylase kinase
km5 = 10 /1000; % mM for phosphorylation of phosphorylase
km6 = 5 /1000; % mM for dephosphorylation of phosphorylase
km7 = 15 /1000; % mM for phosphorylation of glycogen synthase
```

km8 = 0.12 /1000; % mM for dephosphorylation of glycogen synthase

kd = 0.2 /1000; % dissociation of PP1 and phosphorylated PP1 Inhibitor, and also phosphorylase a with synthase PP1

% Total Concentrations

capkt = 0.25 /1000; % mM total R2C2

It = 1.8 /1000; % mM total Inhibitor concentration

kt = 2.5 /1000; % mM total Phosphorylase kinase

pt = 70 /1000; % mM total Glycogen Phosphorylase

pt = 80 /1000; % mM total Glycogen Phosphorylase

st = 3 /1000; % mM total Glycogen synthase

PP1 = 0.25 /1000; % mM PTPase 1

PP2A = 0.025 /1000; % mM PTPase 2

k11 = 0.043 /1000; % mM Dissociation constant of cAMP

k22 = 0.7 /1000; % mM Dissociation constant of cAMP

ki = 100 /1000; % mM cAMP inhibition constant

campt = 10 /1000; % mM maximum cAMP

kg = 349500 /1000; % mM activation constant of glucose-6-phosphate for synthase PP1

g6pt = 700 /1000; % mM maximum glucose-6-Phosphate

kgi = 10000 /1000; % mM activation constant of glucose for phosphorylase phosphatase

s1 = 100; % a multiplicative factor for glucose-6-phosphate effect on glycogen synthase dephosphorylation

kg2 = 500 /1000; % mM inhibition due to glucose-6-phosphate

s2 = 0.0010; % a multiplicative factor for glucose effect on phosphorylase phosphatase

k_a = .001 *60*1000; % min-1 mM-1 dissociation rate constant for PP1_GPa

ka = k_a/kd; % min-1 association rate constant for PP1_GPa

k_gc1 = 1000 *60*1000^2; % dissociation rate constant for [R2C(cAMP)2]+[C]

kgc1 = k_gc1/k11; % association rate constant for [R2C(cAMP)2]+[C]

k_gc2 = 1000 *60*1000^2; % dissociation rate constant for [R2(cAMP)4]+[C]

kgc2 = k_gc2/k22; % association rate constant for [R2(cAMP)4]+[C]

```
par = [k1; k2; k3; k4; k5; k6; k7; k8; km1; km2; km3; km4; km5; km6; km7; km8;
   k_a; ka; k_gc1; kgc1; k_gc2; kgc2; s1; kg2; s2; kgi; capkt; kt; pt; st; PP1];
return
```

par_blood.m

```
% par_blood.m
% called by ode_blood.m

function par = par_blood()

% BLOOD
kf = .5;     % feeding to bloodstream, kf
Imax = 1.3 * 10^(-6);
Imin = .7 * 10^(-6);
k_mIns = 8;
ni = 10;
Gmax = 50 * 10^(-9);
Gmin = 30 * 10^(-9);
k_mGlgn = 8;
ng = 10;

% LIVER/BLOOD transport:
ktL1 = 100;    % gluc <-> B_gluc
ktL2 = .1;    % B_lac -> lac
ktL3 = .1;    % ket -> B_ket
ktL4 = .1;    % %%%%%%%%%%%%%%%%%%%%  DELETE LATER
ktL5 = .1;    % B_ffa -> palm
ktL6 = 1;    % B_alan -> alan
en10 = 10;          % ktL6 * B_alan * kDins^en10/(kDins^en10 + B_ins^en10)

% FAT/BLOOD transport
```

```
ktF1 = .01;       % B_gluc -> F_g6p
ep12 = 10;        %   ktF1 * B_gluc * (1 + B_ins^ep12/(kDins^ep12+B_ins^ep12))
ktF3 = .01;       % F_ffa -> B_ffa
en9 = 20;       %   ktF3 * F_ffa^8 * kDins^en9/(kDins^en9 + B_ins^en9)

% MUSCLE/BLOOD transport
ktS1 = .01;     % B_gluc -> M_g6p
ep13 = 10;      %   ktS1 * B_gluc * (1 + B_ins^ep13/(kDins^ep13+B_ins^ep13))
ktS2 = 1;     % B_ket -> M_ket
ktS3 = .01;     % M_lac -> B_lac
ktS4 = 3;     % M_alan -> B_alan
en11 = 10;     %  ktS4 * M_alan* kDins^en11/(kDins^en11 + B_ins^en11)

% OUTFLOW of blood concentrations
kd_all = 0.01;
kd_Bgluc = kd_all;       % outflow of B_gluc
kd_Bins = kd_all;       % outflow of B_ins
kd_Bglucgn = kd_all;       % outflow of B_glucgn
kd_Bffa = kd_all;       % outflow of B_ffa
kd_Blac = kd_all;       % outflow of B_lac
kd_Bket = kd_all;       % outflow of B_ket
kd_Balan = kd_all;       % outflow of B_alan

k_ins = kd_Bins * Imin;
k1ins = kd_Bins * (Imax-Imin);
k_glucgn = kd_Bglucgn * Gmax;
k1glucgn = kd_Bglucgn * (Gmax-Gmin);

par=[kf; ktL1; ktL2; ktL3; ktL4; ktL5; ktL6;
   ktF1; ktF3;
   ktS1; ktS2; ktS3; ktS4;
```

```
   kd_Bgluc; kd_Bins; kd_Bglucgn; kd_Bffa;
   kd_Blac; kd_Bket; kd_Balan;
   k1ins; k_mIns; ni; k1glucgn; k_mGlgn; ng; k_ins; k_glucgn;
   Imax; Gmax; Imin; Gmin; ep12; ep13; en9; en10; en11];
return
```

par_fat.m

```
% par_fat.m
% called by ode_fat.m

function par = par_fat()

kf1 = .1;     % F_g6p -> F_acyl
ep14 = 10;      %   kf1 * F_g6p * (1 + (B_ins/kDins)^ep14)
kf3 = .2;     % F_acyl -> F_TG
ep15 = 10;      %   kf3 * F_acyl * (1 + (B_ins/kDins)^ep15)
kf4 = .1;     % F_TG -> F_ffa
en12 = 10;    %   kf4 * F_TG * kDins^en12/(kDins^en12 + B_ins^en12)
kf5 = .1;     % F_ffa -> F_acyl,   kf5 * F_ffa^3

par = [kf1; kf3; kf4; kf5; ep14; ep15; en12];
return
```

par_muscle.m

```
% par_muscle.m
% called by ode_muscle.m

function par = par_muscle()

ks1 = .0;       % M_g6p -> M_glyc, ks1 * M_g6p
ks_1 = .0;      % M_glyc -> M_g6p, ks_1 * M_glycgn
```

```
ks2 = .02;       % M_g6p -> M_pyr, ks2 * M_g6p
ks3 = .01;       % M_pyr -> M_lac, ks3 * M_pyr
ks_3 = .01;       % M_lac -> M_pyr, ks_3 * M_lac
ks4 = .07;        % M_pyr -> M_alan, ks4 * M_pyr
ks_4 = 0;      % M_alan -> M_pyr, ks_4 * M_alan * M_ket
ks5 = .5;        % --> M_alan, ks5
ks_dket = .01;    % M_ket decay rate constant

par=[ks1; ks_1; ks2; ks3; ks_3; ks4; ks_4; ks_dket; ks5];
return
```

par_transcripts.m

```
% par_transcripts.m
% Called by ode_blood.m
% This file called by ode_liver.m changes the parameter representing a specific enzyme
% for transcriptional regulation or knockout

function new_par =
par_transcripts(t,k1,k2,k_2,k3,k4,k5,k_5,k6,k7,k11,k12,k13,k14,k16,k17,k18,k19,trans)

%%  trans vector dictates which transcripts are regulated
%   0 -> transcript not regulated, 1 -> transcript regulated, 2 -> transcript knocked out

gk = trans(1);     % k1, glucokinase, gluc -> g6p
gs = trans(2);     % k2, glycogen synthase, g6p -> glyc
gp = trans(3);     % k_2, glycogen phosphorylase, glyc -> g6p
pfk = trans(4);    % k3, phosphofuctose kinase, g6p -> pep
pk = trans(5);     % k4, pyruvate kinase, pep -> pyr
ldh = trans(6);    % k5, k_5, lactate dehydrogenase, pyr <-> lac
pc = trans(7);     % k6, pyruvate carboxylase, pyr -> oa_m
pdh = trans(8);    % k7, pyruvate dehydrogenase, pyr -> acet_m
```

```
mdh = trans(9);    % k11, k12, malate dehydrogenase, oa_m,c <-> malate
pepck = trans(10);  % k13, phosphoenolpyruvate carboxylase, oa_c -> pep
cl = trans(11);     % k14, citrate lyase, cit -> acet_c
fas = trans(12);    % k16, fatty acid synthase, acet_c,malonyl -> palm
cpt = trans(13);    % k17, carnitine O-palmitoyltransferase, palm -> palmCoA
beta_ox = trans(14);     % k18, beta-oxidation, palmCoA -> acet_m
hmgs = trans(15);   % k19, HMG-synthase, acet_m -> ket

%% initialize vectors for transcipt expression factors
tp_k1 = [1 1 1];    tp_k2 = [1 1 1];    tp_k_2 = [1 1 1];
tp_k3 = [1 1 1];    tp_k4 = [1 1 1];    tp_k5 = [1 1 1];
tp_k_5 = [1 1 1];   tp_k6 = [1 1 1];    tp_k7 = [1 1 1];
tp_k11 = [1 1 1];   tp_k12 = [1 1 1];   tp_k13 = [1 1 1];
tp_k14 = [1 1 1];   tp_k16 = [1 1 1];   tp_k17 = [1 1 1];
tp_k18 = [1 1 1];   tp_k19 = [1 1 1];

%  these values represent the proportion of initial mRNA levels taken from
%  transcript data
if gk == 1;    tp_k1 = [ 1 0.606060606 0.787878788 ];   end
if gs == 1;    tp_k2 = [ 1 1.166666667 1.933333333 ];   end
if gp == 1;    tp_k_2 = [ 1 0.769230769 0.307692308 ];  end
if pfk == 1;   tp_k3 = [ 1 0.733333333 0.833333333 ];   end
if pk == 1;    tp_k4 = [ 1 1 0.3 ];                     end
if ldh == 1;   tp_k5 = [ 1 0.972222222 1.208333333 ];    tp_k_5 = tp_k5;    end
if pc == 1;    tp_k6 = [ 1 1.2 1.333333333 ];           end
if pdh == 1;   tp_k7 = [ 1 0.775 0.725 ];               end
if mdh == 1;   tp_k11 = [ 1 0.8 0.75 ];    tp_k12 = tp_k11;     end
if pepck == 1; tp_k13 = [ 1 1.276923077 1.384615385 ];  end
if cl == 1;    tp_k14 = [ 1 0.74 0.2 ];                 end
if fas == 1;   tp_k16 = [ 1 0.75 0.3 ];                 end
if cpt == 1;   tp_k17 = [ 1 1.1 2 ];                    end
```

```
if beta_ox == 1;    tp_k18 = [ 1 1.5 11.5 ];           end
if hmgs == 1;  tp_k19 = [ 1 1.105263158 1.368421053 ];  end

% % knockouts
if gk == 2;    tp_k1 = [ 0 0 0 ];                    end
if gs == 2;    tp_k2 = [ 0 0 0 ];                    end
if gp == 2;    tp_k_2 = [ 0 0 0 ];                    end
if pfk == 2;   tp_k3 = [ 0 0 0 ];                    end
if pk == 2;    tp_k4 = [ 0 0 0 ];                    end
if ldh == 2;   tp_k5 = [ 0 0 0 ];    tp_k_5 = tp_k5;    end
if pc == 2;    tp_k6 = [ 0 0 0 ];                    end
if pdh == 2;   tp_k7 = [ 0 0 0 ];                    end
if mdh == 2;   tp_k11 = [ 0 0 0 ];    tp_k12 = tp_k11;  end
if pepck == 2; tp_k13 = [ 0 0 0 ];                     end
if cl == 2;    tp_k14 = [ 0 0 0 ];                    end
if fas == 2;   tp_k16 = [ 0 0 0 ];                    end
if cpt == 2;   tp_k17 = [ 0 0 0 ];                    end
if beta_ox == 2;    tp_k18 = [ 0 0 0 ];                end
if hmgs == 2;  tp_k19 = [ 0 0 0 ];                    end

%% determine time when regulation occurs
if t < 420
   c=1;
elseif t >= 420 & t < 1020
   c=2;
else
   c=3;
end

%% multiply rate constant by corresponding vector component depending on
%% regulation type and time point
```

```
nk1 = k1 * tp_k1(c);        nk2 = k2 * tp_k2(c);
nk_2 = k_2 * tp_k_2(c);     nk3 = k3 * tp_k3(c);
nk4 = k4 * tp_k4(c);        nk5 = k5 * tp_k5(c);
nk_5 = k_5 * tp_k_5(c);     nk6 = k6 * tp_k6(c);
nk7 = k7 * tp_k7(c);        nk11 = k11 * tp_k11(c);
nk12 = k12 * tp_k12(c);     nk13 = k13 * tp_k13(c);
nk14 = k14 * tp_k14(c);     nk16 = k16 * tp_k16(c);
nk17 = k17 * tp_k17(c);     nk18 = k18 * tp_k18(c);
nk19 = k19 * tp_k19(c);

new_par = [nk1; nk2; nk_2; nk3; nk4; nk5; nk_5; nk6; nk7; nk11;
   nk12; nk13; nk14; nk16; nk17; nk18; nk19];
return
```

C.4 Code for Equations (ode_main.m, ode_liver.m, ode_glycogen.m, ode_blood.m, ode_fat.m, ode_muscle.m)

ode_main.m

```
% ode_main.m
% Called by main.m
% All ode's are grouped according to tissues.  All are called here in the
% ode_main.m file and output is returned in one main vector, f

function f = ode_main(t,y,run,trans,mut)

% liver:
gluc=y(1); g6p=y(2); glycgn=y(3); pep=y(4); pyr=y(5);
lac=y(6); oa_m=y(7); acet_m=y(8); citrate=y(9); aK=y(10);
malate=y(11); oa_c=y(12); acet_c=y(13); malonyl=y(14); palm=y(15);
palmCoA=y(16); ket=y(17); alan=y(18); cAMP=y(19); glutamate=y(20);
co2=y(21);
```

```
% blood:
B_gluc=y(22); B_ins=y(23); B_glucgn=y(24);
B_ffa=y(25); B_lac=y(26); B_ket=y(27); B_alan=y(28);
sink=y(29);

% fat:
F_g6p=y(30); F_acyl=y(31); F_TG=y(32); F_ffa=y(33);

% muscle:
M_g6p=y(34); M_glyc=y(35); M_pyr=y(36); M_lac=y(37);
M_ket=y(38); M_alan=y(39);

% glycogen:
PP1=y(40); PP1_GPa=y(41); PKa=y(42); GPa=y(43); GSa=y(44);
R2C2=y(45); C=y(46); R2_C_cAMP2=y(47); R2_cAMP4=y(48);

% call ode files for each tissue:
f_liver                                                                    =
ode_liver(t,y(1:21),B_gluc,B_ffa,B_ins,B_alan,B_lac,B_glucgn,GSa,GPa,run,trans);
f_blood = ode_blood(t,y(22:29),gluc,lac,ket,F_ffa,M_alan,M_lac,M_ket,run);
f_fat = ode_fat(t,y(30:33),B_gluc,B_ins);
f_muscle = ode_muscle(t,y(34:39),B_gluc,B_ket,B_ins);

% glycogen regulatory circuit ode:
dcAMP1 = f_liver(19);    % involved in ode_liver.m and ode_glycogen.m, combined on
line 38
f_glycogen = ode_glycogen(t,[y(40:48);cAMP],gluc,g6p,mut);
dcAMP2 = f_glycogen(end);

f_glycogen=f_glycogen(1:end-1);
```

```
f_liver(19) = dcAMP1 + dcAMP2;

f = [f_liver; f_blood; f_fat; f_muscle; f_glycogen];    % save all output in one vector
return
```

ode_liver.m

```
% ode_liver.m
% Called by ode_main.m

function f = ode_liver(t,y,B_gluc,B_ffa,B_ins,B_alan,B_lac,B_glucgn,GSa,GPa,
                       run,trans)

% load parameters/variables:
par=par_liver();
k1=par(1); km1=par(2); k_1=par(3); km_1=par(4); k2=par(5);
km2=par(6); k_2=par(7); km_2=par(8); k3=par(9); km3=par(10);
k_3=par(11); km_3=par(12); k4=par(13); km4=par(14); k5=par(15);
km5=par(16); k_5=par(17); km_5=par(18); k6=par(19); k7=par(20);
km7=par(21); k8=par(22); k9=par(23); k10=par(24); k11=par(25);
k_11=par(26); k12=par(27); k13=par(28); k14=par(29); k15=par(30);
k16=par(31); k17=par(32); k18=par(33); k19=par(34); k21=par(35);
k_21=par(36); ki1=par(37); ki2=par(38); ki4=par(39); ki5=par(40);
ki8=par(41); ki13=par(42); p1=par(43); p2=par(44); p7=par(45);
kc1=par(46); kc2=par(47); kcm1=par(48); kcm2=par(49); kDins=par(50);
kDglucgn=par(51); kdcAMP=par(52); kp1=par(53); kp2=par(54); ep1=par(55);
ep2=par(56); ep3=par(57); ep4=par(58); ep5=par(59); ep6=par(60);
ep7=par(61); ep8=par(62); ep9=par(63); ep10=par(64); ep11=par(65);
en1=par(66); en2=par(67); en3=par(68); en4=par(69); en5=par(70);
en6=par(71); en7=par(72); en8=par(73); kDins2=par(74);
k20=par(75); k22=par(76); km6=par(77); km21p=par(78);
km21g=par(79); km_21a=par(80); km_21k=par(81);
```

```
par=par_blood();
kf=par(1); ktL1=par(2); ktL2=par(3); ktL3=par(4); ktL4=par(5);
ktL5=par(6); ktL6=par(7); ktF1=par(8); ktF3=par(9);
ep13=par(34); en9=par(35); en10=par(36); en11=par(37);

% transcriptional regulation
   tr_par=par_transcripts(t,k1,k2,k_2,k3,k4,k5,k_5,k6,k7,k11,k12,k13,k14,k16,k17,k18,
         k19,trans);
   k1 = tr_par(1); k2 = tr_par(2); k_2 = tr_par(3); k3 = tr_par(4);
   k4 = tr_par(5); k5 = tr_par(6); k_5 = tr_par(7); k6 = tr_par(8);
   k7 = tr_par(9); k11 = tr_par(10); k12 = tr_par(11);
   k13 = tr_par(12); k14 = tr_par(13); k16 = tr_par(14); k17 = tr_par(15);
   k18 = tr_par(16); k19 = tr_par(17);

gluc=y(1); g6p=y(2); glycgn=y(3); pep=y(4); pyr=y(5);
lac=y(6); oa_m=y(7); acet_m=y(8); citrate=y(9); aK=y(10);
malate=y(11); oa_c=y(12); acet_c=y(13); malonyl=y(14); palm=y(15);
palmCoA=y(16); ket=y(17); alan=y(18); cAMP=y(19); glutamate=y(20);
co2=y(21);

% LIVER ode eqns:

dgluc = ktL1 * (B_gluc - gluc) ...      % gluc transport, B_gluc <-> gluc
     -  k1 * gluc /(km1 + gluc) * (1 + B_ins^ep1/(kDins^ep1+B_ins^ep1)) ...   % gluc ->
     g6p
     + k_1 * g6p /(km_1 + g6p) * (1 + B_glucgn^ep9/(kDglucgn^ep9+B_glucgn^ep9));
     % g6p -> gluc
dg6p = k1 * gluc /(km1 + gluc) * (1 + B_ins^ep1/(kDins^ep1+B_ins^ep1)) ...        % gluc
     -> g6p
     - k_1 * g6p /(km_1 + g6p) * (1 + B_glucgn^ep9/(kDglucgn^ep9+B_glucgn^ep9)) ...
     % g6p -> gluc
```

```
    - k2 * GSa * g6p / (km2 + g6p) ...          % g6p -> glycgn
    + k_2 * GPa * glycgn / (km_2 + glycgn) ...     % glycgn -> g6p
    - k3 * g6p/(km3+g6p) * (1 + B_ins^ep2/(kDins^ep2+B_ins^ep2)) *
kDglucgn^en1/(kDglucgn^en1 + B_glucgn^en1)  ...         % g6p -> pep
    + k_3 * pep/(km_3+pep) * (1 + B_glucgn^ep8/(kDglucgn^ep8+B_glucgn^ep8)) *
     kDins2^en6/(kDins2^en6 + B_ins^en6);          % pep -> g6p
dglycgn = k2 * GSa * g6p / (km2 + g6p) ...          % g6p -> glycgn
     - k_2 * GPa * glycgn / (km_2 + glycgn);     % glycgn -> g6p
dpep = 2 * k3 * g6p/(km3+g6p) * (1 + B_ins^ep2/(kDins^ep2+B_ins^ep2)) *
     kDglucgn^en1/(kDglucgn^en1 + B_glucgn^en1) ...         % g6p -> pep
    - 2 * k_3 * pep/(km_3+pep) * (1 + B_glucgn^ep8/(kDglucgn^ep8+B_glucgn^ep8)) *
    kDins2^en6/(kDins2^en6 + B_ins^en6) ...       % pep -> g6p
    - k4 * pep / (km4 + pep) * (1 + B_ins^ep3/(kDins^ep3+B_ins^ep3)) *
    kDglucgn^en2/(kDglucgn^en2 + B_glucgn^en2) * ki13/(ki13 + alan) ...
    + k13 * oa_c * (1 + B_glucgn^ep7/(kDglucgn^ep7+B_glucgn^ep7)) *
    kDins^en5/(kDins^en5 + B_ins^en5);          % pep carboxylase, oa_c --> pep
dpyr = k4 * pep / (km4 + pep) * (1 + B_ins^ep3/(kDins^ep3+B_ins^ep3)) *
     kDglucgn^en2/(kDglucgn^en2 + B_glucgn^en2) * ki13/(ki13 + alan) ...           %
     pyruvate kinase, pep -> pyr
    - k5 * pyr / (km5 + pyr)...         % pyr -> lac
    + k_5 * lac / (km_5 + lac)...       % lac -> pyr
    - k6 * pyr / (km6 + pyr) * (1 + p2*acet_m/(kp2 + acet_m)) * (1 +
     B_glucgn^ep4/(kDglucgn^ep4+B_glucgn^ep4)) ...          % pyruvate carboxylase, pyr
     -> oa_m
    - k7 * pyr / (km7 + pyr)  * ki8/(ki8 + acet_m) ...              % pyruvate dehydrogenase,
    pyr -> acet_m
    - k21 ./(km21p + pyr) ./ (km21g + glutamate) * pyr * glutamate *
    kDins^en3/(kDins^en3 + B_ins^en3)  ...          % pyr,glutamate -> alan,aK
    + k_21 ./(km_21a + alan) ./ (km_21k + aK) * alan * aK * acet_m *
    kDins^en3/(kDins^en3 + B_ins^en3) ...   % alan,aK -> pyr,glutamate
```

```
    + k20 * alan * kDins2^en3/(kDins2^en3 + B_ins^en3);             % alternate pathway,
    alan -> pyr
 dlac = k5 * pyr / (km5 + pyr)...        % pyr -> lac
    - k_5 * lac / (km_5 + lac)...       % lac -> pyr
    + ktL2 * B_lac;     % lac transport (bl to liv), B_lac --> lac
doa_m = k6 * pyr / (km6 + pyr) * (1 + p2*acet_m/(kp2 + acet_m)) * (1 +
    B_glucgn^ep4/(kDglucgn^ep4+B_glucgn^ep4)) ...               % pyruvate carboxylase,
    pyr -> oa_m
    - k8 * oa_m * acet_m * ki4/(ki4 + palmCoA) ...  % cit synthase, oa_m + acet_m ->
    citrate
    - k11 * oa_m * (1 + B_glucgn^ep5/(kDglucgn^ep5+B_glucgn^ep5))...                %
    malate dehydrogenase, oa_m -> malate
    + k_11 * malate;      % malate dehydrogenase, malate -> oa_m
dacet_m = k7 * pyr / (km7 + pyr) * ki8/(ki8 + acet_m) ...          % pyruvate
    dehydrogenase, pyr -> acet_m
     - k8 * oa_m * acet_m * ki4/(ki4 + palmCoA) ...  % cit synthase, oa_m + acet_m ->
    citrate
     + 8 * k18 * palmCoA * ki2/(ki2 + malonyl) ...       % beta-oxidation, palmCoA ->
    acet_m
     - 2 * k19 * acet_m^2 * (1 + cAMP^ep11/(kdcAMP^ep11+cAMP^ep11)) *
    kDins^en8/(kDins^en8 + B_ins^en8);         % HMG synthase/lyase, acet_m -> ket
dcitrate = k8 * oa_m * acet_m * ki4/(ki4 + palmCoA) ... % cit synthase, oa_m + acet_m
    -> citrate
    - k9 * citrate ...     % parital TCA cycle, citrate -> alpha-K
    - k14 * citrate * (1 + B_ins^ep10/(kDins^ep10+B_ins^ep10)) *
    kDglucgn^en7/(kDglucgn^en7 + B_glucgn^en7);      % citrate lyase, citrate -> acet_c,
    oa_c


daK = k9 * citrate ...          % parital TCA cycle, citrate -> alpha-K
   - k10 * aK ...               % parital TCA cycle, alpha-K -> malate
   + k21 ./(km21p + pyr) ./ (km21g + glutamate) * pyr * glutamate *
```

```
    kDins^en3/(kDins^en3 + B_ins^en3) ...          % pyr,glutamate -> alan,aK
  - k_21 ./(km_21a + alan) ./ (km_21k + aK) * alan * aK * acet_m *
  kDins^en3/(kDins^en3 + B_ins^en3);   % alan,aK -> pyr,glutamate
dmalate = k10 * aK ...          % parital TCA cycle, alpha-K -> malate
    + k11 * oa_m * (1 + B_glucgn^ep5/(kDglucgn^ep5+B_glucgn^ep5))...        % malate
    dehydrogenase, oa_m -> malate
    - k_11 * malate ...      % malate dehydrogenase, malate -> oa_m
    - k12 * malate * kDins^en4/(kDins^en4 + B_ins^en4)* (1 +
    B_glucgn^ep6/(kDglucgn^ep6+B_glucgn^ep6));         % malate shuttle/DH, malate
    -> oa_c
doa_c = k12 * malate * kDins^en4/(kDins^en4 + B_ins^en4) * (1 +
    B_glucgn^ep6/(kDglucgn^ep6+B_glucgn^ep6))...        % malate shuttle/DH, malate
    -> oa_c
    - k13 * oa_c * (1 + B_glucgn^ep7/(kDglucgn^ep7+B_glucgn^ep7)) *
    kDins^en5/(kDins^en5 + B_ins^en5) ...     % pep carboxylase, oa_c --> pep
    + k14 * citrate * (1 + B_ins^ep10/(kDins^ep10+B_ins^ep10)) *
    kDglucgn^en7/(kDglucgn^en7 + B_glucgn^en7);     % citrate lyase, citrate -> acet_c,
    oa_c
dacet_c = k14 * citrate * (1 + B_ins^ep10/(kDins^ep10+B_ins^ep10)) *
    kDglucgn^en7/(kDglucgn^en7 + B_glucgn^en7) ...        % citrate lyase, citrate ->
    acet_c, oa_c
     - k15 * acet_c * (1 + p1*citrate/(kp1 + citrate)) * ki5/(ki5 + palmCoA) ...      % acet
    carboxylase, acet_c -> malonyl
     - k16 * acet_c * malonyl^7;   % fas, acet_c + malonyl -> palm
dmalonyl = k15 * acet_c * (1 + p1*citrate/(kp1 + citrate)) * ki5/(ki5 + palmCoA) ...     %
    acet carboxylase, acet_c -> malonyl
      - 7 * k16 * acet_c * malonyl^7;  % fas, acet_c + malonyl -> palm
dpalm = k16 * acet_c * malonyl^7 ...  % fas, acet_c + malonyl -> palm
    - k17 * palm * ki1/(ki1 + malonyl) ...          % acyl synth/CPT, palm --> palmCoA
    + ktL5 * B_ffa;       % palm transport (bl to liv), B_palm -> palm
dpalmCoA = k17 * palm * ki1/(ki1 + malonyl) ...       % acyl synth/CPT, palm -->
```

```
    palmCoA
      - k18 * palmCoA * ki2/(ki2 + malonyl);      % beta-oxidation, palmCoA -> acet_m
dket = k19 * acet_m^2 * (1 + cAMP^ep11/(kdcAMP^ep11+cAMP^ep11)) *
    kDins^en8/(kDins^en8 + B_ins^en8) ...        % HMG synthase/lyase, acet_m -> ket
   - ktL3 * ket;              % ket transport (liv to bl) ket -> B_ket
dalan = ktL6 * B_alan * (kDins2)^en10/((kDins2)^en10 + B_ins^en10) ...   % alan
    transport, B_alan -> alan
    + k21 ./(km21p + pyr) ./ (km21g + glutamate) * pyr * glutamate *
    kDins^en3/(kDins^en3 + B_ins^en3) ...    % pyr,glutamate -> alan,aK
    - k_21 ./(km_21a + alan) ./ (km_21k + aK) * alan * aK * acet_m *
    kDins^en3/(kDins^en3 + B_ins^en3) ...    % alan,aK -> pyr,glutamate
    - k20 * alan * kDins2^en3/(kDins2^en3 + B_ins^en3);          % alternate pathway,
    alan -> pyr
dcAMP = kc1 * B_glucgn^10/(kcm1^10 + B_glucgn^10) ...
    - kc2 * B_ins^10/(kcm2^10+B_ins^10) * cAMP;
dglutamate = - k21 ./(km21p + pyr) ./ (km21g + glutamate) * pyr * glutamate *
    kDins^en3/(kDins^en3 + B_ins^en3) ...        % pyr,glutamate -> alan,aK
    + k_21 ./(km_21a + alan) ./ (km_21k + aK) * alan * aK * acet_m *
    kDins^en3/(kDins^en3 + B_ins^en3) ...   % alan,aK -> pyr,glutamate
    - k22 * glutamate;
dco2 = 0;

f = [dgluc; dg6p; dglycgn; dpep; dpyr; dlac; doa_m; dacet_m; dcitrate;
   daK; dmalate; doa_c; dacet_c; dmalonyl; dpalm;
   dpalmCoA; dket; dalan; dcAMP; dglutamate; dco2];
return
```

ode_glycogen.m

```
% ode_glycogen.m
% Called by ode_main.m
```

```
function f=ode_glycogen(t,y,gluc,g6p,mut)

% load parameters/variables:
par=par_glycogen();
kg1=par(1); kg2=par(2); kg3=par(3); kg4=par(4); kg5=par(5);
kg6=par(6); kg7=par(7); kg8=par(8); kmg1=par(9); kmg2=par(10);
kmg3=par(11); kmg4=par(12); kmg5=par(13); kmg6=par(14); kmg7=par(15);
kmg8=par(16); k_a=par(17); ka=par(18); kgc_1=par(19); kgc1=par(20);
kgc_2=par(21); kgc2=par(22); s1=par(23); kg2=par(24); s2=par(25);
kgi=par(26); capkt = par(27); kt = par(28); pt = par(29);
st = par(30); PP1t = par(31);
PP1=y(1); PP1_GPa=y(2); PKa=y(3); GPa=y(4); GSa=y(5);
R2C2=y(6); C=y(7); R2_C_cAMP2=y(8); R2_cAMP4=y(9); cAMP=y(10);

if mut == 'ful'    % full Mutalik circuit, cAMP dependent protein kinase
   kmg5s = kmg5.*(1+s1*g6p./kg2);
   kmg6s = kmg6./(1+s2*gluc./kgi);
   kmg7s = kmg7.*(1+s1*g6p./kg2);
   kmg8s = kmg8./(1+s1*g6p./kg2);
   Jg1 =          0;
   Jg2 =          0;
   Jg3 =          kg3 .* C .* (kt - PKa) ./ (kmg3 + (kt - PKa));
   Jg4 =          kg4 .* (PP1 + PP1_GPa) .* PKa ./ (kmg4 + PKa);
   Jg5 =          kg5 .* PKa .* (pt - GPa) ./ (kmg5s + (pt - GPa));
   Jg6 =          kg6 .* (PP1 + PP1_GPa) .* GPa ./ (kmg6s + GPa);
   Jg7 =          kg7 .* (PKa + C) .* GSa ./ (kmg7s + GSa);
   Jg8 =          kg8 .* (PP1) .* (st - GSa) ./ (kmg8s + (st - GSa));
   Jg9 =          ka .* PP1 .* GPa  -  k_a .* PP1_GPa;
   Jg10 =         kgc1 * R2C2 .* cAMP.^2 - kgc_1 * R2_C_cAMP2 .* C;
   Jg11 =         kgc2 * R2_C_cAMP2 .* cAMP.^2 - kgc_2 * R2_cAMP4 .* C;
elseif mut == 'red'    % reduced glycogen regulatory circuit
```

```
    kmg5s = kmg5.*(1+s1*g6p./kg2);
    kmg6s = kmg6./(1+s2*gluc./kgi);
    kmg7s = kmg7.*(1+s1*g6p./kg2);
    kmg8s = kmg8./(1+s1*g6p./kg2);
    kg5s = 40 * kg5;        % Force the reduced model to have the same
    kg7s = 3500 * kg7;      %   half-max velocity as the full model
    Jg1 =           0;
    Jg2 =           0;
    Jg3 =           0;
    Jg4 =           0;
    Jg5 =           kg5s .* cAMP .* (pt - GPa) ./ (kmg5s + (pt - GPa));
    Jg6 =           kg6 .* PP1 .* GPa ./ (kmg6s + GPa);
    Jg7 =           kg7s .* cAMP .* GSa ./ (kmg7s + GSa);
    Jg8 =           kg8 .* PP1 .* (st - GSa) ./ (kmg8s + (st - GSa));
    Jg9 =           0; ka .* PP1 .* GPa  -  k_a .* PP1_GPa;
    Jg10 =  0;
    Jg11 =  0;
end

%% GLYCOGEN ode eqns:
dPP1 = - Jg9;
dPP1_GPa = Jg9;
dPKa = Jg3 - Jg4;
dGPa = Jg5 - Jg6 - Jg9;
dGSa = Jg8 - Jg7;
dR2C2 = - Jg10;
dC = Jg10 + Jg11;
dR2_C_cAMP2 = Jg10 - Jg11;
dR2_cAMP4 = Jg11;
dcAMP = - 2*Jg10 - 2*Jg11;
```

```
f = [dPP1; dPP1_GPa; dPKa; dGPa; dGSa;
   dR2C2; dC; dR2_C_cAMP2; dR2_cAMP4; dcAMP];
return
```

ode_blood.m

```
% ode_blood.m
% Called by ode_main.m

function f = ode_blood(t,y,gluc,lac,ket,F_ffa,M_alan,M_lac,M_ket,run)

% load parameters/variables:
par=par_blood();
kf=par(1); ktL1=par(2); ktL2=par(3); ktL3=par(4); ktL4=par(5);
ktL5=par(6); ktL6=par(7); ktF1=par(8); ktF3=par(9);
ktS1=par(10); ktS2=par(11); ktS3=par(12); ktS4=par(13);
kd_Bgluc=par(14); kd_Bins=par(15); kd_Bglucgn=par(16); kd_Bffa=par(17);
kd_Blac=par(18); kd_Bket=par(19); kd_Balan=par(20);
k1ins=par(21); k_mIns=par(22); ni=par(23); k1glucgn=par(24);
k_mGlgn=par(25); ng=par(26); k_ins=par(27); k_glucgn=par(28);
Imax=par(29); Gmax=par(30); Imin=par(31); Gmin=par(32); ep12=par(33);
ep13=par(34); en9=par(35); en10=par(36); en11=par(37);
par=par_liver();
kDins=par(50); kDglucgn=par(51); kDins2=par(74);
B_gluc=y(1); B_ins=y(2); B_glucgn=y(3);
B_ffa=y(4); B_lac=y(5); B_ket=y(6); B_alan=y(7);
sink=y(8);

% FEEDING pattern:
if run==1          % constant feeding
     kfeed = kf;
```

```
elseif run==2
   if t<0
      kfeed = kf;     % constant feeding
   else
      u = 0;
      sd = 1/(kf*sqrt(2*pi));  % gives range of [0,kf]
      % kfeed = exp(-(.014*t-u).^2./(2.*sd^2))./(sd.*sqrt(2.*pi));  % decrease feeding
      kfeed = .25*cos(.01*t) + .25;       % oscillatory feeding
      %kfeed = .25*cos(.005*t) + .25;            % oscillatory feeding
   end
end

dB_gluc = kfeed ...        % feeding
       - ktL1 * (B_gluc - gluc) ...   % gluc transport, B_gluc <-> gluc
       - ktF1 * B_gluc * (1 + B_ins^ep12/(kDins^ep12+B_ins^ep12)) ...    % transport,
     B_gluc -> F_g6p
       - ktS1 * B_gluc * (1 + B_ins^ep13/(kDins^ep13+B_ins^ep13)) ...        % gluc
     transport, B_gluc -> M_gluc
       - kd_Bgluc * B_gluc;          % output of B_gluc
dB_ins = k_ins ...              % basal insulin secretion
      + k1ins*B_gluc^ni / (k_mIns^ni + B_gluc^ni)...    % pos reg by B_gluc
      - kd_Bins * B_ins;                                % insulin decay
dB_glucgn = k_glucgn - k1glucgn*B_gluc^ng / (k_mGlgn^ng + B_gluc^ng)...     % neg
     reg by gluc
       - kd_Bglucgn * B_glucgn;                                % glucgn decay
dB_ffa = - ktL5 * B_ffa ...         % palm transport (bl to liv), B_ffa -> palm
        + ktF3 * F_ffa^8 * (kDins2)^en9/(kDins2^en9 + B_ins^en9) ...    % transport, F_ffa
        -> B_ffa
       - kd_Bffa * B_ffa;          % output of B_ffa
dB_lac = ktS3 * M_lac ...     % lac transport, mus to blood
      - ktL2 * B_lac ...     % lac transport (bl to liv), B_lac --> lac
```

```
      - kd_Blac * B_lac;     % output of B_lac
dB_ket = ktL3 * ket ...         % ket transport (liv to bl) ket -> B_ket
      - ktS2 * B_ket ...       % ket transport, blood to mus
      - kd_Bket * B_ket;       % output of B_ket
dB_alan = ktS4 * M_alan* (.75.*10^(-6))^en11/((.75.*10^(-6))^en11 + B_ins^en11)...
     % alan transport, M_alan -> B_alan
      - ktL6 * B_alan * (.75.*10^(-6))^en10/((.75.*10^(-6))^en10 + B_ins^en10) ...
     % alan transport, B_alan -> alan
      - kd_Balan * B_alan;            % output of B_alan
dsink = 6* kd_Bgluc * B_gluc ...            % output of B_gluc
      + 16* kd_Bffa * B_ffa ...          % output of B_ffa
      + 3* kd_Blac * B_lac ...     % output of B_lac
      + 4* kd_Bket * B_ket ...       % output of B_ket
      + 3* kd_Balan * B_alan;           % output of B_alan

f = [dB_gluc; dB_ins; dB_glucgn; dB_ffa; dB_lac; dB_ket; dB_alan; dsink];
return
```

ode_fat.m

```
% ode_fat.m
% Called by ode_main.m

function f = ode_fat(t,y,B_gluc,B_ins)

% load parameters/variables:
par = par_fat();
kf1=par(1); kf3=par(2); kf4=par(3); kf5=par(4);
ep14=par(5); ep15=par(6); en12=par(7);
par=par_liver();
kDins=par(50); kDglucgn=par(51);
par=par_blood();
```

```
ktL5=par(6); ktL6=par(7); ktF1=par(8); ktF3=par(9);
Imax=par(29); Gmax=par(30); Imin=par(31); Gmin=par(32); ep12=par(33);
ep13=par(34); en9=par(35); en10=par(36); en11=par(37);
F_g6p=y(1); F_acyl=y(2); F_TG=y(3); F_ffa=y(4);

dF_g6p = ktF1 * B_gluc * (1 + B_ins^ep12/(kDins^ep12+B_ins^ep12))...      %
    transport, B_gluc -> F_g6p
     - kf1 * F_g6p * (1 + B_ins^ep14/(kDins^ep14+B_ins^ep14));            % F_g6p ->
    F_acyl
dF_acyl = kf1 * F_g6p * (1 + B_ins^ep14/(kDins^ep14+B_ins^ep14))...      % F_g6p ->
    F_acyl
     - kf3 * F_acyl * (1 + B_ins^ep15/(kDins^ep15+B_ins^ep15))...   % F_glyc3p,
    F_acyl -> F_TG
      + kf5 * F_ffa^3;        % F_ffa2 -> F_acyl
dF_TG = kf3 * F_acyl  * (1 + B_ins^ep15/(kDins^ep15+B_ins^ep15))...  % F_glyc3p,
    F_acyl -> F_TG
    - kf4 * F_TG * kDins^en12/(kDins^en12 + B_ins^en12);             % F_TG -> F_glyc,
    F_ffa
dF_ffa = 0;   % hold fat levels constant
     3* kf4 * F_TG * kDins^en12/(kDins^en12 + B_ins^en12)...             % F_TG ->
     F_glyc, F_ffa
     - 3 * kf5 * F_ffa^3 ...        % F_ffa2 -> F_acyl
     - 8 * ktF3 * F_ffa^8 * (.75*10^(-6))^en9/((.75*10^(-6))^en9 + B_ins^en9);       %
    transport, F_ffa2 -> B_ffa

f = [dF_g6p; dF_acyl; dF_TG; dF_ffa];
return
```

ode_muscle.m

```
% ode_muscle.m
```

```
% Called by ode_main.m

function f = ode_muscle(t,y,B_gluc,B_ket,B_ins)

% load parameters/variables:
par=par_muscle();
ks1=par(1); ks_1=par(2); ks2=par(3); ks3=par(4);
ks_3=par(5); ks4=par(6); ks_4=par(7); ks_dket=par(8);
ks5=par(9);
par=par_liver();
kDins=par(50);
par=par_blood();
ktS1=par(10); ktS2=par(11); ktS3=par(12); ktS4=par(13);
ep13=par(34); en9=par(35); en10=par(36); en11=par(37);
M_g6p=y(1); M_glycgn=y(2); M_pyr=y(3); M_lac=y(4);
M_ket=y(5); M_alan=y(6);

dM_g6p = ktS1 * B_gluc * (1 + B_ins^ep13/(kDins^ep13+B_ins^ep13)) ...     % gluc
     transport, B_gluc -> M_gluc
      - ks1 * M_g6p ...       % M_g6p -> M_glycgn
      + ks_1 * M_glycgn ...   % M_glycgn -> M_g6p
      - ks2 * M_g6p;          % M_g6p -> M_pyr
dM_glycgn = ks1 * M_g6p ...     % M_g6p -> M_glycgn
        - ks_1 * M_glycgn;    % M_glycgn -> M_g6p
dM_pyr = 2 * ks2 * M_g6p ...    % M_g6p -> M_pyr
      - ks3 * M_pyr ...        % M_pyr -> M_lac
      + ks_3 * M_lac ...       % M_lac -> M_pyr
      - ks4 * M_pyr ...        % M_pyr -> M_alan
      + ks_4 * M_alan * M_ket;    % M_alan -> M_pyr
dM_lac = ks3 * M_pyr ...        % M_pyr -> M_lac
      - ks_3 * M_lac ...       % M_lac -> M_pyr
```

```
      - ktS3 * M_lac;          % lac transport, mus to blood
dM_ket = ktS2 * B_ket ...       % ket transport, blood to mus
      ... - ktS4 * M_alan* M_ket * kis1/(kis1 + (B_ins-Imin)/Imax) ...      % alan transport,
M_alan -> B_alan
      - ks_dket * M_ket;       % decay term for M_ket (no other output)
dM_alan = 0;    % hold alanine levels constant
       ks5 ...              % --> M_alan
       + ks4 * M_pyr ...        % M_pyr -> M_alan
       - ks_4 * M_alan * M_ket...      % M_alan -> M_pyr
       - ktS4 * M_alan* kDins^en11/(kDins^en11 + B_ins^en11);     % alan transport,
     M_alan -> B_alan

f = [dM_g6p; dM_glycgn; dM_pyr; dM_lac; dM_ket; dM_alan];
return
```

REFERENCES

1. Young, F.G., *Claude Bernard and the discovery of glycogen; a century of retrospect.* Br Med J, 1957. **1**(5033): p. 1431-7.

2. Arias, I.M. and J.L. Boyer, *The liver : biology and pathobiology*. 4th ed. 2001, Philadelphia: Lippincott Williams & Wilkins. xvi, 1064 p., [16] p. of plates.

3. Nunemaker, C.S., et al., *Glucose modulates [Ca2+]i oscillations in pancreatic islets via ionic and glycolytic mechanisms.* Biophys J, 2006. **91**(6): p. 2082-96.

4. Soria, B. and F. Martin, *Cytosolic calcium oscillations and insulin release in pancreatic islets of Langerhans.* Diabetes Metab, 1998. **24**(1): p. 37-40.

5. Sturis, J., et al., *Computer model for mechanisms underlying ultradian oscillations of insulin and glucose.* Am J Physiol, 1991. **260**(5 Pt 1): p. E801-9.

6. Tolic, I.M., E. Mosekilde, and J. Sturis, *Modeling the insulin-glucose feedback system: the significance of pulsatile insulin secretion.* J Theor Biol, 2000. **207**(3): p. 361-75.

7. Kvapil, M. and P. Stolba, *[A minimal model of insulin and glucose kinetics].* Vnitr Lek, 1992. **38**(6): p. 608-16.

8. Toffolo, G., et al., *A minimal model of insulin secretion and kinetics to assess hepatic insulin extraction.* Am J Physiol Endocrinol Metab, 2006. **290**(1): p. E169-E176.

9. Lehninger, A.L., D.L. Nelson, and M.M. Cox, *Lehninger principles of biochemistry*. 4th ed. 2005, New York: W.H. Freeman. 1119 p., [91].

10. Murray, R.K., *Harper's illustrated biochemistry*. 2003, Lange Medical Books/McGraw-Hill: New York. p. v.

11. Kurland, I.J. and D.Z. D'Argenio, *A minimal model of liver glycogen metabolism; feasibility for predicting flux rates.* J Theor Biol, 1988. **135**(3): p. 343-58.

12. Kleckner, N.W., Z. Kizaki, and R.G. Thurman, *Potential intercellular futile cycling of carbohydrates in diabetes.* Biochem J, 1987. **246**(2): p. 417-23.

13. Boyle, J.P., et al., *Projection of diabetes burden through 2050: impact of changing demography and disease prevalence in the U.S.* Diabetes Care, 2001. **24**(11): p. 1936-40.

14. Im, S.S., et al., *Transcriptional regulation of glucose sensors in pancreatic beta cells and liver.* Curr Diabetes Rev, 2006. **2**(1): p. 11-8.

15. Frias, J.P. and S.V. Edelman, *Incretins and their role in the management of diabetes.* Curr Opin Endocrinol Diabetes Obes, 2007. **14**(4): p. 269-76.

16. Balks, H.J. and K. Jungermann, *Regulation of peripheral insulin/glucagon levels by rat liver.* Eur J Biochem, 1984. **141**(3): p. 645-50.

17. Jungermann, K. and F. Stumpel, *Role of hepatic, intrahepatic and hepatoenteral nerves in the regulation of carbohydrate metabolism and hemodynamics of the liver and intestine.* Hepatogastroenterology, 1999. **46 Suppl 2**: p. 1414-7.

18. Cornish-Bowden, A., *Fundamentals of enzyme kinetics*. Rev. ed. 1995, London Brookfield, Vt., USA: Portland ; Ashgate Pub. Co. [distributor]. xiii, 343 p.

19. Mutalik, V.K. and K.V. Venkatesh, *Quantification of the glycogen cascade system: the ultrasensitive responses of liver glycogen synthase and muscle phosphorylase are due to distinctive regulatory designs.* Theor Biol Med Model, 2005. **2**: p. 19.

20. Cardenas, M.L. and A. Goldbeter, *The glucose-induced switch between glycogen phosphorylase and glycogen synthase in the liver: outlines of a theoretical approach.* J Theor Biol, 1996. **182**(3): p. 421-6.

21. Buraczewski, S., et al., *The course of digestion of different food proteins in the rat. 2. The effect o feeding carbohydrate with proteins.* Br J Nutr, 1971. **25**(2): p. 299-306.

22. Curtis, K.J., et al., *Protein digestion and absorption in the rat.* J Physiol, 1978. **274**: p. 409-19.

23. Massillon, D., et al., *Quantitation of hepatic glucose fluxes and pathways of hepatic glycogen synthesis in conscious mice.* Am J Physiol, 1995. **269**(6 Pt 1): p. E1037-43.

24. Mvumbi, L., M. Bollen, and W. Stalmans, *Calcium ions and glycogen act synergistically as inhibitors of hepatic glycogen-synthase phosphatase.* Biochem J, 1985. **232**(3): p. 697-704.

25. Tu, J. and B.E. Tuch, *Glucose regulates the maximal velocities of glucokinase and glucose utilization in the immature fetal rat pancreatic islet.* Diabetes, 1996. **45**(8): p. 1068-75.

26. Jitrapakdee, S., M.E. Walker, and J.C. Wallace, *Functional expression, purification, and characterization of recombinant human pyruvate carboxylase.* Biochem Biophys Res Commun, 1999. **266**(2): p. 512-7.

27. Guionie, O., et al., *Identification and characterisation of a new human glucose-6-phosphatase isoform.* FEBS Lett, 2003. **551**(1-3): p. 159-64.

28. Jeng, J., et al., *Pyruvate dehydrogenase E1 alpha isoform in rat testis: cDNA cloning, characterization, and biochemical comparison of the recombinant testis and liver enzymes.* Comp Biochem Physiol B Biochem Mol Biol, 1998. **120**(1): p. 205-16.

29. Huang, K.P. and J.C. Robinson, *Purification and properties of the glucose-6-phosphate-dependent form of human placental glycogen synthase.* Arch Biochem Biophys, 1976. **175**(2): p. 583-9.

30. Medicus, R. and J. Mendicino, *Role of enzyme interactions in the regulation of glycolysis and gluconeogenesis. Purification and properties of the phospho- and dephospho-forms of glycogen phosphorylase from swine kidney.* Eur J Biochem, 1973. **40**(1): p. 63-75.

31. Nicolau, J., D.N. Souza, and G. Nunez-Burgos, *Regulation of phosphofructokinase-1 on submandibular salivary glands of rats after isoproterenol administration.* Arch Physiol Biochem, 2000. **108**(5): p. 437-43.

32. Adams, A., C. Redden, and S. Menahem, *Characterization of human fructose-1,6-bisphosphatase in control and deficient tissues.* J Inherit Metab Dis, 1990. **13**(6): p. 829-48.

33. Srivastava, L.K. and N.Z. Baquer, *Purification and properties of rat brain pyruvate kinase.* Arch Biochem Biophys, 1985. **236**(2): p. 703-13.

34. LeVan, K.M. and E. Goldberg, *Properties of human testis-specific lactate dehydrogenase expressed from Escherichia coli.* Biochem J, 1991. **273 (Pt 3)**: p. 587-92.

35. Mendiola, P. and J. De Costa, *The effects of temperature and pH on the kinetic properties of heart muscle lactate dehydrogenase from anuran amphibians.* Comp Biochem Physiol B Biochem Mol Biol, 1991. **98**: p. 529-534.

36. Ruscak, M., J. Orlicky, and V. Zubor, *Isoelectric focusing of the alanine aminotransferase isoenzymes from the brain, liver and kidney.* Comp Biochem Physiol B, 1982. **71**(1): p. 141-4.

37. DeRosa, G. and R.W. Swick, *Metabolic implications of the distribution of the alanine aminotransferase isoenzymes.* J Biol Chem, 1975. **250**(20): p. 7961-7.

38. Ward, C.W. and P.J. Schofield, *Glycolysis in Haemonchus contortus larvae and rat liver.* Comp Biochem Physiol, 1967. **22**(1): p. 33-52.

39. Gubern, G., et al., *Subcellular distribution of alanine aminotransferase activity in human liver.* Biochem Soc Trans, 1990. **18**(6): p. 1287-8.

40. Ingebritsen, T.S. and P. Cohen, *Protein phosphatases: properties and role in cellular regulation.* Science, 1983. **221**(4608): p. 331-8.

41. Foulkes, J.G., et al., *A kinetic analysis of the effects of inhibitor-1 and inhibitor-2 on the activity of protein phosphatase-1.* Eur J Biochem, 1983. **132**(2): p. 309-13.

42. Nimmo, G.A. and P. Cohen, *The regulation of glycogen metabolism. Phosphorylation of inhibitor-1 from rabbit skeletal muscle, and its interaction with protein phosphatases-III and -II.* Eur J Biochem, 1978. **87**(2): p. 353-65.

43. Shacter, E., P.B. Chock, and E.R. Stadtman, *Energy consumption in a cyclic phosphorylation/dephosphorylation cascade.* J Biol Chem, 1984. **259**(19): p. 12260-4.

44. Meinke, M.H. and R.D. Edstrom, *Muscle glycogenolysis. Regulation of the cyclic interconversion of phosphorylase a and phosphorylase b.* J Biol Chem, 1991. **266**(4): p. 2259-66.

45. Killilea, S.D., et al., *Evidence for the coordinate control of activity of liver glycogen synthase and phosphorylase by a single protein phosphatase.* J Biol Chem, 1976. **251**(8): p. 2363-8.

46. Cohen, P., *Control of enzyme activity*. 2nd ed. 1983, London ; New York: Chapman and Hall. 96 p.

47. Aiston, S., et al., *Glucose 6-phosphate causes translocation of phosphorylase in hepatocytes and inactivates the enzyme synergistically with glucose.* Biochem J, 2004. **377**(Pt 1): p. 195-204.

48. Beavo, J.A., P.J. Bechtel, and E.G. Krebs, *Activation of protein kinase by physiological concentrations of cyclic AMP.* Proc Natl Acad Sci U S A, 1974. **71**(9): p. 3580-3.